Bipartite GINS binding mode of TopBP1 to activate the metazoan Mcm2-7 replicative helicase

Inaugural Dissertation

for

the doctoral degree of

Dr. rer. nat.

from the Faculty of Biology

University of Duisburg-Essen

Submitted by

Bilal Tetik

Born in Izmir-Turkey

August 2023

The experiments underlying the present work were conducted at the Faculty of Biology at the Department of Molecular Genetics II at the University of Duisburg-Essen.

1. Examiner: Prof. Dr. Dominik Boos

2. Examiner: Prof. Dr. Stefan Westermann

Chair of the Board of Examiners: Prof. Dr. Hemmo Meyer

Date of the oral examination: 21.11.2023

DOI: 10.17185/duepublico/81325
URN: urn:nbn:de:hbz:465-20240202-113320-1

In the context of this doctoral work, the following article has been submitted:

Matthew Day*, Bilal Tetik*, Milena Parlak*, Almeida-Hernandez Y, Sanchez-Garcia E, Kaschani F, Räschle M, Siegert H, Pearl L, Oliver A, Boos D

TopBP1 utilises a bipartite GINS binding mode to activate the replicative helicase.

bioRxiv (2023) doi: https://doi.org/10.1101/2023.03.31.535063

Under revision at Nature Communications

* equal contribution

In the context of this doctoral work, the following articles were published:

Pedro Ferreira, Verena Höfer, Nora Kronshage, Anika Marko, Karl-Uwe Reusswig, Bilal Tetik, Christoph Dießel, Kerstin Köhler, Nikolai Tschernoster, Janine Altmüller, Nina Schulze, Boris Pfander, Dominik Boos

MTBP phosphorylation controls DNA replication origin firing

In: Biology Vol. 11 (2022) Nr. 6

Table of Content

List of figures

List of extended figures

List of tables

Summary

Genome replication must be complete, accurate and occur exactly once during each cell cycle to generate two faithful copies of the DNA, one for each emerging daughter cell. This is at the heart of genetic homeostasis over the successive cell generations.

Replication initiation is the first step of replication and regulates exactly when and where replication takes place. In yeast, the molecular processes and the main proteins involved in initiation have been described. The loading of the Mcm2-7 helicase takes place in G1-phase and its activation occurs in the S-phase. In the first step, origin licensing, the Mcm2-7 helicase is loaded onto the origin of DNA and the pre-replicative complex (pre-RC) is formed. Mcm2-7 is helicase-inactive at that stage. The second step is origin firing, the pre-RCs are converted to the helicase-active CMG (Cdc45-Mcm2-7-GINS) and replisomes are formed. Activation of the Mcm2-7 helicase in S-phase begins with the stepwise assembly of a transient preinitiation complex (pre-IC), and GINS and Cdc45 are recruited to the Mcm2-7 during the pre-IC formation. In yeast, Sld3-Sld7, the orthologue of Treslin-MTBP in vertebrate, mediates the recruitment of Cdc45 to the Mcm2-7. GINS, Dpb11, Sld2 and Polε form pre-loading complex (pre-LC) and this complex recruits GINS to the Mcm2-7. When helicase-active CMG complex is formed, Sld3-Sld7, Dpb11 and Sld2 leave the complex and mature replisomes are formed. Although the origin firing factors are conserved between yeast and vertebrates, the molecular details of the recruitment of Cdc45 and GINS to the Mcm2-7 are poorly investigated in vertebrates due to the lack of *in vitro*-reconstitution efforts. In this project, we use recombinant proteins to reveal molecular details of the TopBP1-GINS interaction, providing insight how TopBP1 contributes to GINS recruitment to the inactive Mcm2-7 helicase to form helicase-active CMG.

In our research, we conducted biochemical and structural studies, which revealed that the helicase activator GINS interacts with TopBP1 through two distinct binding surfaces. The first binding surface involves the previously poorly described GINI domain. We here showed that the GINI domain is located between BRCT3 and BRCT4 domains of TopBP1 and it consists of highly conserved amino acids among metazoans. Our cryo-EM model demonstrated that GINI domain forms an short α-helix structure and this α-helix structure is crucial for the interaction with GINS. The second binding surface is located on TopBP1-BRCT4 which is a novel binding site for GINS. Both of these binding surfaces interact with the opposite ends of the A domain of the GINS subunit Psf1, and their cooperation is necessary for a stable biochemical interaction between TopBP1 and GINS. Moreover, we carried out rescue experiments for DNA replication in TopBP1 depleted *Xenopus* egg extract by adding-back of either recombinant TopBP1-

BRCT0-5-WT or recombinant TopBP1 with different sets of mutations in either interface. These rescue experiments showed that this cooperation between GINI and BRCT4 domains is also required during replication origin firing. Furthermore, we here propose that the interaction between TopBP1 and GINS is not compatible simultaneously with the binding of Polε to GINS when GINS is already bound to Mcm2-7-Cdc45. Based on our TopBP1-GINS model, we propose that three molecular processes are coordinated: The arrival of DNA polymerase epsilon, the ejection of TopBP1, and the integration of GINS into Mcm2-7-Cdc45 during replication origin firing.

Zusammenfassung

Die Genomreplikation muss vollständig, genau und während jedes Zellzyklus genau einmal erfolgen, um zwei originalgetreue Kopien der DNA zu erzeugen, eine für jede entstehende Tochterzelle. Dies steht im Mittelpunkt der genetischen Homöostase über die aufeinanderfolgenden Zellgenerationen.

Replikationsinitiation ist der erste Schritt der Replikation und reguliert, wann und wo genau die Replikation stattfindet. Die molekularen Prozesse und essenziellen Proteine, die an Replikationsinitiation beteiligt sind, wurden im Hefen-Modell beschrieben. Das Laden der Mcm2-7 Helikase findet in der G1-Phase statt, die Aktivierung erfolgt in der S-Phase. In dem ersten Schritt, der Lizenzierung (origin licensing), wird die inaktive Mcm2-7-Helikase auf den DNA-Origins geladen und der Prä-Replikative Komplex (Prä-RK) gebildet. Der zweite Schritt ist das Origin-Firing, in welchem der inaktive Prä-RK zu der aktiven CMG Helikase (Cdc45-Mcm2-7-GINS) umgewandelt und die Replisomen gebildet werden. Die Aktivierung der Mcm2-7 Helikase in der S-Phase beginnt mit dem schrittweisen Aufbau eines transienten Prä-Initiationskomplexes (Prä-IK), und während der prä-IK Assemblierung werden GINS und Cdc45 an die Mcm2-7 Helikase rekrutiert. In Hefe vermittelt Sld3-Sld7, das Ortholog von Treslin-MTBP bei Wirbeltieren, die Rekrutierung von Cdc45 an Mcm2-7. GINS, Dpb11, Sld2 und DNA polymerase epsilon (Polε) bilden einen Prä-Ladekomplex (Prä-LK) und dieser Komplex rekrutiert GINS an Mcm2-7. Wenn der aktive CMG Helikase-Komplex gebildet wird, verlassen Sld3-Sld7, Dpb11 und Sld2 den Komplex und es werden reife Replisomen gebildet. Obwohl die Origin-Firing-Faktoren zwischen dem Modellorganismus Hefe und Wirbeltieren konserviert sind, sind die molekularen Details der Rekrutierung von Cdc45 und GINS an die Mcm2-7-Helikase bei Wirbeltieren aufgrund mangelnder Bemühungen zur In-vitro-Rekonstitution noch unbekannt. In diesem Projekt verwenden wir rekombinante Proteine, um molekulare Mechanismen der TopBP1-GINS-Interaktion aufzudecken und Einblicke zu geben, wie TopBP1 zur GINS-Rekrutierung für die inaktive Mcm2-7-Helikase beiträgt, um Helikase-aktives CMG zu bilden.

Im Rahmen unserer Forschung führten wir biochemische und strukturelle Studien durch, die zeigten, dass der Helikase Aktivator GINS über zwei unterschiedliche Domänen mit TopBP1 interagiert. Bei der ersten Bindungsdomäne handelt es sich um die bisher nicht vollständig beschriebene GINS-Interaktionsdomäne (GINI). Wir zeigen hier, dass die GINI zwischen den BRCT3- und BRCT4-Domänen von TopBP1 lokalisiert ist und, dass sie aus hoch konservierten Aminosäuren in Metazoen besteht. Unser Kryo-EM-Modell hat gezeigt, dass die GINI-Domäne

eine kurze α-Helix-Struktur bildet und diese α-Helix-Struktur für die Interaktion mit GINS entscheidend ist. Die zweite Bindungsdomäne befindet sich auf TopBP1-BRCT4, einer neuartigen Bindestelle für GINS. Beide Bindungsdomänen interagieren mit den gegenüberliegenden Enden der A-Domäne der GINS-Untereinheit Psf1 und ihre Kooperation ist für eine stabile biochemische Interaktion zwischen TopBP1 und GINS notwendig. Darüber hinaus führten wir Rettungsexperimente zur DNA-Replikation in TopBP1-depletiertem Xenopus-Eiextrakt durch, indem wir entweder rekombinantes TopBP1-BRCT0-5-WT oder rekombinantes TopBP1 mit unterschiedlichen Mutationssätzen in beiden Bindestellen einfügten. Diese Rettungsexperimente zeigten, dass diese Kooperation zwischen GINI- und BRCT4-Domänen auch bei dem Origin-Firing erforderlich ist. Darüber hinaus schlagen wir hier vor, dass die Interaktion zwischen TopBP1 und GINS nicht gleichzeitig mit der Bindung von Polε an GINS kompatibel ist, wenn GINS bereits an Mcm2-7-Cdc45 gebunden ist. Basierend auf unserem TopBP1-GINS-Modell schlagen wir vor, dass drei molekulare Prozesse koordiniert sind: das Eintreffen von Polε, die Dissoziation von TopBP1 und die Integration von GINS in Mcm2-7-Cdc45 während des Origin-Firing.

Abbreviations

APC/C	Anaphase promoting complex
APS	Ammonium persulfate
ATP	Adenosine triphosphate
BRCA1	Breast cancer gene 1
BRCT	BRCA1 (Breast cancer associated 1) C-terminal domain
C-terminus	Carboxyl-terminus
Cdc45	Cell division control protein 45
Cdc6	Cell division control protein 6
CDC7	Cell division cycle 7-related protein kinase
Cdh1	Cadherin-1
CDK	Cyclin-dependent kinase
Cdt1	Chromatin licensing and DNA replication factor 1
CMG	Cdc45-Mcm2-7-GINS
CMGE	Cdc45-Mcm2-7-GINS-Polε
Dbf4	DBF4 Zinc Finger
DDK	Dbf4-dependent kinase
DMEM	Dulbecco's Modified Eagle Medium
DMSO	Dimethyl sulfoxide
DNA	Deoxyribonucleic acid
Dpb11	DNA Polymerase B (II)
dsDNA	Double stranded DNA
FCS	Fetal calf serum
FKH	Forkhead
GINI	GINS interaction

GINS	go-ichi-ni-san protein complex
IPTG	Isopropyl-β-D-thiogalactopyranosid
ISC	Intra S-phase checkpoint
kDa	Kilodalton
kb	Kilobase
LB	Luria Bertani
Mcm2-7	Minichromosome maintenance complex components 2-7
ml	Milliliter
mM	Millimolar
MTBP	Mdm2-binding protein
N-terminus	Amino-terminus
nM	Nanomolar
ORC	Origin recognition complex
PBS	Phosphate buffered saline
PCNA	Proliferating cell nuclear antigen
PCR	Polymerase chain reaction
PMSF	Phenylmethylsulfonyl fluoride
Pol	Polymerase
POLE2	DNA polymerase epsilon subunit 2
PP	Lambda protein phosphatase
pRb	Retinoblastoma
pre-IC	Pre-initiation complex
pre-LC	Pre-loading complexes
pre-RC	Pre-replicative complex
Rad53	Serine/threonine-protein kinase RAD53

RecQ4	RecQ like Helicase 4
Rpm	Rounds per minute
SDS-PAGE	Sodium dodecyl sulfate polyacrylamide gel electrophoresis
SDS complex	Sld3/Sld7-Dpb11-Sld2
Sld2,3,5,7	Synthetic Lethality with Dpb11
TBS	Tris buffered saline
TCA	Trichloroacetic acid
TEMED	tetramethylethylenediamine
TMT	Treslin-MTBP-TopBP1
TopBP1	DNA Topoisomerase II Binding Protein 1
Tris	Tris(hydroxymethyl)aminomethane
TRP	Temporal replication program
TTR	Timing transition region
v/v	Volume percentage
w/v	Weight percentage
WT	Wild type
α-32P dCTP	Deoxycytidine 5'-[alpha-32P] triphosphate
µg	Microgram
µl	Microliter
µM	Micromolar
°C	Degree Celsius

1. Introduction

To preserve genetic homeostasis in the cells through generations, genome must be duplicated completely and exactly once in each cell cycle. Genome duplication takes place in a process called DNA replication. The first step of DNA replication is initiation which leads to the establishment of two bidirectional replication forks at the specialized sites within DNA called as replication origin. Elongation is the second step, where the new DNA is synthesized bidirectionally by the established replication forks. During the last step, termination, the newly synthesized DNA is ligated into a continuous strand, the replisomes are disassembled and DNA replication terminates. To ensure complete and error-free DNA replication and thus maintenance of genetic stability, these processes are strictly regulated and coordinated (Huberman and Riggs 1968; Shima et al. 2007; Toledo et al. 2013). Replication initiation plays a crucial role in this regulation and control, because it regulates where in the genome, when and under which circumstances replication forks are formed (Zaffar et al. 2022).

Replication initiation involves two steps: Replication origin licensing and origin firing. During origin licensing, two inactive replicative Mcm2-7 helicases are loaded onto the replication origin in a head-to-head orientation. During origin firing, the inactive helicases become activated and two bi-directional mature replisomes are formed. An essential aspect of the activation of the helicase is the loading of two helicase components, Cdc45 and GINS, onto the Mcm2-7 helicase. However, the specific molecular details of helicase activation during origin firing in metazoans are still largely unknown. This research project aims to advance our understanding of how the firing factor TopBP1 facilitates the recruitment of the GINS helicase activator to the replicative helicase at a molecular level.

1.1. DNA replication in eukaryotes

1.1.1. Fundamental aspects of genome replication in eukaryotes

DNA replication is specifically carried out during the S phase of the cell cycle, which is facilitated by the increase in cyclin-dependent kinase (CDK) and Dbf4-dependent kinase (DDK) levels during the S phase. Since eukaryotic cells have large genomes, numerous replication origins are required to ensure complete replication within one S phase (Hyrien, Marheineke, and Goldar 2003). However, it is crucial to prevent excessively large inter-origin distances, known as the random gap problem, which may hinder the complete duplication of the genome. To avoid this, a sufficient number of origins must be activated, and they must be positioned close enough to ensure efficient replication within the allotted time (Boos and Ferreira 2019).

In addition to spatial regulation through replication origin positioning, higher eukaryotes have a temporal replication program (TRP) (Dimitrova and Gilbert 1999; Leonard and Mechali 2013). Due to limited availability of certain firing factors in somatic cells, not all origins can fire simultaneously (Wong et al. 2011; Tanaka and Araki 2011; Collart et al. 2013; Mantiero et al. 2011). To overcome this limitation and prevent large inter-origin distances, replication occurs in replication domains, which consist of clusters of replicons (Berezney, Dubey, and Huberman 2000; Nakamura, Morita, and Sato 1986). Replicons are groups of approximately five origins that fire in close vicinity. Replication domains appear as typical replication foci under a microscope (Sporbert et al. 2002). This domain-wise replication approach promotes efficient replication by minimizing isolated replication events. Isolated replication events, where replication forks lack opposing forks for termination, pose a high risk of stalling and collapsing, which may lead to single-stranded DNA (ssDNA) and potential genome instability. To prevent such events, adjacent replication domains in the genome replicate sequentially, resembling a domino-like model where replication progress from the initial domain to the adjacent domain (Sadoni et al. 2004; Maya-Mendoza et al. 2010; Sporbert et al. 2002). Timing transition regions (TTRs) serve as boundaries between adjacent early and late replication domains. These TTRs are replicated in a unidirectional manner, aligning with the two outermost forks moving out of their respective domains (Berezney, Dubey, and Huberman 2000; Boos and Ferreira 2019).

This domino-like model here is highly simplified and raises many open questions. What are the mechanisms to determine the timing of the first replication domain (the first domino)? How is the spreading of the sequential replication events achieved and blocked at TTRs? Additionally, chromatin processes and various parameters seem to influence the timing of replication. It has been shown that euchromatin regions that are transcriptionally active tend to replicate early in the S phase, while compact heterochromatin replicates later (Boos and Ferreira 2019; Rhind 2006; Yekezare, Gomez-Gonzalez, and Diffley 2013; Nakamura, Morita, and Sato 1986; Leonhardt et al. 2000). However, the majority of the molecular mechanisms and regulatory factors that enable these processes are still not well comprehended.

1.1.2. Cell cycle regulation of the initiation of DNA replication

Re-replication of the origins that already have been replicated might result in over-replication, and this might lead to genetic instability. In order to prevent this, the replication of DNA in eukaryotes is tightly controlled so that the replication of genomic DNA is restricted to occur exactly once per cell cycle. Two distinct steps in the initiation of DNA replication, origin

licensing and origin firing, play key roles to achieve this strict control (Diffley 1996; Diffley 2001; Sclafani and Holzen 2007).

During origin licensing, the inactive replicative helicase is loaded onto specific origins, forming a pre-replicative complex (pre-RC). The subsequent origin firing step involves the conversion of the pre-RCs into active replisomes. These two processes are temporally separated into distinct phases of the cell cycle to ensure that genome duplication occurs only once per cell cycle. Origin licensing exclusively takes place during mitotic exit and in the G1 phase of the cell cycle, while origin firing is strictly coupled to the S-phase (Diffley 1996; Diffley 2001; Sclafani and Holzen 2007; Boos and Ferreira 2019). The regulation of this temporal separation is achieved through the oscillating of CDK levels. In the late mitosis and G1 phase, relatively high levels of the anaphase-promoting complex/cyclosome (APC/C) activity lead to degradation of the S phase and G2/M phase cyclins, while the G1 cyclins are resistant for the APC/C-mediated degradation (Siddiqui, On, and Diffley 2013). These low S-CDK levels allow origin licensing but prevent their firing in G1 phase (Figure 1). During the transition from G1 to S phase, Cdh1, the adaptor of APC/C, is phosphorylated by G1-CDK, resulting in inactivation of APC/C and subsequent increase in the levels of S and G2/M phase cyclins (Peters 2002) (Figure 1). In S phase, high S-CDK levels inhibit origin licensing, but high S-CDK levels are required for origin firing (Diffley 1996; Diffley 2001; Siddiqui, On, and Diffley 2013; Tanaka and Araki 2010)**.** This CDK dependency strictly couples origin firing to the S phase. In addition to CDKs, the coupling of origin firing to the S phase also relies on another cell cycle kinase called Dbf4-dependent kinase (DDK), which includes the catalytic subunit Cdc7 and the regulatory subunit Dbf4. DDK is inactive in G1 phase due to the degradation of its regulatory subunit Dbf4 by APC/C. However, DDK accumulates in S phase fallowing inactivation of APC/C (Figure 1).

The temporal separation of origin licensing and origin firing, which is dependent on CDK and DDK activity, is conserved in both yeast and human cells (Sclafani and Holzen 2007).

Figure 1. DNA replication initiation is a two-step process
Origin licensing occurs during the G1 phase of the cell cycle when the activity of cyclin-dependent kinases (CDKs) and Dbf4-dependent kinase (DDK) is low, and the activity of the anaphase-promoting complex/cyclosome (APC/C) is high. As the cell progresses into the S phase, the activity of CDKs and DDK increases and remains elevated until the end of the M phase. In the M phase, the APC/C facilitates the transition into anaphase. Adapted from (Galanti and Pfander 2018).

1.1.3. Molecular functions of DNA replication initiation in yeast

The molecular mechanisms of replication initiation are well established in budding yeast, however poorly understood in metazoans. Therefore, the yeast model is used as a reference for investigating these processes in vertebrates. Genetic screening, cell biology, and biochemistry have identified the critical factors involved in origin firing and characterized their fundamental activities and regulations (Zaffar et al. 2022).

Origin licensing is the first step of replication initiation in yeast and involves the formation of the pre-RCs, which consists of an inactive double hexamer of the replicative Mcm2-7 helicase at the origin of DNA replication (Costa and Diffley 2022). In order to prevent premature replication, the Mcm2-7 helicase remains inactive in pre-RCs during the G1 phase. Mcm2-7 helicase is composed of ring-shaped hetero-hexamers, and two of the Mcm2-7 rings are positioned in a head-to-head configuration, resulting in their N-terminal domains being directed towards each other. (Evrin et al. 2009; Remus et al. 2009; Zaffar et al. 2022). The *in vitro* reconstitution studies showed that the process of licensing requires several essential replication factors, such as origin recognition complex (ORC), Mcm2-7-Cdt1, Cdc6 and ATP (Remus et al. 2009; Evrin et al. 2009; Zaffar et al. 2022). ORC is a protein complex consisting of six subunits, with five forming a crescent moon shape (Orc1-5) and Orc6 binding at the periphery. Orc1-5 contains an N-terminal AAA+-ATPase and a C-terminal DNA-binding domain (Costa and Diffley 2022). In yeast, the ORC binds specifically to the ARS consensus sequences (ACS), which are located at the central region of origins (Bell and Stillman 1992). Once ORC specifically binds to the replication origin, the AAA+-ATPase Cdc6 associates with ORC (Bell 2002). The licensing factor Cdt1 binds to the helicase, stabilizing the formation of an open Mcm2-7 ring, which facilitates the loading of the replicative helicase onto double-stranded DNA (Frigola et al. 2017). The complex of the Mcm2-7 heptamer and Cdt1 is then recruited to

the ORC/Cdc6 complex, depending on ATP hydrolysis by the AAA+-ATPase complexes ORC/Cdc6 (Ticau et al. 2015; Coster and Diffley 2017; Frigola et al. 2013; Kang, Warner, and Bell 2014; Siddiqui, On, and Diffley 2013). The Mcm2-7 hexamers are sequentially loaded to form a double hexamer structure(Remus et al. 2009). Once the Mcm2-7 helicase is loaded and Cdc6 and Cdt1 dissociate, the double hexamer is referred to as the pre-replicative complex (pre-RC) (Figure 3-Licensing). To prevent licensing during the S phase, CDK inhibits the essential loading factors ORC, Cdc6, Cdt1, and Mcm2-7 (Drury, Perkins, and Diffley 1997, 2000; Nguyen, Co, and Li 2001; Labib, Diffley, and Kearsey 1999; Elsasser et al. 1999).

The second step of the initiation, origin firing, occurs in S-phase, where CDK and DDK activities are high. In the origin firing step, the inactive double hexametric Mcm2-7 helicase is converted into two bi-directional mature replisomes. The process of helicase activation initiates through the step-wise assembly of the transient pre-initiation complex (pre-IC) on pre-RCs. The activation step requires elevated levels of two kinases, S-CDK and DDK (Zegerman and Diffley 2007). DDK phosphorylates Mcm4 and Mcm6 subunits of the Mcm2-7 preferentially in the pre-RC configuration (Deegan, Yeeles, and Diffley 2016; De Jesus-Kim et al. 2021). This phosphorylation recruits Sld3-Sld7 together with the helicase activator Cdc45 to the Mcm2-7 (Itou et al. 2014; Francis et al. 2009; Greiwe et al. 2022; Saleh et al. 2022). Sld2 and Sld3 are the only essential substrates of S-CDK for initiating DNA replication (Zegerman and Diffley 2007). Sld2 contains one essential S-CDK phosphorylation site, Thr84 (Masumoto et al. 2002), while Sld3 has two essential S-CDK phosphorylation sites, Thr600 and Ser622 (Zegerman and Diffley 2007; Tanaka et al. 2007). On the other hand, Dbp11 is a protein that possesses multiple pairs of BRCA1 C-terminal (BRCT) repeats, which enable it to bind to phospho-Sld3 and phospho-Sld2 at BRCT1/2 and BRCT3/4, respectively. This interaction leads to the formation of the Sld3/Sld7-Dpb11-Sld2 (SDS) complex, as depicted in Figure 2.

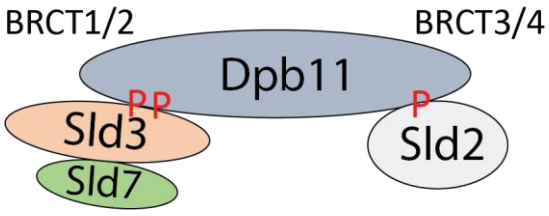

Figure 2. The SDS complex in yeast
Phosphorylation of Sld3 and Sld2 by CDK facilitates their interaction with two BRCT tandem domains present in Dpb11, leading to the assembly of the Sld3/Sld7-Dpb11-Sld2 (SDS) complex

Studies in yeast cells and *in vitro* showed that CDK phosphorylated-Sld2 binds to Dpb11 and may form the pre-loading complex (pre-LC) along with GINS and DNA polymerase epsilon (Polε), resulting in recruiting of these essential firing factors to the pre-RCs which are already associated with CDK phosphorylated-Sld3-Sld7-Cdc45 (Muramatsu et al. 2010; De Jesus-Kim et al. 2021). The resulting complex might be the molecular representation of the pre-initiation complex (pre-IC), which has been defined to form in CDK-dependent manner (Zou and Stillman 1998). Once the helicase activators Cdc45 and GINS are successfully delivered, the regulatory firing factors, including Sld3-Sld7, Sld2, and Dpb11, dissociate from the helicase, resulting in the formation of the Cdc45-Mcm2-7-GINS (CMG) complex (Gambus et al. 2006; Kanemaki and Labib 2006). Polε remains associated with the helicase and performs essential functions within replisomes during DNA synthesis (Figure 3-Firing).

Before elongation starts, the fallowing steps must be completed. (1) Separation of the Mcm2–7 double hexamers into single hexamers, (2origin DNA melting, (3) opening of both Mcm2–7 rings, likely at the Mcm2-5 gate, to extrude single DNA strands from their centers in opposite directions. (4) incorporation of Cdc45, GINS, and DNA polymerase epsilon with Mcm2–7 to activate its helicase activity, (5) the CMG helicases passing each other in the N-terminal direction to replicate the DNA bidirectionally during elongation (Figure 3-Elongation) (Douglas et al. 2018; Fu et al. 2011; Zaffar et al. 2022). *In vitro* biochemical reconstitution studies of yeast origin firing have demonstrated that the kinases CDK and DDK, along with the essential initiation factors Sld3, Sld7, Sld2, Dpb11, Mcm10, Mcm2-7, Cdc45, GINS, and Polε, are sufficient for replication origin firing (Yeeles et al. 2015). These factors constitute the core initiation factors involved in yeast replication.

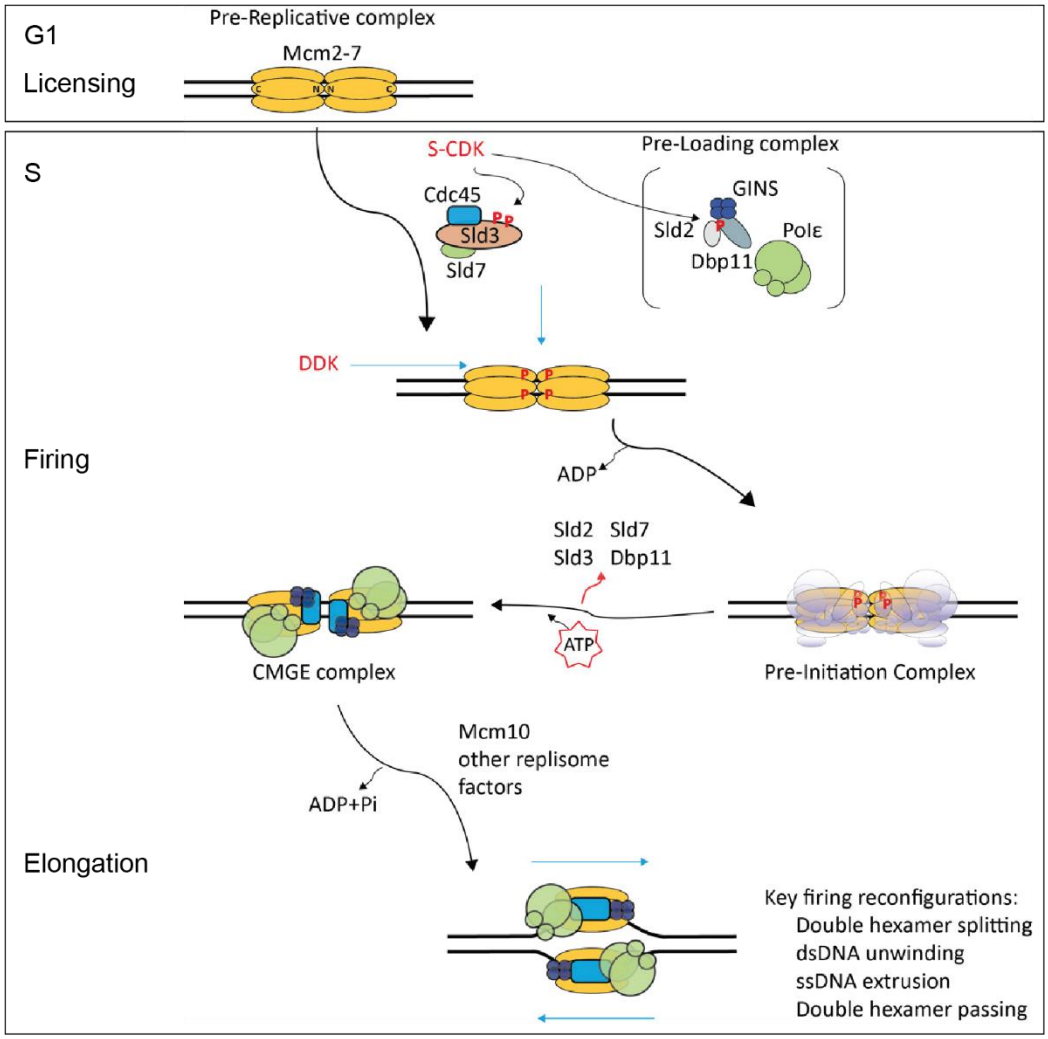

Figure 3. DNA replication initiation in yeast
Licensing: In the G1 phase, when CDK activity is low, the inactive Mcm2-7 replicative helicase is loaded onto the origin of replication. The recruitment of the helicase leads to the formation of the pre-replicative complex (pre-RC). **Firing:** Phosphorylation of the Mcm2-7 helicase by DDK facilitates the recruitment of Sld3-Sld7 and the helicase component Cdc45 to the pre-RC. During the G1-S transition, CDK activation promotes the phospho-dependent binding of Sld3 and Sld2 to Dpb11. Phosphorylated Sld3 is essential for the binding of the pre-loading complex (pre-LC), consisting of Sld2, Dpb11, GINS, and Polε, to the pre-RC through its interaction with Dpb11. These binding events lead to the formation of the pre-initiation complex (pre-IC). The addition of Mcm10 triggers ATPase-powered DNA unwinding by the MCM complex, allowing two Cdc45-Mcm2-7-GINS (CMG) complexes to intersect, establishing bidirectional replication forks. **Elongation:** The SDS complex dissociates from the origin of replication, while the helicase components Cdc45 and GINS, along with Mcm10, activate the helicase. This activation enables the ATP-dependent unwinding of DNA by the helicase. The key re-configurations to form bi-directional replication forks from pre-RCs: splitting of double Mcm2-7 hexamers into the single hexamers, unwinding of dsDNA, ssDNA extrusion and passing of the CMG helicases each other in the N-terminal direction. Adapted from (Zaffar et al. 2022).

1.2. The Sld3/Sld7-Dpb11-Sld2 (SDS) complex is the major regulatory hub of the replication initiation

The SDS complex is the major regulatory platform of the origin firing in yeast, and it plays a crucial role in regulating cell cycle progression and DNA damage checkpoints. It is governed by the control mechanisms that ensure the accurate and complete replication of the genome.

SDS complex plays a key role in the CDK and DDK dependent S-phase coupling of the origin firing. Moreover, recent studies have shown that in order to create a temporal gap between the origin licensing and origin firing, the firing factor Sld2 undergoes degradation during the M phase. This degradation provides robust separation of the licensing and origin firing and ensures that origin firing is still inhibited and cannot take place in the transition from low to high levels of CDK and DDK during the G1 phase. In this way, Sld2 prevents over replication and contributes to genome stability (Reusswig et al. 2016).

In addition to the origin firing, the SDS complex has a key function in the inhibition of origin firing upon DNA damage or other sources of replication stress. DNA damage hampers replisome progression and results in mutations and genomic re-arrangements. Therefore, origin firing must be tightly regulated under DNA damage conditions or other sources of replication stress (Reusswig et al. 2016; Zegerman and Diffley 2010). The formation of the SDS complex is the main target of the intra S phase checkpoint kinase (ISC) in the inhibition of the origin firing upon DNA damage conditions. This inhibition prevents replication in unfavourable conditions. In yeast, the ISC kinase Rad53 is activated when DNA damage occurs. Activated Rad53 phosphorylates Sld3, and this phosphorylation blocks the interaction with Dpb11, resulting in inhibition of origin firing (Zegerman and Diffley 2010). Additionally, the DDK pathway is inhibited by phosphorylation of Dbf4 by Rad53. A recent study revealed that DDK docks onto one MCM ring and phosphorylates the opposed ring. Rad53-phosphorylated Dbf4 prevents phosphorylation of the Mcm2-7 helicase, involving a blockage of DDK binding to the Mcm2-7 double hexamers (Greiwe et al. 2022). Consequently, upon DNA damage the ISC regulation of the CDK and DDK pathways are essential for origin firing control.

Chromatin structure has an impact on replication initiation, indicating the existence of specific regulatory mechanisms to meet the specific requirements of certain genomic regions for origin firing. Replication time is an example for this. A recent study has revealed an interaction between Sld3 and the acetyl transferase Esa1 at the silent HMLα locus. The Sld3-Esa1 interaction controls both origin firing time and transcriptional repression of the locus (Tanaka 2021; Zaffar et al. 2022). Generally, heterochromatin is replicated later in S-phase, while euchromatin is replicated earlier in S-phase. However, an exception is observed in pericentromeric heterochromatin, which supports robust sister chromatid cohesion and facilitates proper biorientation of sister kinetochores (Tanaka and Diffley 2002; Natsume et al. 2013). Pericentromeric heterochromatin replicates early, because DDK is accumulated at the pericentromeric origins. This accumulation of DDK is facilitated by the Ctf19 kinetochore complex in telophase. This promptly recruits Sld3-Sld7 to pericentromeric replication origins

and initiate replication early in S-phase (Natsume et al. 2013). Early replication of transcriptionally active euchromatin regions indicates that transcription factors can stimulate origin activity. It has been shown that the presence of Fkh1 and Fkh2 is crucial for the clustering of early origins and their interaction with the essential initiation factor Cdc45 during the G1 phase. This implies that Fkh1 and Fkh2 play a selective role in recruiting origins to emerging replication factories to induce early replication initiation in the S phase (Knott et al. 2012).

1.3. Initiation of DNA replication in vertebrates

In vertebrates, the exact molecular mechanisms of pre-RC and pre-IC formation have not been elucidated yet. However, it is known that all the core factors of pre-RC and pre-IC formation steps in yeast have orthologues in vertebrates, indicating that the basic mechanisms are conserved. Additionally, these orthologues in vertebrates have evolved vertebrate specific regions, presumably due to higher complexity of vertebrate genome requires more finely tuned regulation. This might explain why most of the orthologues contain vertebrate specific regions.

TopBP1 and Treslin (vertebrate orthologues of Dpb11 and Sld3, respectively) couple origin firing to the S phase in vertebrates, similar to yeast. In this process, Treslin binds to TopBP1 in a S-CDK phosphorylation-dependent manner, as Sld3-Dpb11 interaction in yeast. It was shown that S-CDK-phosphorylated Treslin binds to the equivalent phospho-binding domain of Dpb11, where phospho-Sld3 binds, in TopBP1, and this phospho-binding domain is essential for DNA replication (Kumagai, Shevchenko, and Dunphy 2011; Boos et al. 2011). Under DNA damage conditions or situations that cause DNA replication stress, Chk1,orthologue of Rad53, inhibits the firing of replication origins by interfering with the interaction between Treslin and TopBP1 (Boos et al. 2011; Kelly et al. 2022; Guo et al. 2015). It has been recently shown in the Boos laboratory that MTBP is the orthologue of Sld7, and it is essential for DNA replication (Kohler et al. 2019). MTBP forms a complex with Treslin, like Sld3 and Sld7 in yeast, and Treslin-MTBP-TopBP1 (TMT) form a stable complex in cells (Figure 4) (Kohler et al. 2019; Boos, Yekezare, and Diffley 2013; Ferreira et al. 2022).

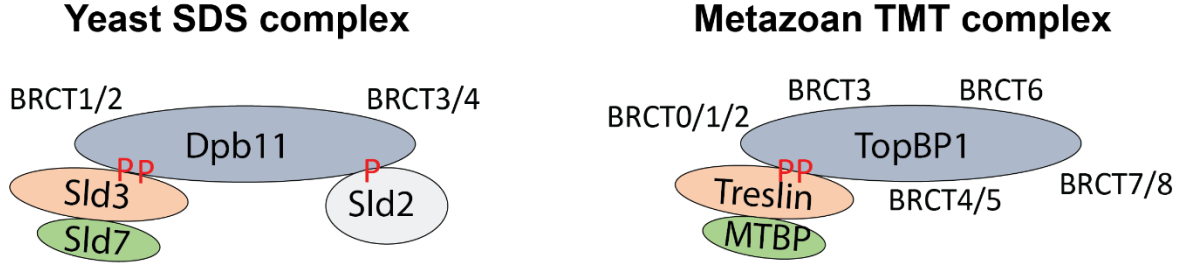

Figure 4. Yeast SDS and metazoan TMT complexes

In yeast, CDK-phosphorylated Sld3 and Sld2 binds to Dpb11 BRCT1/2 and BRCT3/4, respectively and form the SDS (Sld3-Dpb11-Sld2) complex. In metazoan, CDK phosphorylation of Treslin enables its phospho-dependent interaction with TopBP1-BRCT0/1/2 and forms the TMT (Treslin-MTBP-TopBP1) complex.

As mentioned above, the core factors of pre-RC and pre-IC formation steps are evolved to have vertebrate specific regions to carry out the vertebrate specific functions. One of these core factors is RecQ4, the orthologue of yeast Sld2. RecQ4 and Sld2 are essential for replication initiation. However, it is unlikely that phospho-dependent binding of RecQ4 to TopBP1 is conserved (Matsuno et al. 2006; Sangrithi et al. 2005). The studies in *Xenopus* egg extract have shown that Dpb11-BRCT3/4 is required for DNA replication due to its interaction with Sld2, by contrast, the equivalent TopBP1-BRCT4/5 domain is dispensable for DNA replication (Kumagai, Shevchenko, and Dunphy 2010; Tak et al. 2006). In addition to RecQ4, the TMT complex proteins have also evolved additional protein domains that serve specific functions in metazoans. siRNA studies in cultured human cells have revealed that MTBP is essential for DNA replication. However, studies in yeast have shown that despite the involvement of Sld7 in normal replication progression and resistance against low doses of hydroxyurea, it is not an essential factor (Boos, Yekezare, and Diffley 2013; Tanaka and Araki 2011; Kohler et al. 2019). A recent study in the Boos laboratory has revealed that MTBP is the target of at least three kinase pathways: Cdk8/19-cyclin C kinase, M-CDK, and Chk1/2. RNAi-replacement experiments of the endogenous MTBP with the RNAi resistant phospho-mimetic mutants of MTBP in the cultured human cells indicated that phosphorylation of MTBP at CDK consensus sites may promote origin firing, while phosphorylation of checkpoint consensus sites inhibits replication (Ferreira et al. 2021). Treslin and Sld3 share three homologous domains: the middle domain (M domain), the Sld3-Treslin domain, and the adjacent TopBP1/Dpb11 interaction domain. These shared domains in Treslin are flanked by vertebrate-specific N- and C-terminal domains. The RNAi-replacement experiments of Treslin demonstrated that the mutant Treslin containing only the shared three homologous domains was unable to rescue DNA replication in the siRNA treated cells. This indicates that the vertebrate-specific N- and C-terminal domains are required for replication in human cells (Ferreira et al. 2022). Similar to Treslin and MTBP, TopBP1 has vertebrate-specific regions. Since these regions are the subject of this project, they will be discussed in more detail in the following section.

As mentioned earlier, in metazoan, origin licensing and origin firing are strictly separated to prevent re-replication. This strict separation of origin licensing and origin firing is regulated by various mechanisms. One such mechanism is the restriction of loading the Mcm2-7 helicase to the G1 phase of the cell cycle. This regulation is similar to yeast. During the G1 phase, active

APC/C plays a role in inactivating key kinases involved in origin firing, S-CDK and DDK. APC/C achieves this by degrading S-cyclins and the regulatory subunit Dbf4. Additionally, in metazoan, the activity of Cdt1, an essential factor for the Mcm2-7 loading, is regulated by multiple mechanisms to prevent re-licensing in S phase. One of these mechanisms is the inhibition of geminin. Geminin, when bound to Cdt1, hampers the formation of pre-replication complexes (pre-RCs). However, when geminin is degraded, Cdt1 is released, allowing it to load the replicative helicase onto the DNA origins. This step is essential for the licensing of origins. Active APC/C also plays a role in the degradation of geminin in G1 phase. In S-phase, the low APC/C activity allows accumulation of geminin, thereby preventing re-licensing (Wohlschlegel et al. 2000; Tada et al. 2001; Siddiqui, On, and Diffley 2013). Another mechanism to regulate the Cdt1 activity to prevent re-licensing in S phase is the ubiquitin-mediated degradation of Cdt1 facilitated by CRL4 ubiquitin ligase (Havens and Walter 2011; Siddiqui, On, and Diffley 2013).

Taken together, the fundamental aspects of origin licensing and origin firing are conserved between yeast and vertebrates. Additionally, the orthologues of the core factors in vertebrates have vertebrate specific regions. The conservation of the basic mechanisms of the initiation between yeast and vertebrates makes yeast a “useful model” to investigate the molecular mechanisms of the initiation in vertebrates, while the vertebrate specific functions of the core factors ensure the complete replication of their complex genome.

1.3.1. TopBP1 and Dpb11 are orthologues with differences

TopBP1 is one of the major factors among pre-IC factors that integrates the signals from cellular pathways, like its yeast counterpart Dpb11. TopBP1 functions in DNA replication initiation, checkpoint signalling, DNA repair and influences transcriptional control.

TopBP1 acts as a scaffold to assemble protein complexes in a regulated way via its multiple BRCT repeats. TopBP1 contains nine BRCT repeats, and some of these repeats share homologous sequences with Dpb11 (Garcia, Furuya, and Carr 2005; Yamane, Kawabata, and Tsuruo 1997). In TopBP1, BRCT1-2 and BRCT4-5 are the equivalent of BRCT1-2 and BRCT3-4 in Dpb11 present, respectively. Despite the similarities, TopBP1 shows differences in domain structure compared to the domain structure of Dpb11. Dpb11 contains four BRCT domains, and no have equivalent of BRCT0, BRCT3 and BRCT7/8 domains of TopBP1 (Figure 5- white boxes) (Yamane, Kawabata, and Tsuruo 1997; Garcia, Furuya, and Carr 2005). TopBP1 binds to the S-CDK-phosphorylated Treslin and contributes to couple the origin firing to the S phase, like its yeast counterpart Dpb11 (Boos et al. 2011; Kumagai, Shevchenko, and Dunphy 2010, 2011). Another function of TopBP1 in DNA replication is recruitment of GINS to the Mcm2-7

helicase. As explained previously, GINS is the essential component of the active helicase. In yeast, GINS binds to the GINI domain between BRCT3 and BRCT4 in Dpb11 and it is recruited to the helicase by the pre-LC. In vertebrates, the existence of the pre-LC is unknown, but it was suggested that the similar GINI domain is present between BRCT3 and BRCT4 in TopBP1 (Tanaka et al. 2013). In this thesis, we characterized binding of GINS to TopBP1 in details.

In addition to their function in the initiation, TopBP1 and Dp11 have a conserved functional role in DNA damage signalling. In yeast, C-terminal part of Dpb11 serves as a ATR activator domain, and it binds to Mec1 to stimulate the checkpoint kinase activity of Mec1. The C-terminal part of TopBP1 also acts as a ATR activator domain like Dpb11. TopBP1 binds to ATR via its C-terminal domain and stimulate the activation of ATR under DNA damage conditions (Kumagai et al. 2006; Mordes et al. 2008). TopBP1 and Dpb11 share also a conserved functional role in DNA repair pathways. DNA repair protein Rad9 binds to BRCT1/2 repeats of Dpb11 in a phospho-dependent manner upon DNA double strand break (DSB) formation. TopBP1 binds to DNA damage response protein 53BP1 via its BRCT1/2 and BRCT5 domains in a phosphorylationr-dependent manner and promotes the repair of DNA double strand breaks (Pfander and Diffley 2011; Bigot et al. 2019).

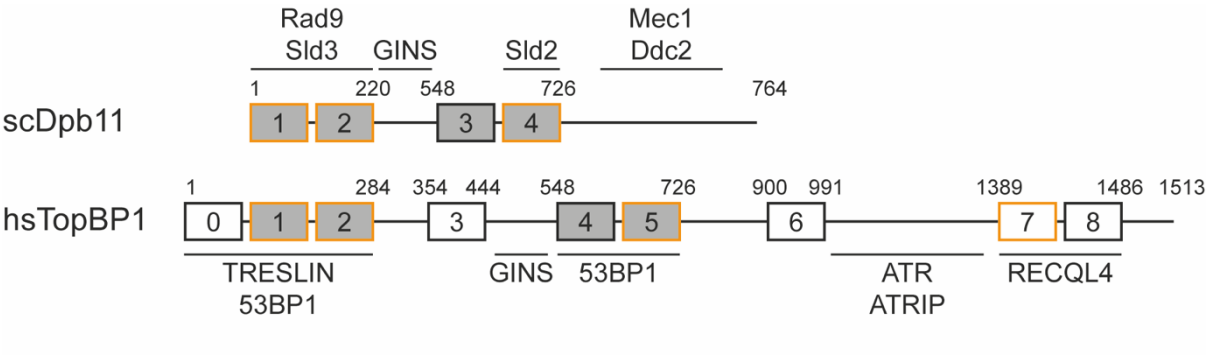

Figure 5. Scheme of yeast Dpb11 and metazoan TopBP1 interactors
The structural arrangement of Dpb11 in Saccharomyces cerevisiae and TopBP1 in Homo sapiens is represented in the domain model. The BRCT1/2 and BRCT3/4 domains of Dpb11, depicted as grey boxes, are conserved in TopBP1. The interaction between these domains and their respective interacting proteins is highlighted using orange colour for phosphorylation-dependent binding and black colour for phosphorylation-independent binding. (Adapted from Milena Parlak's PhD thesis "TopBP1 loads GINS onto the Metazoan Mcm2-7 Helicase during Replication Origin Firing").

The evolutionary adaptations of TopBP1 have enabled its interactions with various other proteins, including additional DSB repair proteins, as indicated in Table 1 (Table 1). Studies have demonstrated that TopBP1 associates with DSB repair proteins BRCA1, MDC1, BLM, and CIP2A (Adam et al. 2021; Greenberg et al. 2006; Sun et al. 2017; Wang, Gong, and Chen

2011). BRCA1 and TopBP1 have been found to interact with hyperphosphorylated FANCJ during DSB repair, contributing to both repair processes and activation of the S phase checkpoint (Sakasai et al. 2012). The association between MDC1 and TopBP1 facilitates the recruitment of TopBP1 to phosphorylated histone H2AX (γH2AX), which serves as a biomarker for DSB presence in mammalian cells (Georgoulis et al. 2017). The binding between the ATP-dependent RecQ-like helicase BLM and TopBP1 is crucial for maintaining genome stability. BLM plays a critical role in resolving intermediates of homologous recombination to prevent events such as sister chromatid exchange (SCE), which can lead to genetic crossover events. Impaired binding between BLM and TopBP1 has been associated with increased SCE and subsequent genome instability (Blackford et al. 2015; Sun et al. 2017). It has been shown that CIP21 directly interacts with TopBP1 and coordinates DNA damage-induced mitotic checkpoint and proliferation, indicating that the association of TopBP1 with the phosphatase CIP2A is also vital for maintaining genome stability, although the specific mechanisms remain to be fully understood (Adam et al. 2021; Laine et al. 2021).

Table 1 TopBP1 interacting proteins
(Adapted from Milena Parlak's PhD thesis "TopBP1 loads GINS onto the Metazoan Mcm2-7 Helicase during Replication Origin Firing")

BRCT repeats	**DNA replication**	**DNA repair**	**Cell cycle**	**Transkription**
0/1/2	Cdc45, Treslin-MTBP	BRCA1; MDC1; RAD9 (HUS1;RAD1); RHNO1; SMARCAD1	53BP1	TCOF1
Inter 3/4 (GINI)	GINS			
4/5		BLM; BRCA1	53BP1; MDC1	TCOF1
Inter 4/5		CIP2A		
6	CDC45	PARP1	FANCJ	E2F1; TOP2A; TOP2B
AAD		ATR; ATRIP	ATR	

7/8		BRCA1; PLK1	PHF8	TOP2A; TOP2B

1.3.2. GINS is a heterotetrameric complex

GINS forms the CMG complex along with Cdc45 and Mcm2-7, and the CMG complex acts as the core component of the replicative helicase (Yeeles et al. 2015). Cryo-EM studies suggested that Cdc45 and GINS are recruited to the N-tier of Mcm2-7, when GINS and Cdc45 engage with the helicase, double hexamer interface of the Mcm2-7 is disrupted. This allows the Mcm2-7 helicase to move along the single-stranded DNA (ssDNA) in the 5' to 3' direction, facilitating bidirectional replication(Costa et al. 2011; Yuan et al. 2016; Costa and Diffley 2022).

GINS is a heterotetrameric complex consisting of four subunits: Sld5, Psf1, Psf2, and Psf3. These four subunits bear a structural resemblance and are likely to derive from a single protein through gene duplication fallowed by domain swap. (Goswami et al. 2018; Jones et al. 2021; Kanemaki et al. 2003; Kubota et al. 2003; Marinsek et al. 2006). They share a common fold that is built-up of two regions: the α-helical A domain and the smaller β rich B domain. Sld5 and Psf1 have the A domain at the N-terminus and the B domain at the C-terminus, while these two regions are swapped in Psf2 and Psf3. The B domain of Psf1 shows sensitivity against proteolysis, suggesting that it is linked to the core of the complex via a flexible linker. Sld5 forms a heterodimer with Psf1 and Psf2, while it forms another heterodimer with Psf3. These two heterodimers form a heterotetramer in a 1:1:1:1 composition of each subunit (Carroni et al. 2017; MacNeill 2010).

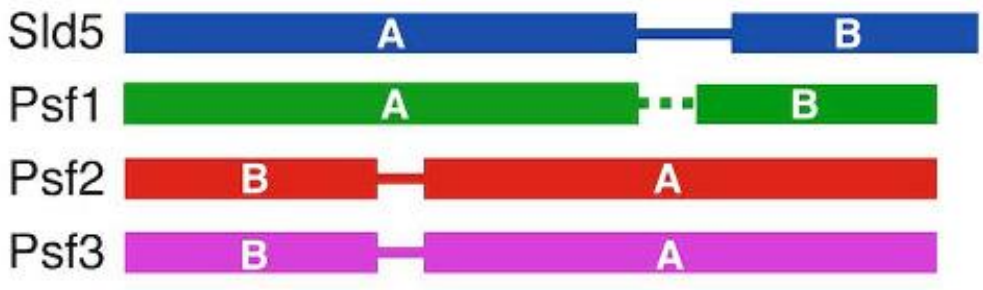

Figure 6. The schematic domain structure of the eukaryotic GINS heterotetramer
At the N-termini of Sld5 and Psf1, as well as the C-termini of Psf2 and Psf3, there is an α-helical A-domain. Conversely, the β-sheet rich B-domain is situated at the C-termini of Sld5 and Psf1, as well as the N-termini of Psf2 and Psf3. Adapted from (Carroni et al. 2017).

Cryo-EM and X-ray studies revealed that the human GINS complex dimerizes in solution. This may indicate that GINS double tetramers might be recruited to the double-hexameric MCM2-7 complexes at replication origins to form two active helicases with opposite polarities (Carroni et al. 2017). Cryo-EM studies also showed that Psf1, Sld5 and Psf3 are highly flexible, and they form stable heterotetrameric complex with Psf2 (Chang et al. 2007; Kamada et al. 2007). Considering the visible structure of the GINS tetramer, it has been proposed that these flexible domains of Sld5, Psf1, and Psf3 are situated close to each other. The coexistence of these flexible domains on the GINS surface suggests that they may form a binding surface for other replication proteins. *In vitro* reconstitution studies of human replisome propose that the B domain of Psf1 is flexible, when the CMG complex is formed, the B domain of Psf1 adopts to the discrete confirmation that allows the interaction with the N-terminus of PolE2 subunit of Pol ε to form the CMG-Polε complex (CMGE) (Chang et al. 2007; Jones et al. 2021).

2. Aim of the Study

To generate two faithful copies of the DNA, genome replication must be complete, accurate and exactly once during each cell cycle. Here, the initiation of DNA replication serves as a critical regulatory step. In yeast, *in vitro* reconstitution experiments have shown that Sld3-SLd7, Sld2, Dpb11 and DNA polymerase epsilon (Polε) are the core firing factors and sufficient with Mcm2-7, GINS and Cdc45 to support origin firing (Yeeles, Deegan et al. 2015, Yeeles, Janska et al. 2017). Origin firing includes the assembly and the activation of the CMG (Cdc45-Mcm2-7-GINS) complex (Gambus, Jones et al. 2006, Kanemaki and Labib 2006). In yeast, it has been shown that CDK-phosphorylated Sld2 and Dpb11 form the pre-loading complex (pre-LC) along with Polε and GINS, then GINS is recruited to the Mcm2-7 by the pre-LC, while the recruitment of Cdc45 is mediated by Sld3 (Muramatsu, Hirai et al. 2010, Itou, Muramatsu et al. 2014). In metazoan, it was proposed that Treslin mediates the recruitment of Cdc45 to the Mcm2-7, while the existence of pre-LC has not been shown yet. Previous yeast two-hybrid experiments loosely defined a GINS interaction domain (GINI domain) between TopBP1 BRCT3 and BRCT4, and this GINI domain is required for efficient DNA replication in eukaryotes (Tanaka et al. 2013). However, the molecular details of this interaction and how this interaction contributes to the recruitment of GINS to the Mcm2-7 helicase are poorly understood. Therefore, we aimed to characterize the molecular underpinnings of TopBP1-GINS interaction and provide insight how TopBP1-GINS interaction contributes replication origin firing in metazoan.

In this project, we utilized cryo-EM and structural prediction algorithms, along with *in vitro* biochemical binding assays and crosslinking mass spectrometry to elucidate how TopBP1 and GINS interact. We performed multiple amino acid sequence alignment of TopBP1 among vertebrates to identify the conserved GINS interaction domain, and we confirmed the results of this alignment using *in vitro* biochemical binding assays. We assess the requirement of TopBP1-GINS interaction in DNA replication. For this, we carried out the rescue experiment of DNA replication in *Xenopus* egg extract by adding-back of the recombinant TopBP1 to the endogenous TopBP1 depleted extract. Furthermore, we checked the requirement of TopBP1-GINS interaction in origin firing by mass spectrometry of chromatin-bound proteins. Our project proposes a potential model where TopBP1 recruits GINS to the Mcm2-7 helicase, and then it is recycled.

3. Results

3.1. Purification of pre-IC factors

Pre-IC assembly, which plays a crucial role in the CMG formation, represents the major regulatory step in replication origin firing. Therefore, our ultimate goal is to biochemically reconstitute the pre-IC formation step *in vitro* to investigate the detailed molecular mechanisms of pre-IC formation in vertebrates. For this purpose, we isolated the pre-RCs from *Xenopus* egg extract and purified the proteins and kinases involved in pre-IC formation from the insect cells and *E.coli*.

3.1.1. Purification of TopBP1 from insect cells

We intended to purify most of the pre-IC factors from insect cells. Since the insect cell culture was new in our lab, we first established how to work with the insect cells. Since TopBP1 is one of the important regulatory core factors among the pre-IC factors, we started the purification of pre-IC factors with TopBP11-766-strep (TopBP1-BRCT0-5-WT). It was cloned into the pLib plasmid with C-terminal strep-tag. Then, pLib-TopBP1-BRCT0-5-Strep was transformed into the E.coli-MultiBac cells to generate the bacmids. Sf9 insect cells were infected with these pLib-based bacmids. We assessed the infection ratio of the infected cells by utilizing the GFP tag on pLib. For this, we used automated-fluorescence counter. To efficiently infect the insect cells, a high virus titer is needed.

We first tested which virus stage is better to infect the cells to efficiently express the protein. For this, we checked the infection ratio by utilizing the GFP-tag on pLib and expression of the recombinant protein. Since the titer of the virus in super natant is relatively low after the first infection, the titer of the virus is increased by repeatedly infecting the cells using the supernatant of the infected cells. After V3 stage, the infection ratio was not increased any more. In addition to the infection ration, we also checked the expression of the protein. Since the infection ratio and the expression of the recombinant protein reached to maximum at V3 stage (GFP signal was more than 90%), we decided to over express TopBP1 at V3 stage for large scale expression.

TopBP1-BRCT0-5-Strep was expressed in Sf9 insect cells for 72 hours after infection with V2 stage viral supernatant. Lysates of these cells were loaded to the streptactin affinity column (StrepTrapHP-1ml column, Cytiva, 28907546) using an Äkta FPLC. The column was washed and then the bound protein was eluted with 2.5 mM desthiobiotin in the elution buffer. The coomassie stained SDS-PAGE gel in Figure 7 shows that the purified TopBP1 is relatively clean and the concentration of the most concentrated fractions is around 2 µg/µl (Figure 7). The yield is around 4 mg recombinant protein from 500 ml Sf9 insect cell culture.

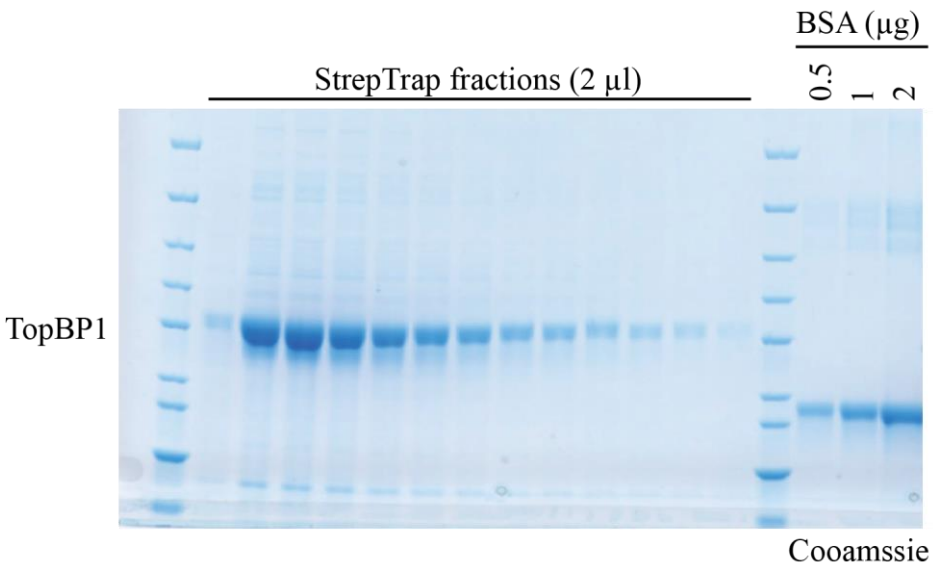

Figure 7. Purification of TopBP1-BRCT0-5-strep from insect cells
Cells Sf9 insect cells were infected with the baculovirus of TopBP1-BRCT0-5-strep, and the cells were grown as suspension culture at 27 °C for 72 hours. Then, the lysate was applied onto StrepTactin HP 1ml column (Cytiva, 28907546) on FPLC. The bound protein was eluted with 2.5 mM of desthiobiotin in the elution buffer.

3.1.2. Purification of GINS from insect cells

GINS was also purified from Sf9 insect cells. GINS is composed of four subunits: Sld5, Psf1, Psf2 and Psf3. To generate the pLib-based baculovirus of GINS, Sld5 subunit was cloned into the pLib vector with N-terminal 6xHis and 3xFlag-tag (pLib-6xHis-3xFlag-Sld5). The other GINS subunits, Psf1, Psf2 and Psf3, were separately cloned into the untagged pLib vector. 1 liter Sf9 insect cells were co-infected with all four pLib based GINS-baculoviruses and cultured for 72 h. The cell lysate was used for purification of His-Flag-Sld5 using Ni-NTA agarose beads, and the bound protein was eluted from the beads with 250 mM of imidazole in the elution buffer. Coomassie stained-SDS-PAGE showed that all four GINS subunits were eluted from the beads together, indicating that they were in a complex (Figure 8A). We determined which protein was which subunit by western blotting.

Since the purified GINS complex was contaminated with non-specifically co-purified proteins (many other bands) after Ni-NTA step (Figure 8A), the eluates were pooled and applied onto the cation ex-change column on FPLC (Figure 8B), and followed by size exclusion chromatography (Figure 8C). After size exclusion chromatography, SDS-PAGE and Coomassie staining showed that the purified GINS complex was relatively clean, and the subunits formed a stoichiometric complex. The concentration of the most concentrated fractions were roughly 250 ng/µl. The yield was between 750 ng and 1 mg protein from 1 liter insect cells.

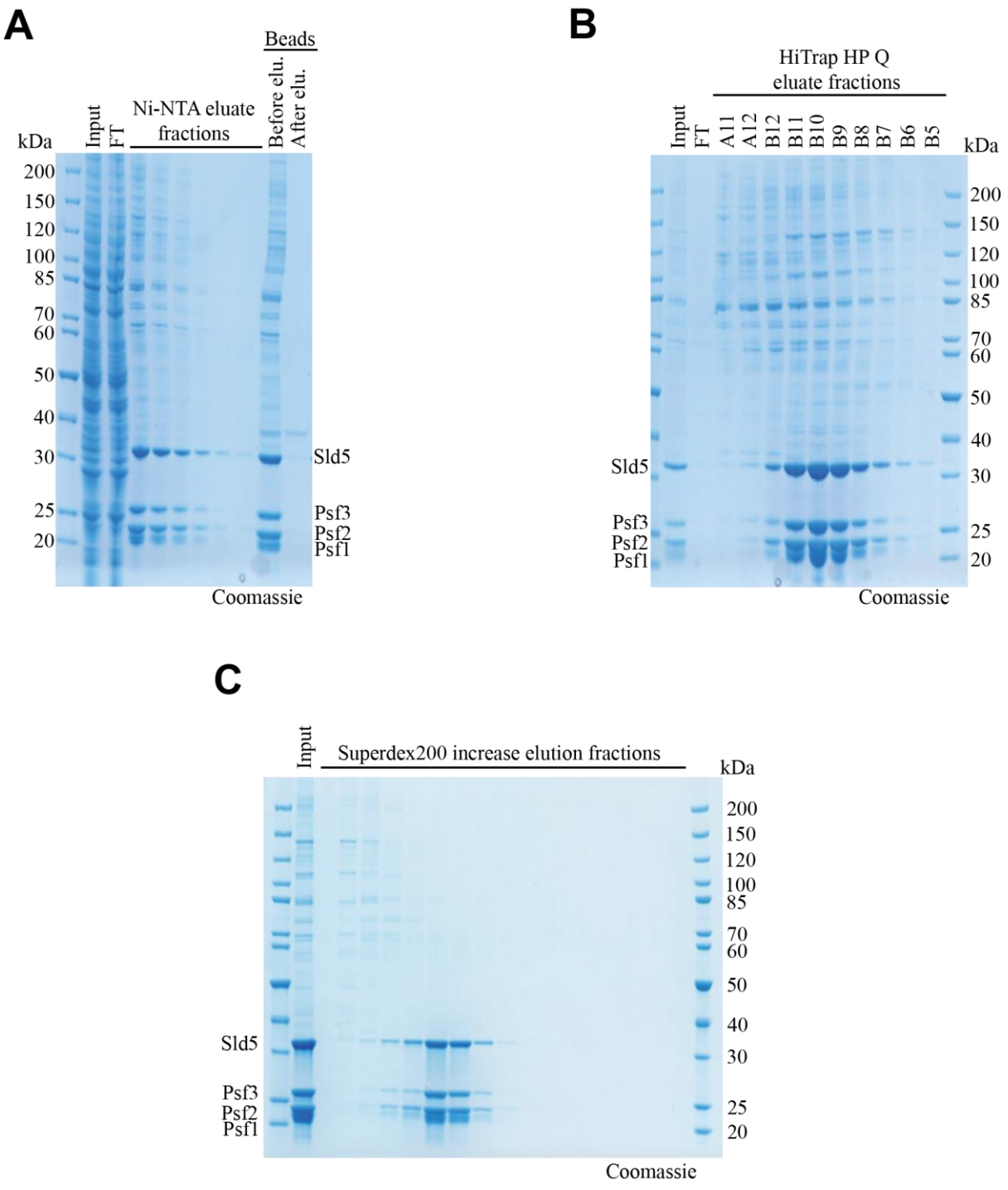

Figure 8. Purification of GINS from insect cells
Sf9 insect cells were co-infected with the individual baculoviruses of Psf1, Psf2, Psf3 and 6xHis-3xFlag-Sld5, and they were grown as suspension culture at 27 °C for 72 hours. **A)** The lysate was first incubated with Ni-NTA beads, and then the bound protein was eluted from the beads using 250 mM imidazole in the elution buffer. Each fraction was 2ml, and 3 µl of each fraction was loaded for the SDS-PAGE analysis. **B)** The imidazole eluates were pooled and applied onto an HiTrap HP Q anion exchange column (Cytiva, 17115301). The bound protein was eluted from the column with the linear gradient of NaCl (150 mM to 1 M). Each fraction was 500 µl, and 3 µl of each was loaded for the SDS-PAGE analysis. **C)** Peak fractions after the anion ex-change column including GINS were pooled and loaded onto Superdex200 increase gel filtration column (Cytiva, 28-9909-44). Each fraction was 1ml and loaded 5 µl for SDS-PAGE.

3.1.3. Purification of other pre-IC factors

In addition to TopBP1 and GINS, we purified all other pre-IC factors of which the orthologues in yeast have been shown to be required and sufficient to support DNA replication *in vitro*

(Yeeles et al. 2015). These proteins are Treslin-MTBP, DNA Pol ε, Cdc45, RecQ4, DDK, CDK, TopBP1 and GINS. Because these proteins are less important for this thesis, I will describe these purifications only briefly.

6xHis-Treslin1-1258 and MTBP-strep was purified as a complex from Sf9 insect cells co-infected with individual baculovirus of 6xHis-Treslin1-1258 and MTBP-strep in two steps using streptactin affinity beads and size exclusion chromatography (Figure 9A). DNA Polymerase ε (Polε) was purified as a complex of 6xHis-3xFlag-PolE11263-2287 and PolE2 from insect cells. Polε is consists of four subunits, but C-terminal part of PolE1 (PolE11263-2287) and PolE2 subunits are sufficient to support DNA replication, therefore we decided to purify only these two subunits. We purified Polε in 3 steps using metal-ion affinity column, cation exchange chromatography and size exclusion chromatography (Figure 9B). Cdc45-6xHis was purified from *E.coli* in collaboration with our M.Sc. student Yannik Glahn using Ni-NTA agarose beads (Figure 9C). RecQ4-strep was purified from insect cells using streptactin affinity column (Figure 9D). DDK (GST-Cdc7 and Dbf4) was purified from *E.coli* using glutathione beads (the construct was provided by the Santocanale lab) (Figure 9E).

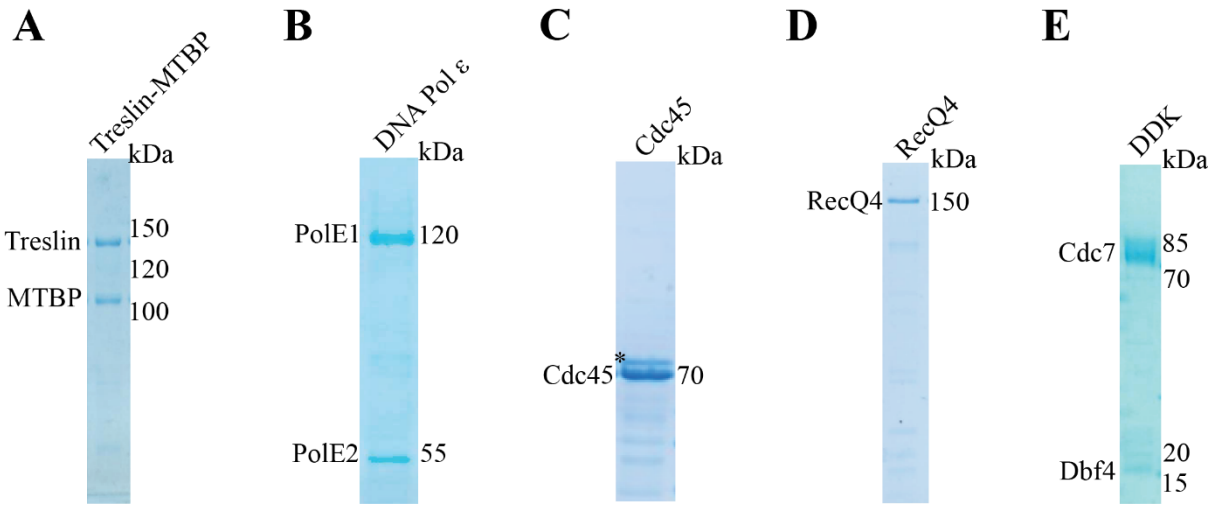

Figure 9. Purification of the rest of the preIC factors
A) Insect cells were co-infected with 6xHis-Treslin11-1258 and MTBP-strep, and the lysate was first incubated with streptactin agarose beads and followed by size exclusion chromatography using Superose6 column. **B)** Insect cells were coinfected with 6xHis-3xFlag-PolE11263-2287 and PolE2, and then the lysate applied onto the metal ion affinity chromatography, followed by cation exchange chromatography and finally fallowed by size exclusion chromatography. **C)** Cdc45-6His was expressed in E.coli at 20 °C for O/N, and then the lysate incubated with Ni-NTA beads. The bound protein was eluted with 250 mM imidazole in the elution buffer. (By Yannik Glahn) **D)** RecQ4-strep was expressed in insect cells for 72 hours, and then the lysate was loaded onto the strep-tag affinity column. **E)** GST-Cdc7/Dbf4 bacterial construct was provided by Santocanale lab. The construct was expressed in E.coli at 20°C for O/N, and the cells were pelleted and the lysate was incubated with glutathione beads. The bound protein was eluted by using the precision protease.

3.2. First attempts towards reconstitution of pre-LC *in vitro*

Next, we aimed to biochemically reconstitute pre-LC *in vitro* using the recombinant proteins. In yeast, the pre-LC is composed of Dpb11^{TopBP1}, Sld2^{RecQ4}, GINS and DNA Polymerase ε (Polε), and the formation of the complex is dependent on CDK activity (Muramatsu et al. 2010) (Figure 10). We aimed at reconstitution of pre-LC *in vitro* to investigate vertebrate pre-LC interactions predicted from the known pre-LC factors in yeast.

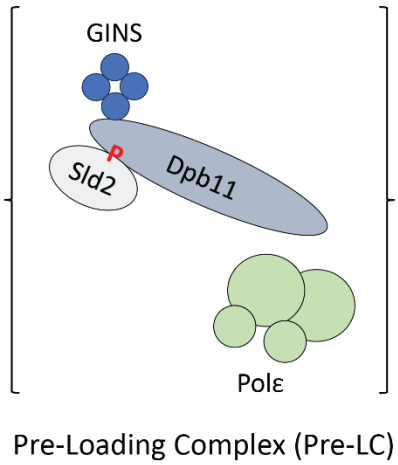

Figure 10. Pre-Loading Complex in yeast
In yeast, CDK-phosphorylated-Sld2 and GINS bind to Dpb11. However, it is not known how Polε interacts with the other pre-LC factors. Since the structure of pre-LC is not known yet, it is here depicted in brackets.

I first attempted to generate pre-LC *in vitro* using purified TopBP1, RecQ4, Pol ε and GINS. For this, the purified RecQ4-strep was immobilized onto the streptactin beads, and subsequently treated with CDK, CDK buffer or Lambda phosphatase (PPase). As a pull-down control, the beads were not coupled with the RecQ4. After the treatment, the beads were washed, and purified TopBP1, GINS and Pol ε were added and incubated for 1 hour at 4 °C. The unbound proteins were washed away from the beads, and the complex formation was analysed by silver staining (Figure 11A-I). Figure 11A-I shows that TopBP1 and Pol ε bind to the RecQ4 indicating that they might together form a complex with RecQ4. The formation of this complex is not dependent on CDK, because the proteins bound to the CDK treated, CDK buffer treated and PPase treated RecQ4 similarly. Since we could not detect binding of GINS to the RecQ4 by the silver staining, we analysed the same samples with anti-Sld5 western blot (Figure 11A-II). According to the western blot, the signal for RecQ4 pulldown was stronger than the control pulldown, but it was still not clear specific signal. Therefore, the binding of GINS with the RecQ4 was difficult to judge.

I next characterised the binding of Pol ε to RecQ4 *in vitro* closer. In yeast, C-terminal part of $Dpb2^{PolE1}$ includes the inactive DNA polymerase fold, and it is sufficient to support DNA replication *in vitro* (Goswami et al. 2018). Since the full length PolE1 was relatively big (~250 kDa), we decided to purify the Pol ε as a complex of PolE1-C, PolE11263-2287, and full-length PolE2. We also purified Pol ε with the PolE1-C short, 1918-2287. To check the interaction between RecQ4 and Pol ε, the RecQ4-strep was immobilized on the streptactin beads, and then the beads were incubated with 2 different complexes of Pol ε, PolE1-C/PolE2 or PolE1-C short/PolE2. Figure 11B shows that Pol ε bound to RecQ4, and shorter fragment of PolE1 makes the interaction weaker, suggesting that the C-terminal part of PolE1 involves in binding to RecQ4 (Figure 11B).

I moved on to test whether TopBP1 interacts with Pol ε *in vitro*. Although TopBP1-BRCT 0/1/2 are homologous to Dpbp11-BRCT1/2 and TopBP1-BRCT4/5 are homologous to Dpb11-BRCT3/4, BRCT3 exists as an metazoan-specific BRCT domain between BRCT0/1/2 and BRCT4/5 in TopBP1 (Tanaka et al. 2013). In addition to test if the TopBP1-Pol ε complex exist, we also wanted to test if this BRCT3 has a role in the interaction with Pol ε. To check the interaction, Dynabeads protein G were coupled with anti-TopBP1 antibody, and then TopBP1-BRCT0-5-WT or TopBP1-BRCT0-5-ΔBRCT3 was immobilized to the beads and incubated with Pol ε. I first ran silver stained-SDS-PAGE gels to analyse the pulldown (Figure 11C-I). Since the silver stained-SDS-PAGE gel did not give clear result, the pulldown was also analysed by anti-PolE1 western blot (Figure 11C-II). The western blot analysis of the pulldown suggested that TopBP1 interacts with Pol ε, and BRCT3 domain of TopBP1 is not required for this interaction.

TopBP1-GINS interaction previously has been shown by yeast two hybrid screening (Tanaka et al., 2013). To confirm this interaction *in vitro* with the purified proteins, GINS was immobilized to beads by exploiting the 3xFlag tag on Sld5 subunit, and then incubated with TopBP1-BRCT0-5-strep. The silver-stained-SDS-PAGE gel shows that TopBP1 binds to GINS (Figure 11D). We decided to further characterized this interaction, because we wanted understand better how GINS and TopBP1 interact and how this interaction contributes to the recruitment of GINS to the Mm2-7. However, the other detected interactions are also interesting, but need further characterization for future research.

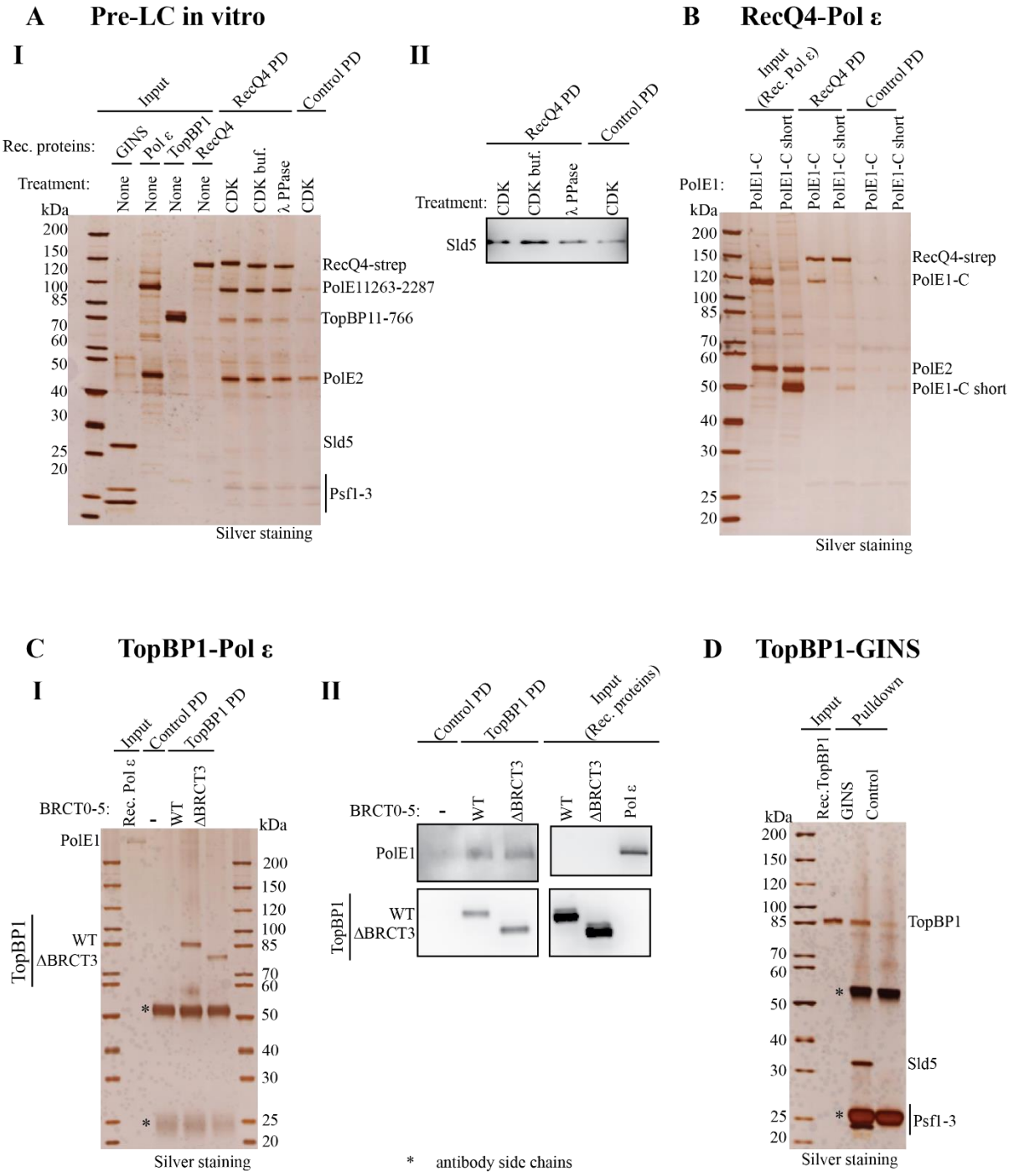

Figure 11. Reconstitution of Pre-LC *in vitro*
A) Immobilized recombinant RecQ4-strep was used to pulldown GINS, Pol ε and TopBP1. Pulldown was analyzed by silver-stained SDS gel (I) and anti-Sld5 western blot (II). **B)** Pol ε binds to RecQ4 in vitro. Immobilized recombinant RecQL4-strep was used to pulldown Pol ε. Pulldown was analyzed by silver-stained SDS gel. **C)** TopBP1 interacts with Pol ε. The recombinant TopBP1 was immobilized to the pre-coupled beads with anti-TopBP1 (TopBP11-360, self-made) antibody and used to pulldown Pol ε. Pulldown was analyzed by Silver stained SDS gel (I) or anti-TopBP1 and anti-Flag (6xHis-3xFlag-PolE1) western blot (II). **D)** TopBP1 interacts with GINS. GINS was immobilized to the magnetic anti-Flag beads, and then incubated with TopBP1. The pulldown was analyzed with silver-stained SDS gel

3.3. Characterization of TopBP1-GINS interaction

3.3.1. TopBP1 interacts with GINS *in vivo* and *in vitro*

We next analysed the TopBP1-GINS complex using analytical size exclusion chromatography (SEC) (in collaboration with Matthew Day). When TopBP1-BRCT0-5 and GINS were combined, they eluted from the column earlier in comparison to the individual running of the proteins during SEC (Figure 12A). This indicates that the proteins bind to each other and form a stable complex in solution. SDS-PAGE analysis of the elution fractions clearly shows the stoichiometric co-elution of TopBP1 with GINS (Figure 12B). These results showed that TopBP1 and GINS form a stable complex *in vitro*, and TopBP1-BRCT0-5 is sufficient to form this complex.

After confirmation of the TopBP1-GINS interaction *in vitro*, we checked whether this interaction occurs in human cells. For this purpose, HEK-293T cells were transiently transfected with 6xMyc-TopBP11-766 (TopBP1-BRCT0-5), and anti-Myc-tag immunoprecipitation (IP) from the transfected cell lysates was carried out using magnetic anti-Myc beads. The IP from the transfected cells showed a weak but specific signal for the GINS subunit Sld5 (Figure 12C). In addition to the anti-Myc IP from the transfected cells, we could detect TopBP1-GINS interaction in human cells using proximity biotinylation experiments in cooperation with Milena Parlak (data not shown). Taken together, these results show that TopBP1-GINS interaction occurs in human cells as well, and TopBP1-BRCT0-5 is sufficient to interact with GINS *in vitro* and *in vivo*.

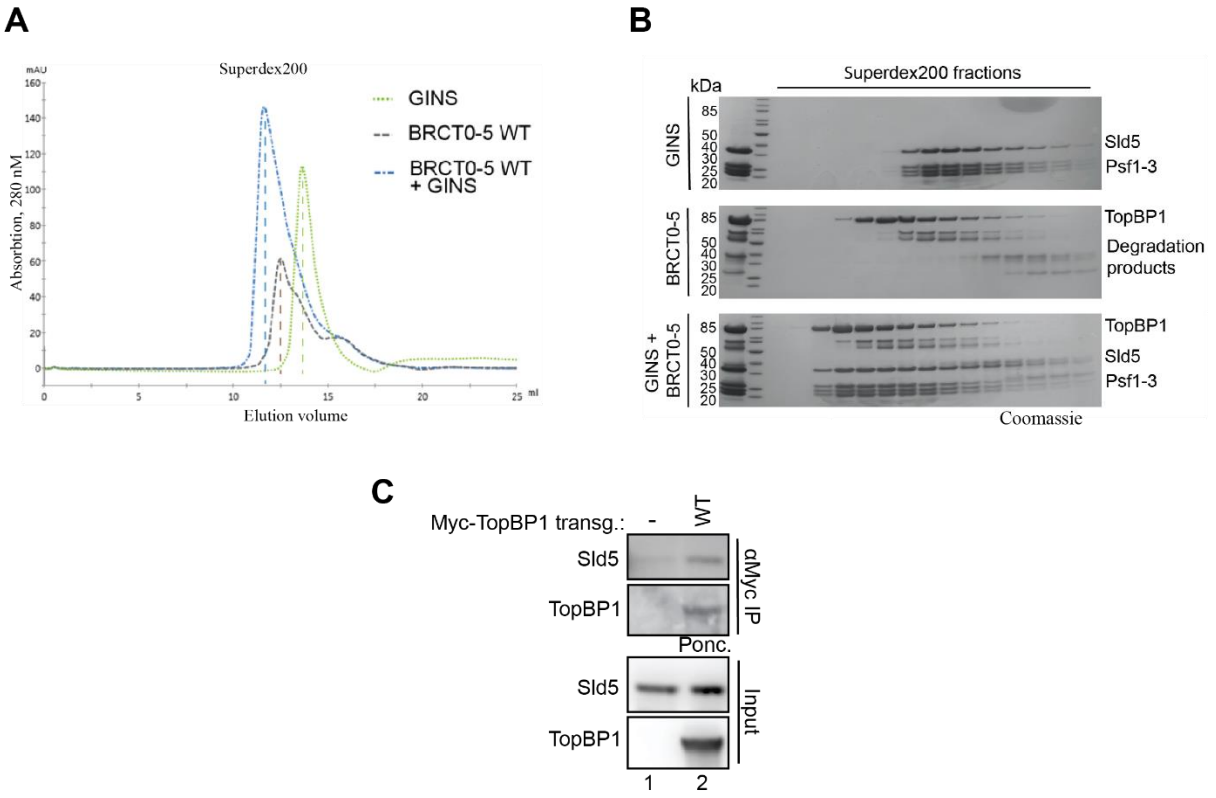

Figure 12. TopBP1 and GINS forms stable complex *in vivo* and *in vitro*
Recombinant TopBP1-BRCT0-5 and GINS were incubated before SEC, and Superdex200 column was used to run the complex or individual proteins. **A)** Chromatograms of SEC runs of TopBP1 and GINS alone and in combination (Experiment by Matthew Day) **B)** Coomassie-stained SDS gel of fractions from the SEC runs shown in A. **C)** TopBP1 interacts with GINS in human cells. Immunoblots showing immunoprecipitation of 6Myc-TEV2-TopBP1-BRCT0-5 from transiently transfected HEK-293T lysates using anti-Myc antibodies. Untransfected cell lysates were used for control IPs. Immunoprecipitated TopBP1 was detected using Ponceau (Ponc.) staining. A weak but specific co-IP of Sld5 was detectable.

3.3.2. TopBP1 requires the BRCT4/5, but not the BRCT0-2 and BRCT3 domains to bind GINS

We next utilized deletion and mutation analysis to determine which domain of TopBP1 is required to bind to GINS. Since the previous yeast two-hybrid experiments suggested that the GINI domain should be located between BRCT3 and BRCT4 (Tanaka et al. 2013), we did not expect that deletion of the Treslin binding module BRCT0-2 is required for the GINS interaction. In order test that, BRCT0-2 domain was deleted from TopBP1 (TopBP1-ΔBRCT0-2), and the interaction with GINS was tested by using analytical SEC (Fig 13A) (In cooperation with Matthew Day). The combining of TopBP1-ΔBRCT0-2 and GINS resulted in earlier elution from the column, while the individual runs of the proteins were eluted later. This indicates that deletion of the BRCT0-2 did not affect the binding, and TopBP1 and GINS still can form stable complex.

We next checked the requirement of the TopBP1-BRCT3 and BRCT4-5 domains for binding to GINS. For this purpose, either TopBP1 deletion mutants lacking BRCT3 domain or BRCT4/5 domains were (TopBP1-ΔBRCT3 and TopBP1-ΔBRCT4/5 respectively) tested for binding to

recombinant GINS using the GINS pulldown assay (Figure 13B). TopBP1-ΔBRCT3 bound to GINS. Surprisingly, deletion of BRCT4/5 abolished binding to GINS. We concluded that TopBP1-BRCT4/5 may be an essential binding region for GINS.

We then decided to check whether the canonical phospho-binding pocket of BRCT5 domain is required for binding. Therefore, we mutated S654, K661 and K704 on the canonical phospho-binding pocket of BRCT5 domain to V, R and E, respectively (Bigot et al. 2019), and then purified the mutant protein, TopBP1-B5mut, from insect cells using strep-tag on C-terminus of the protein. TopBP1-B5mut purified very similarly as TopBP1-BRCT0-5-WT, suggesting that the mutations did not cause misfolding (Extended Figure 6). In order to confirm that the canonical phospho-binding site was inhibited in the TopBP1-B5mut, we tested whether it interacts with 53BP1. 53BP1 mainly binds to the canonical phosphorylation site on K704 in the BRCT5 domains of TopBP1 in a phosphorylation dependent manner (Bigot et al. 2019). To check binding to 53BP1, the streptactin agarose beads were first coupled with the recombinant TopBP1-B5mut, and then incubated with untrasfected HEK-293T cell lysate. Figure 13C shows that the TopBP1-B5mut does not bind to 53BP1, indicating that the phospho-binding site is inactive (Figure 13C). To test the effect of this mutation on binding to GINS, we used the same GINS pulldown assay in the previous experiments. TopBP1-B5mut bound to GINS similarly to TopBP1-BRCT0-5-WT, indicating that the canonical phospho-binding is not required for binding to GINS (Figure 13D).

These experiments showed that, TopBP1-BRCT4/5 was not able to bind to GINS. This was surprising, because a similar fragment of *Xenopus* TopBP1 was sufficient for interaction in the yeast two-hybrid experiments and rescued DNA replication in TopBP1-depleted *Xenopus* egg extracts (Tanaka et al. 2013). Taken together, BRCT0-2 and BRCT3 domains are not required to bind to GINS, but BRCT4/5 domain is required while the phospho-binding site on BRCT5 domain is not required.

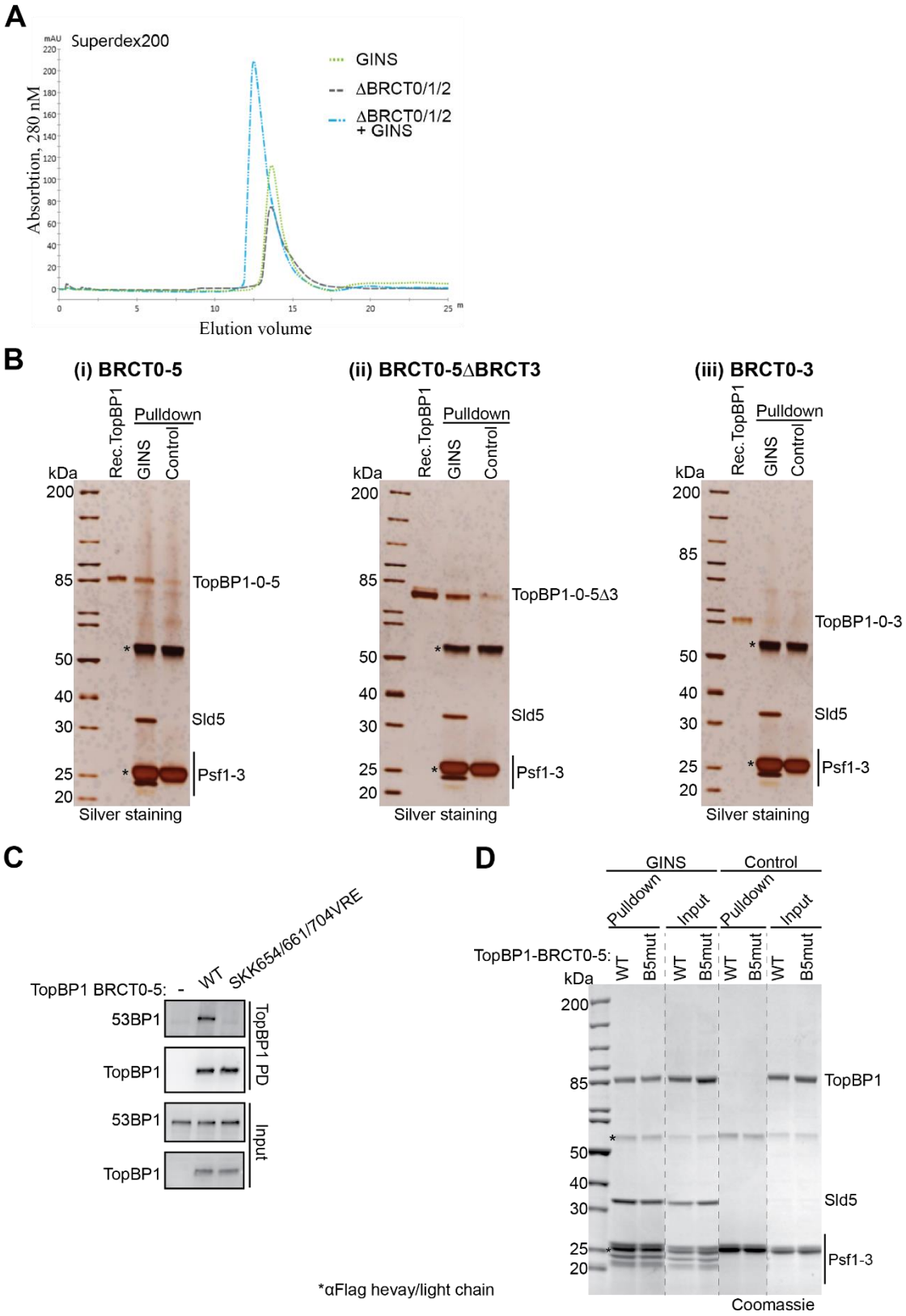

Figure 13. BRCT0-2 and BRCT3 are not required for binding to GINS, while BRCT4/5 is required
A) Chromatograms of SEC runs of TopBP1-ΔBRCT0-2 and GINS alone and in combination (by Matthew Day). **B)** GINS was immobilized to the magnetic anti-Flag beads and used to pulldown TopBP1. The pulldown was analyzed with silver-stained SDS gel. **C)** Immobilized recombinant GINS was used to pulldown TopBP1-BRCT0-5 or B5mut. The pulldown was analysed with Coomassie-stained SDS gel. **D)** TopBP1-B5mut was immobilized to the streptactin Sepharose beads and used to pulldown 53BP1 from non-transfected HEK-293T cells. The interaction was analyzed with anti-TopBP1 and anti-53BP1 western blots.

3.3.3. Cryo-EM structure of TopBP1-BRCT4/5 in complex with GINS

We next sought to uncover how TopBP1 interacts with the GINS complex. For this purpose, the peak fractions of the SEC run of TopBP1-BRCTΔ0-2 and GINS combination in Figure 13A were subjected to cryo-EM in a collaboration with Matthew Day. The resulting model showed that the arrangement of the two BRCT domains facilitates a direct contact between BRCT4 and the Psf1 subunit of GINS (Figure 14A). Unlike the standard BRCT fold, TopBP1-BRCT4 does not possess an alpha-helix between beta strands 3 and 4. This omitted helix creates a novel surface that helps in the interaction with Psf1. BRCT4 domain directly contacted the A domain of Psf1 close to where the B domain docks to the CMG helicase once GINS and Cdc45 have engaged with the MCM ring.

According to our cryo-EM model, Val590, Thr606 and Val610 are the amino acids that interact with the side chains of Trp92 and Ile97 in Psf1 (Figure 14B). To confirm these predictions, the amino acids in TopBP1 were mutated to glutamate, arginine and glutamate, respectively. The mutant protein (TopBP1-B4mut) was purified from Sf9 insect cells similarly to TopBP1-BRCT0-5-WT, suggesting stable protein folding (Extended Figure 8). To rule out whether the mutations on the BRCT4 domain effected the folding of the protein, we utilized the interaction of TopBP1 with 53BP1. In order to test the binding to 53BP1, streptactin beads were coupled with the recombinant TopBP1 proteins using the strep-tag on the C-terminus of the proteins. Subsequently, the pre-coupled beads were incubated with the lysate of non-transfected HEK-293T cells. The analysis of the pulldown of 53BP1 from the lysate showed that TopBP1-B4mut bound to 53BP1 similarly to TopBP1-BRCT0-5-WT, while TopBP1-ΔBRCT4/5 bound weakly (Extended Figure 9). Since TopBP1-BRCT0-5 contains both binding sites for 53BP1, explaining its stronger binding to 53BP1 compared to the TopBP1-BRCT-ΔBRCT4/5. We then tested whether the mutant protein binds to GINS in the GINS pulldown assay. TopBP1-B4mut was unable to bind GINS (Figure 14C). Binding was indistinguishable from ΔBRCT4/5.

We also confirmed the predictions of our cryo-EM model by mutating the opposite interaction surface of Psf1. For this, we mutating Ile97 in Psf1 to arginine (Psf1-I97R), and purified the mutant protein from the insect cells. The purified Psf1-I97R was capable to form GINS tetramers, indicating that the mutation did not alter the folding of the protein (Figure 14D). We used the GINS pulldown assay to test if Psf1-I97R binds to TopBP1-BRCT0-5-WT. GINS pulldown assay demonstrated that Psf1-I97R bound to TopBP1-BRCT0-5 poorly (Figure 14E), indicating that Psf1-I97 involves in the interaction. Taken together, we identified a GINS interaction site on BRCT4 domain of TopBP1, which had not been described previously, and

TopBP1-VTV590/606/610 in BRCT4 forms an interaction surface involving T92 and I97 on the Psf1 side.

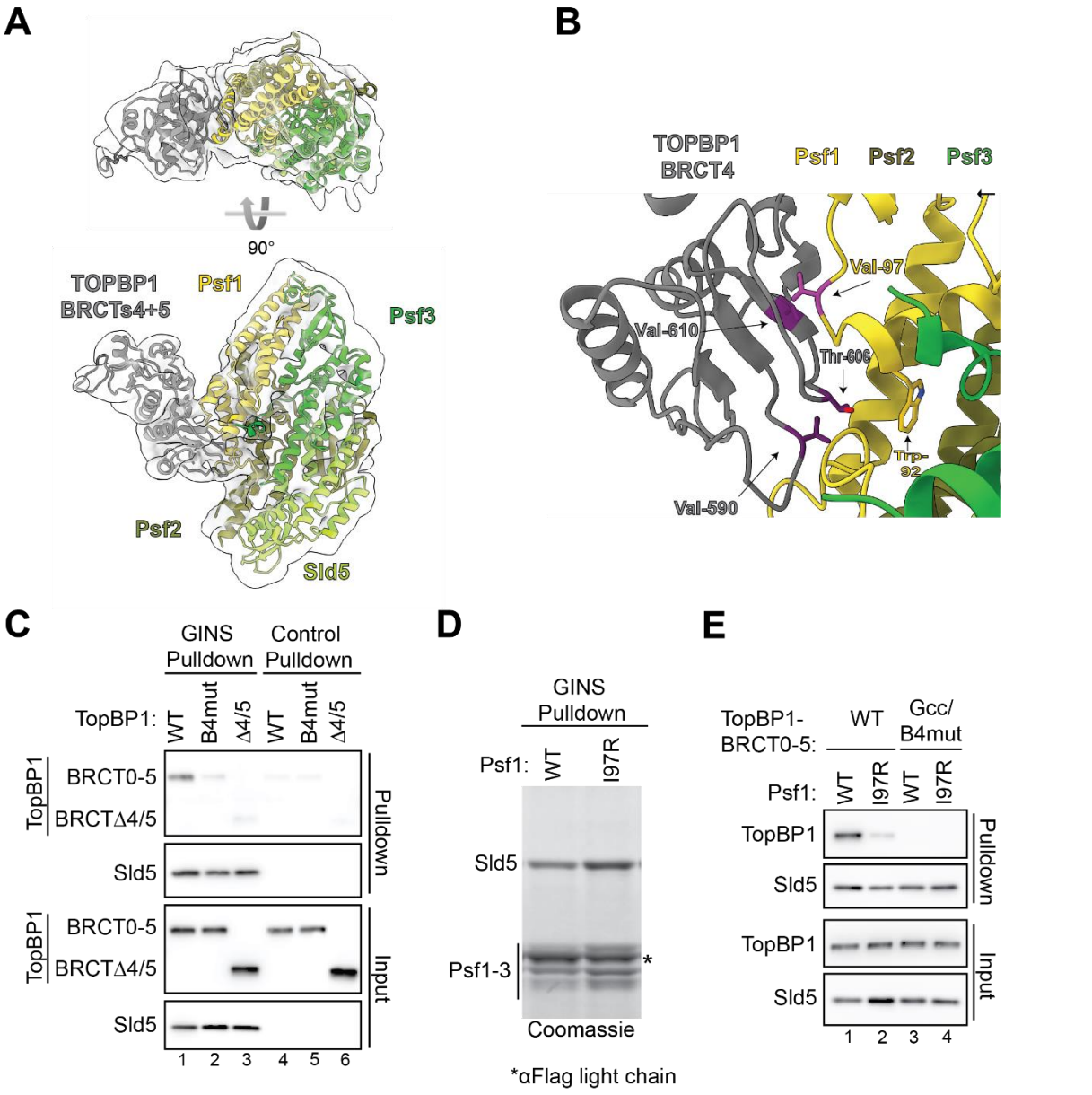

Figure 14. Interaction between GINS and TopBP1-BRCT4/5
A) Cryo-EM structure of the GINS-TopBP1-BRCT4/5 complex produced by using the peak fractions from the SEC run of GINS-TopBP1-BRCT3-5 combination in Figure 12A (By Matthew Day). **B)** Details of the interaction between BRCT4 and PSF1. The residues depicted in stick representation appear vital for the interface. Mutations to break the interaction are shown as pink and purple in Psf1-I97R (valine in the main variant shown here) and TopBP1-B4mut, respectively. **C)** Immobilized recombinant GINS was used to pulldown of indicated recombinant TopBP1-strep versions. The pulldown was analyzed by immunoblotting. **D)** GINS tetramer formation upon the mutation on Psf1 was tested by immobilizing the recombinant GINS onto the beads. Tetramer formation was analysed by Coomassie staining. **E)** Pulldown of TopBP-BRCT0-5 using beads-immobilized WT GINS or Psf1-I97R. The pulldown was analysed by immunoblotting.

3.3.4. TopBP1 requires the conserved core of the GINI region for GINS binding

We then addressed the role of the TopBP1-GINI domain in GINS binding. The GINI region, had been suggested by yeast two-hybrid experiments, is located between TopBP1-BRCT and BRCT4, but the interaction was not characterized in more detail (Tanaka et al. 2013). Unfortunately, the GINI region was not resolved in our initial cryo-EM model. We generated a multiple amino acid sequence alignment of the inter BRCT3 and BRCT4 among vertebrate species using T-Coffee algorithm (Figure 15A). Comparison of the amino acid sequences revealed that the region between Glu487 and Tyr494 almost completely consists of identical amino acids. We named this region the GINI center core (Gcc) and mutated it to investigate its effect in GINS binding. In addition to the TopBP1-Gcc mutant, we also mutated other regions that includes conserved amino acids. These are GINI core (Gcore) and Regions I-III (RI-III) (Figure 15A). Then, the mutant TopBP1 proteins with strep-tag were purified from insect cells. The purity and the concentration of the recombinant mutant TopBP1 proteins were very similar to the WT TopBP1 (Extended Figure S7). We confirmed that TopBP1-Gcc binds to 53BP1 similar to TopBP1-BRCT0-5-WT, indicating that the mutation did not change the protein folding (Extended Figure S9). GINS pulldown experiments revealed that TopBP1-Gcc and Gcore were severely compromised in its ability to bind GINS, whereas RI-III could still bind to GINS (Figure 15B). Taken together, these findings show that the GINI core region that is located between Asp487 and Tyr494 is essential for the GINS interaction.

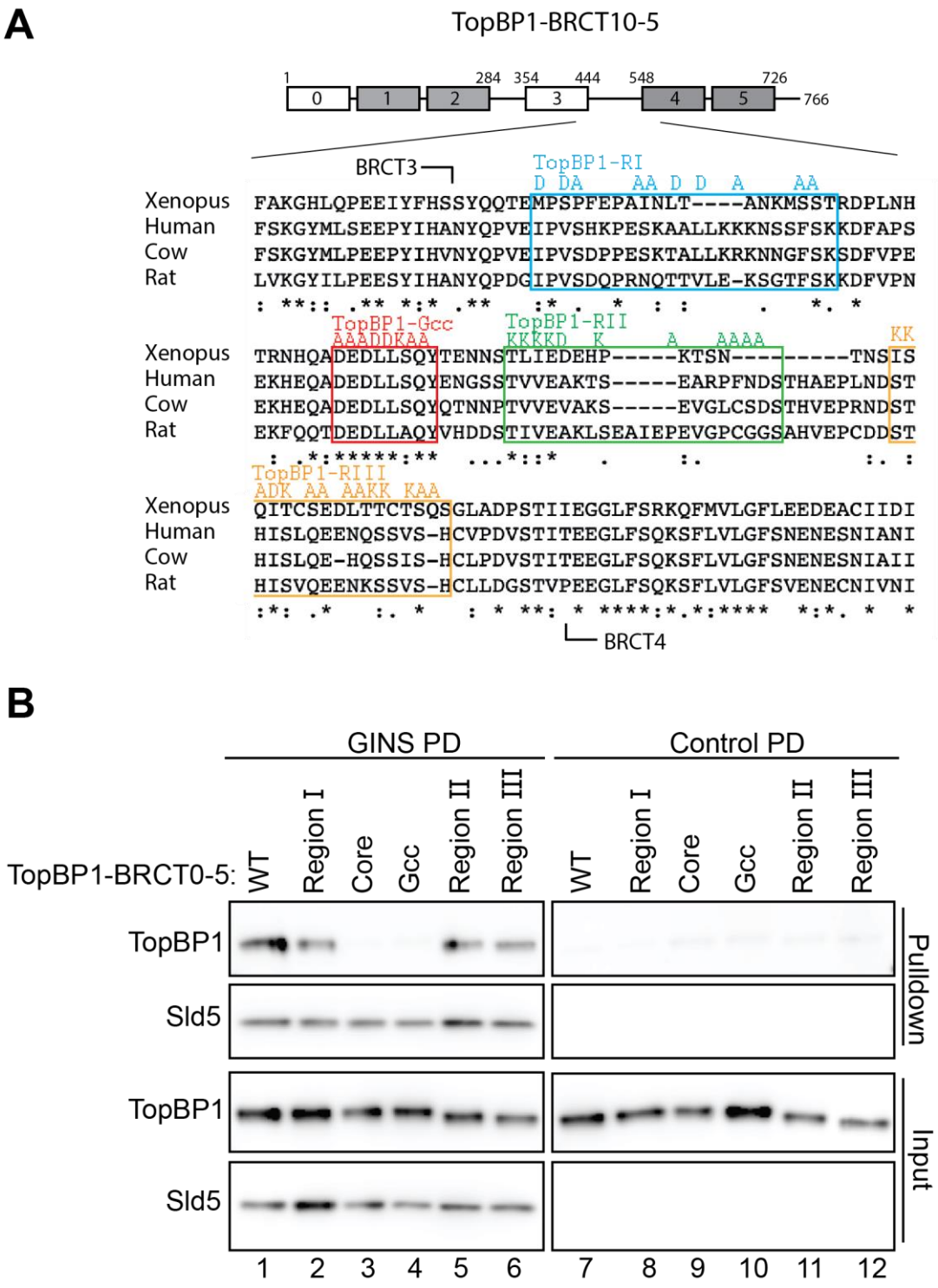

Figure 15. The highly conserved Gcc (GINI centre core region) is required for the interaction with GINS
A) The alignment of TopBP1 proteins was carried out using T-COFFEE algorithm. The following TopBP1 proteins were used in this alignment: Humans (Q92547), Xenopus laevis (Q7ZZY3), Bos taurus (A0A3Q1LWE4) and Rattus norvegicus (A0A8I6GFZ6). Substitutions of amino acids and names for mutations in the core region of the GINI region are shown. Coloured boxes represent regions I (blue), core helix (red), II green) and III (orange). **B)** Immobilized recombinant GINS was used to pulldown of indicated recombinant TopBP1-strep versions. The pulldown was analyzed by immunoblotting.

3.3.5. The GINI core helix interacts with Psf1-A domain

We next sought to understand how the GINI domain interacts with GINS. For this purpose, we utilized AlphaFold2 structure prediction program. In our first AlphaFold2 prediction experiment, we subjected Psf1 subunit of GINS and TopBP1-BRCT3-5 to the AlphaFold2 program. The Alphafold2 model accurately predicted the interaction between BRCT4 of TopBP1 and Psf1 subunit of GINS, which we found out in our initial cryo-EM model (Figure 16A). This showed the potential of Alphafold2 to predict unknown complexes accurately. To have more comprehensive predictions of the TopBP1-GINS interaction, we subjected GINS with all subunits and TopBP-BRCT3-5 to AlphaFold2 program in cooperation with Yasser Almeida-Hernandez. According to the new Alphafold2 model, the GINI domain forms an α-helix, and this helix mainly interacts with the distal part of the Psf1-A domain (Figure 16B). In addition to the Psf1, the adjacent region of Psf3 also is involved. This site is completely separate of Psf1 from the BRCT4 binding site almost at the opposite end.

In order to test the contribution of this α-helix structure to the GINS-interaction surface, we first mutated the central leucine-leucine motif in the GINI domain to proline-proline to break the helix (TopBP1-Gpp), and then the mutant protein TopBP1-Gpp with strep-tag was purified from the insect cells. The purified TopBP1-Gpp behaved similarly to the purified TopBP1-BRCT0-5-WT (Extended Figure 7). We confirmed that TopBP1-Gpp binds to 53BP1 similar to TopBP1-BRCT0-5-WT, indicating that the mutation did not change the protein folding (Extended Figure 9). To check the interaction with GINS, I used the GINS pulldown assay. In the GINS pulldown assay, TopBP1-Gpp showed severely compromised interaction with GINS in comparison to TopBP1-BRCT0-5-WT (Figure 16C), indicating that this α-helix involves in the interaction with GINS.

In addition to the GINS pulldown experiment, we also performed the fluorescence polarization (FP) experiments to test the contribution of this α-helix structure in the GINI domain to the GINS-interaction surface. We performed FP experiment using fluorescently labelled either the WT GINI-core peptide (aa Ala478- Gly497) or the GINI core peptide including PP mutation (aa Ala478- Gly497) and the recombinant GINS tetramer in collaboration with Matthew Day. The fluorescently labelled WT GINI-core peptide moderately bound to GINS, and we determined a dissociation constant Kd of ~8 μM (Figure 16D). When we used the fluorescently labelled GINI-core peptide with the PP mutation, we did not detect FP signal, indicating that it did not bind to the GINS. The FP assays showed that the α-helix structure in the GINI domain is crucial to form the interaction surface with Psf1.

Taken together, the GINI region is a bona fide GINS interaction site with moderate binding affinity, and the helix structure is crucial for the interaction. The interaction occurs dependently on residues of distal part of the Psf1-A domain and the adjacent region of Psf3 that were formed central interaction residues in our alphaFold2 predictions.

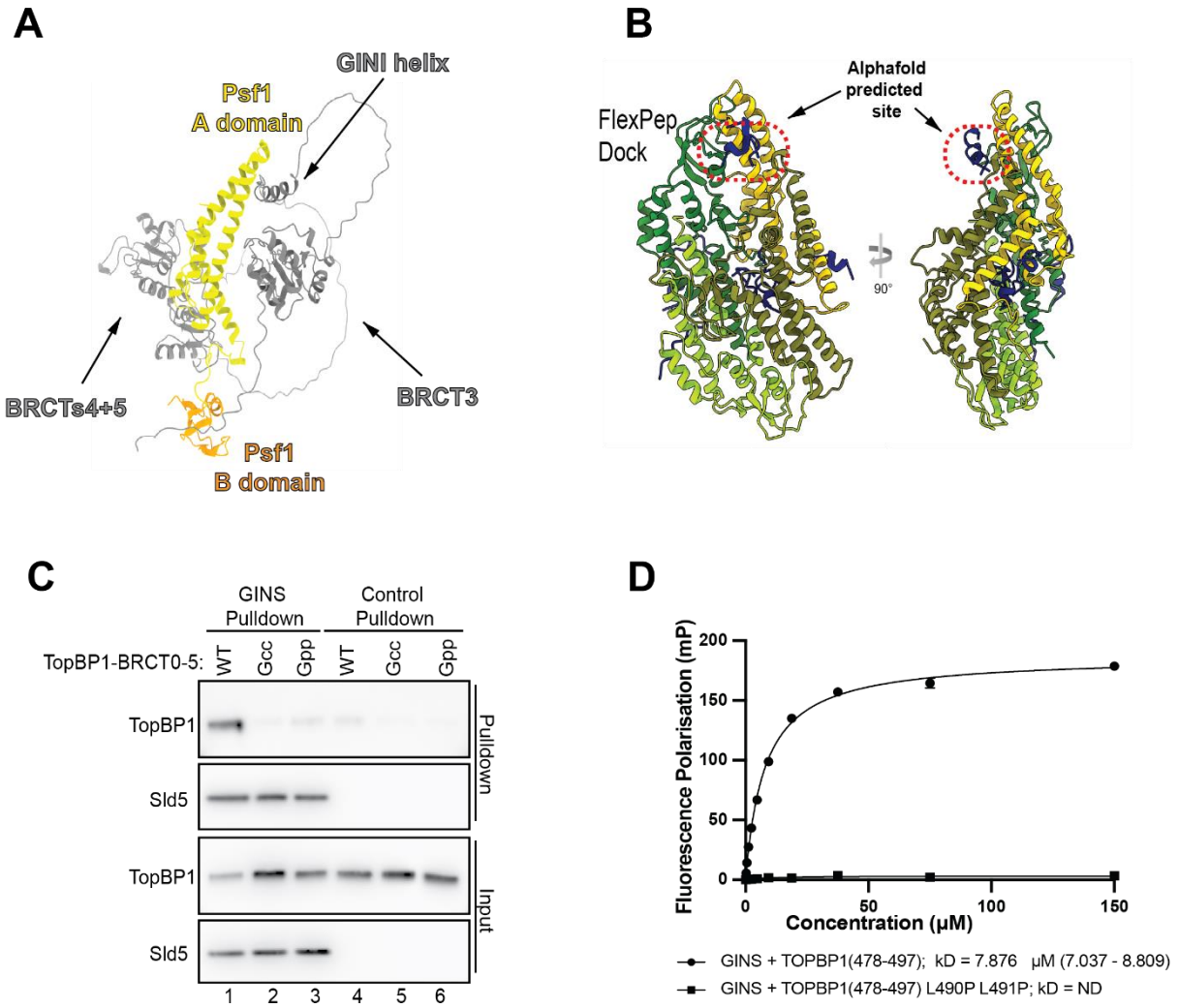

Figure 16. Binding of the GINI domain to GINS

A) AlphaFold2 model of TopBP1 BRCT3-5 with Psf1 subunit of GINS. Alphafold2 accurately predicts the previously unknown BRCT4 interaction with Psf1 in addition to predicting the GINI domain as an another interaction site for GINS. **B)** AlphaFold2 model of TopBP1 BRCT3-5 with all subunits of GINS (Experiment by Yasser Almeida-Hernandez). **C)** Immobilized recombinant GINS was used to pulldown of indicated recombinant TopBP1-strep versions. The pulldown was analyzed by immunoblotting. **D)** FP (fluorescence polarisation) experiments using recombinant GINS and fluorescently labelled TopBP1 peptides. The dissociation constant, Kd, was determined as roughly 8 μM. (Experiment by Matthew Day)

3.3.5.1. Crosslinking mass spectrometry analysis of the TopBP1-GINS complex

We further validated the AlfaFold2 predictions using the crosslinking mass spectrometry. For this purpose, the TopBP1-GINS complex was crosslinked by BS3-crosslinker, and followed by mass spectrometry in collaboration with our MSc student Heike Siegert and Dr. Farnusch Kaschani at the mass spectrometry facility of our institute. The chemical crosslinker BS3

(bis(sulfosuccinimidyl)suberat) covalently crosslinks lysine residues of proteins within a distance of about 12 Å. Then, the crosslinked proteins were further processed and analysed by mass spectrometry.

We first determined the optimal BS3 concentration that ensures efficient crosslinking while preventing excessive crosslinking by incubating TopBP1-GINS with the increasing amounts of BS3. The crosslinked samples were analysed by silver-stained SDS PAGE gel (Figure 17). Disappearance of the individual proteins and emergence of a high molecular weight crosslinking products indicate crosslinking. From 600 µM BS3 upwards, monomers of TopBP1 and of GINS started to disappear in the SDS PAGE gels, and high molecular weight products appeared above TopBP1. We decided to use 600 µM and 2500 µM BS3.

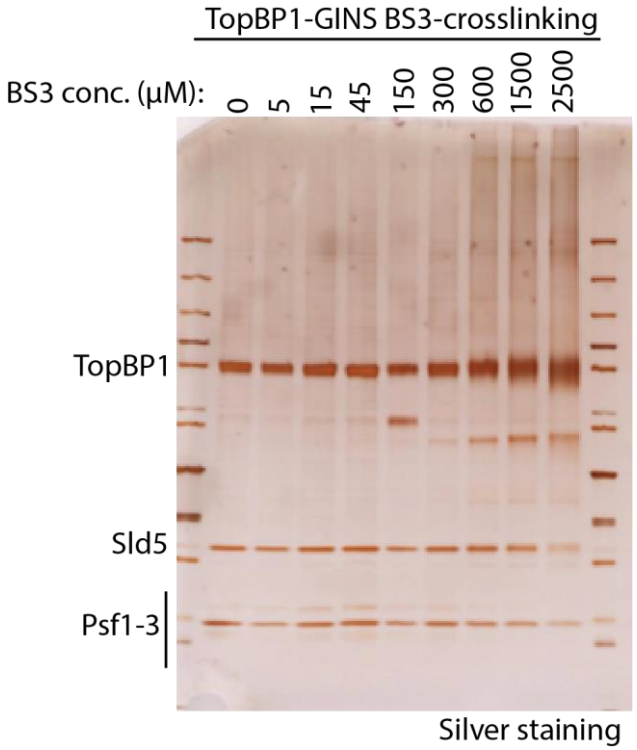

Figure 17.Titration of the crosslinker BS3
Crosslinking conditions were optimized by incubating the recombinant TopBP1-BRCT0-5 and GINS with increasing concentrations of the crosslinker BS3. Samples were analyzed by silver stained-SDS gel.

We next performed the crosslinking of the recombinant GINS and TopBP1-BRCT0-5 complex using either 600 µM or 2500 µM BS3 crosslinker. We used 90% of the crosslinked sample for mass spectrometry analysis (in solution experiment), the rest of the crosslinked sample was loaded on the SDS-Page gel. The coomassie-stained gel was cut in slices above the molecular weight of monomeric TopBP1-BRCT0-5-strep for subsequent mass spectrometry analysis of the crosslinked sample (gel extracted experiment). The GINI domain itself does not contain

lysine residues. However, we detected crosslinks between the adjacent lysin residues of the GINI region, K466, K468, K474, K475, K480 and K482, and the lysin residues at the distal end of the Psf1 A domain and the adjacent region of Psf3 in the both of the in solution and gel extracted experiments (Figure 18A). In addition to Psf1 and Psf3, we also detected crosslinks between the lysin residues of the GINI domain and Sld5. However, the number of this crosslinks were relatively less than the crosslinks between the GINI and Psf1 or Psf3 (Figure 18B-C). This findings indicate that the interaction is mainly between the GINI domain and the distal end of the Psf1 A domain and the adjacent region of Psf3, and in addition to Psf1 and Psf3, Sld5 may involve in this interaction.

Surprisingly, we did not observe significant crosslinking between BRCT4 and GINS. Only one crosslink was identified between residue 576 of BRCT4 and residue 210 on Psf3. One possible explanation for the scarcity of crosslinks is that the conformation of the region on Psf1 that interacts with BRCT4 prevents the binding of BRCT4. The presence of crosslinks between the C-terminal helix of Psf3 and the Psf1 B domain indicates that crosslinking has stabilized the GINS complex in its CMG bound state, bringing these two regions in close proximity. This particular form of the GINS tetramer may interfere with the formation of the TOPBP1 BRCT4-GINS complex.

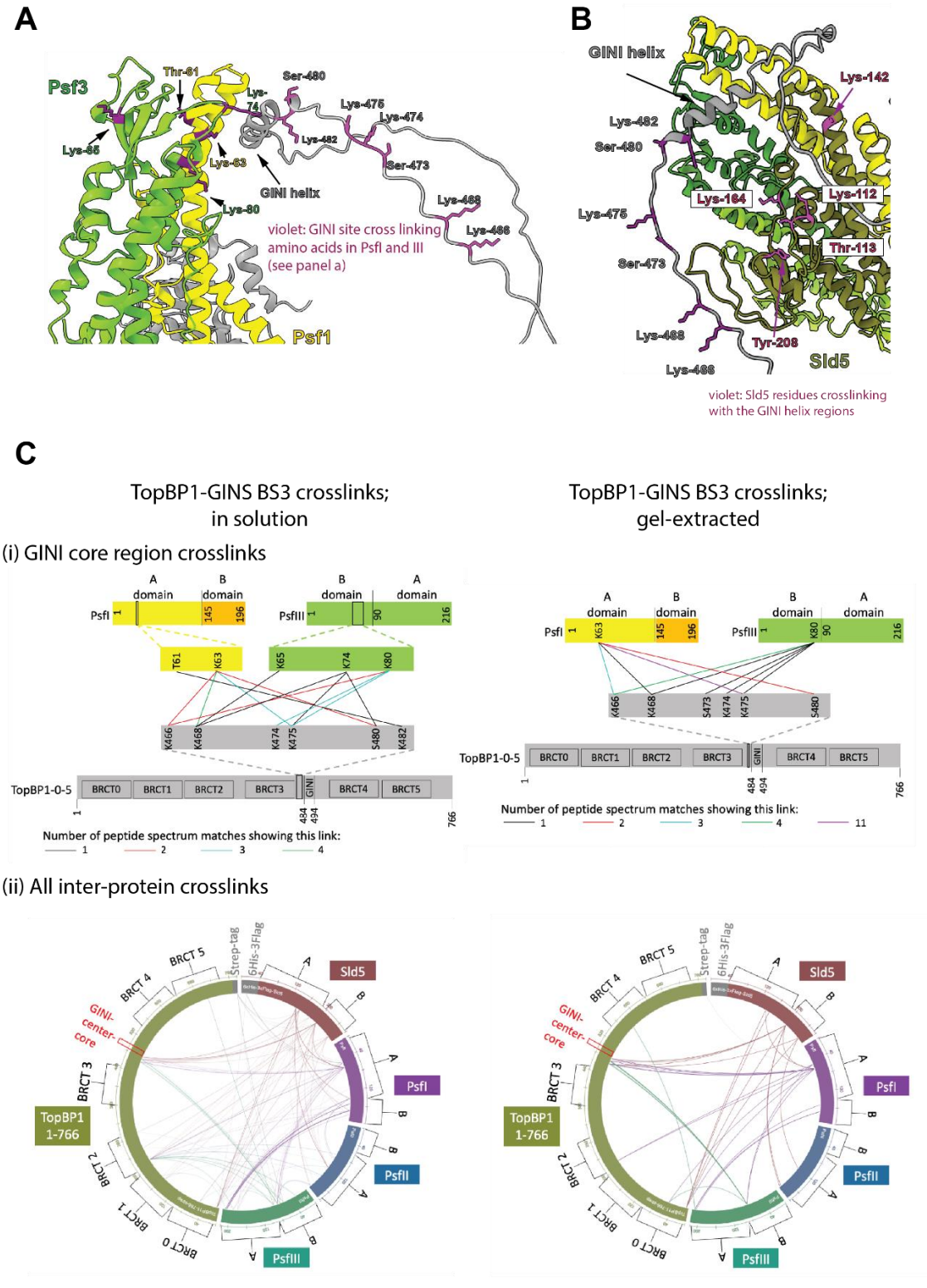

Figure 18. Schematic representation of crosslinked TopBP1-BRCT0-5-Strep and GINS complex using the crosslinker BS3

A) The predicted structure of the TopBP1-PsfI-PsfII complex, generated using AlphaFold2, is presented here. The amino acids that were found to be involved in crosslinking are highlighted in pink. **B)** The crystal structure of the GINS complex is docked onto the predicted AlphaFold2 structure of the TopBP1-PsfI-PsfII complex. The amino acids of the Sld5 protein that participated in crosslinking are highlighted in violet. **C)** Schematic representation of the crosslinks formed between TopBP1-BRCT0-5-Strep and GINS using BS3 crosslinker. **(i)** illustrates the crosslinks involving the GINI domain of TopBP1, while **(ii)** presents circular plots displaying all the inter-protein crosslinks that were identified. Crosslinked samples were analyzed using mass spectrometry. The ProXL (Protein Cross-Linking Database) tool was used for data analysis and visualization purposes. The crosslinks are color-coded based on the number of peptide spectrum matches indicating the presence of each specific link. (with Heike Siegert)

3.3.5.2. Cryo-EM structure of the GINI core region in interaction with GINS

We next aimed to enhance the resolution of our initial cryo-EM data to gain physical structural data about the TopBP1-GINI-GINS interaction, because the resolution of the GINI domain was not enough in the initial cryo-EM model. In order to gain physical structural data about the TopBP1-GINI-GINS interaction, we aimed to enhance the resolution of our initial cryo-EM data. Therefore, we purified an alternative GINS tetramer that the Psf1 B domain was deleted to improve the detail around the Psf1 A domain, the predicted interaction region. We confirmed that this GINS mutant binds TopBP1 using pulldown experiments

Using this recombinant mutant GINS and TopBP1-BRCT3-5 proteins, we then performed another cryo-EM experiment in collaboration with Matthew Day. The new cryo-EM model showed the GINI domain as a short α-helix in consistent with the Alphafold2 predictions. We then docked the AlphaFold2 GINI helix into the cryo-EM density (Figure 19A). According to our final cryo-EM model, the hydrophobic side of the GINI-core helix faces with the two helices of the Psf1 A domain, and the side chains of Leu490 and Leu491 of the GINI domain interact with the side chain of Val47, Lys51, Ile62, Lys63, and His66 of the Psf1 A domain. In addition to these interactions, Tyr494 of the GINI domain and Tyr40, Asn43, Leu69 and His66 form additional interaction surface.

We next confirmed these predictions by mutating two separate pairs of residues, Asn43/Lys51 and Lys63/His66, in Psf1 that seemed critical for TopBP1-GINI interaction. We generated Psf1-NK43/51AE and Psf1-NK63/66AE mutants, and then purified these mutants from Sf9 insect cells in the same way with the purification of the WT GINS. We first tested the tetramer formation ability of the purified mutant GINS proteins by immobilized them onto the anti-Flag beads using 3xFlag tag on Sld5 subunit (Figure 19B). GINS pulldown experiment revealed that KH63/66AE mutant was not able to form tetramer, Psf1 subunit was missing. Therefore, we excluded this mutant from the future experiments. In contrast, NK43/51AE mutant could form tetramer similar to WT GINS. In order to check the binding ability of NK43/51AE to TopBP1-BRCT0-5-WT, the GINS pulldown assay was used. The GINS pulldown assay showed that NK43/51AE mutant was severely defective to bind to TopBP1 (Figure 19C). This indicates that the GINI domain forms interaction surface with the Psf1 A domain, and NK43/51 are the critical amino acids on Psf1 for this interaction surface. Overall, the cryo-EM model of the GINI region exhibited consistency with the Alphafold2 model that predicted binding of the GINI region to the distal end of the Psf1 A domain and the adjacent regions in Psf3.

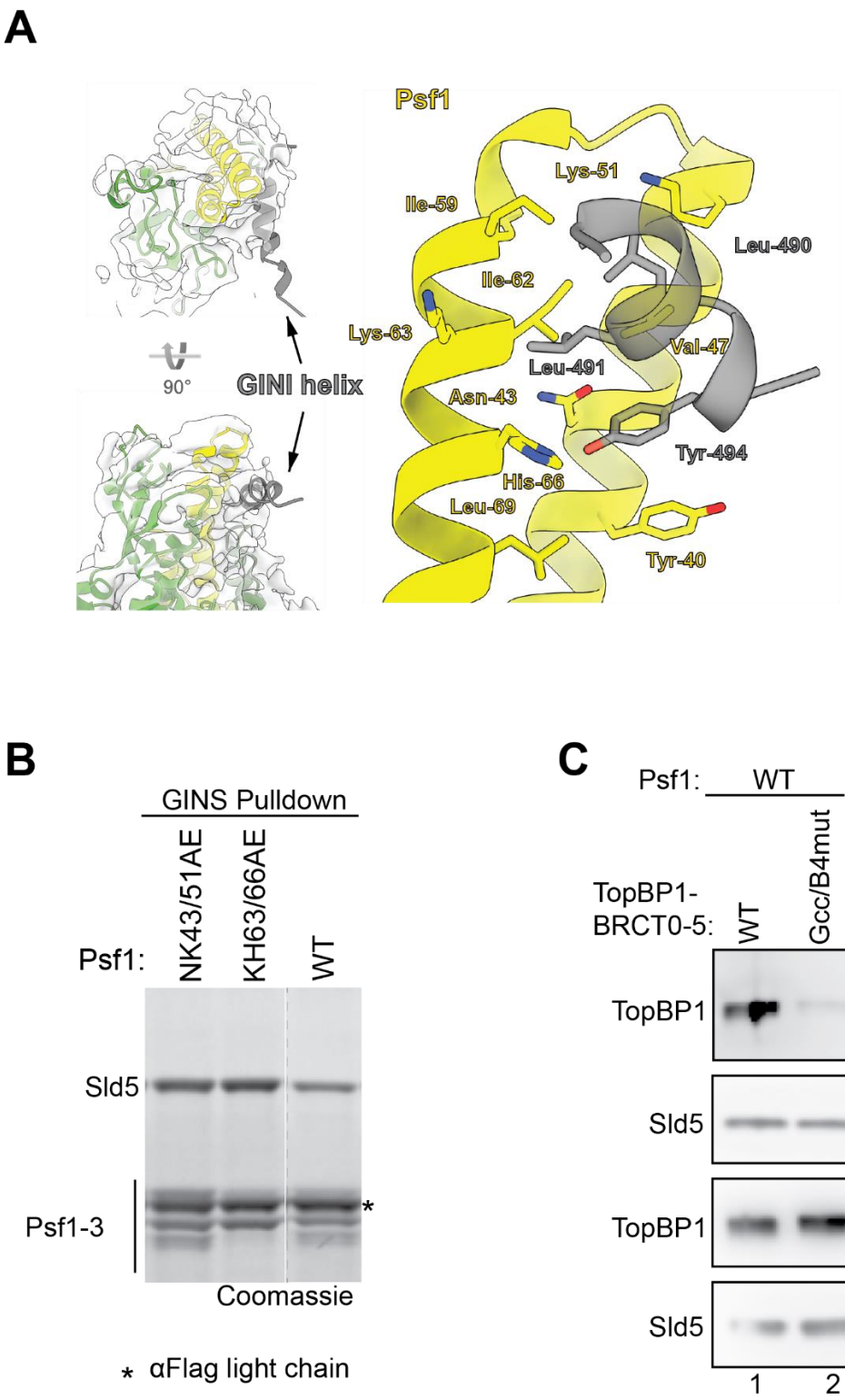

Figure 19. Cryo-EM density and AlphaFold2 prediction of the GINI region reveals the binding of the GINI region to the Psf1 A domain

A) On the left hand side, cryo-EM volume shows α-helix structure is coloured as gray. On the right hand side, zoom-in of the TopBP1-GINI and the Psf1 A domain interaction surface on the Alphafold2 model. (Experiment by Matthew Day) **B)** GINS tetramer formation upon he mutation on Psf1 was tested by immobilizing the recombinant GINS onto the beads. Tetramer formation was analyzed by Coomassie staining. **C)** Immobilized recombinant GINS was used to pulldown of indicated recombinant TopBP1-strep versions. The pulldown was analyzed by immunoblotting.

3.3.6. The GINI domain and the BRCT4 domain cooperate to support DNA replication

We next tested whether both GINS binding regions contribute to DNA replication. For this, we utilized *Xenopus* egg extract system to analyse the DNA replication (in collaboration with Milena Parlak). We first depleted the endogenous TopBP1 in the *Xenopus* egg extract using two independent TopBP1 antibodies (#ab1 and #ab2). Figure 20A shows that both of the anti-TopBP1 antibodies depleted more than 90% of the endogenous TopBP1 in the extract (Figure 20A). After depletion of the extract, either recombinant TopBP1-BRCT0-5-WT or the mutant TopBP1 was added to the depleted extract in the presence of radiolabelled α32P-dCTP (Figure 20B). Depletion of endogenous TopBP1 from the extract suppressed DNA replication in comparison to the extracts depleted with IgG-control antibody (Figure 20C). Addition of the recombinant TopBP1-BRCT0-5-WT to the depleted extract efficiently rescued DNA replication (Figure 20C). This results indicate that our anti-TopBP1 antibodies can successfully deplete the endogenous TopBP1 from the extract, resulting in suppression of the DNA replication in the egg extract, and our recombinant TopBP1-BRCT0-5-WT is able to rescue DNA replication similar to the physiological levels. This allows us to investigate the GINS binding mutants of TopBP1 in the depleted *Xenopus* egg extract.

In comparison to TopBP1-BRCT0-5-WT, the addition of either TopBP1-BRCT0-5-Gcc or TopBP1-BRCT0-5-Gpp to the depleted extract showed moderate reduction in the DNA replication. TopBP1-ΔBRCT4/5 (GINI domain intact) supported the DNA replication to the similar level with the WT TopBP1-BRCT0-5. This was consistent with the previous studies (Kumagai, Shevchenko, and Dunphy 2010; Tanaka et al. 2013). TopBP1-B4mut (GINI domain intact) showed a similar behaviour as TopBP1-ΔBRCT4/5 (Figure 20D). However, when the mutations on the GINI domain and BRCT4 domain were combined, the DNA replication was almost not rescued in the depleted extract (Figure 20D). Taken together, the presence of either functional GINI domain or BRCT4 domain is sufficient to support DNA replication, but the presence both of the functional GINI domain and BRCT4 domain efficiently rescues DNA replication, indicating that the GINI domain and BRCT4 domain cooperate to support DNA replication.

Our rescue experiments demonstrated a discrepancy between the severity of the effects of the GINI and BRCT4 mutations on supporting replication. To check if there is a discrepancy on the binding to GINS as well, we decided to test the interaction in less stringent conditions using 100 mM NaAc instead of 150 mM NaCl in the binding buffer (Figure 20E). The GINS pulldown assay showed that mutating either the GINI domain or BRCT4 domain weaken the interaction

between TopBP1 and GINS. Mutating the GINI domain has more severe effect comparison to the BRCT4 domain. When the GINI domain and the BRCT4 domain are both mutated, the interaction is abolished (Figure 20E). These results indicate that mutating one of the binding sites makes another binding site essential for binding to GINS, and both binding sites cooperate to form stable interaction with GINS.

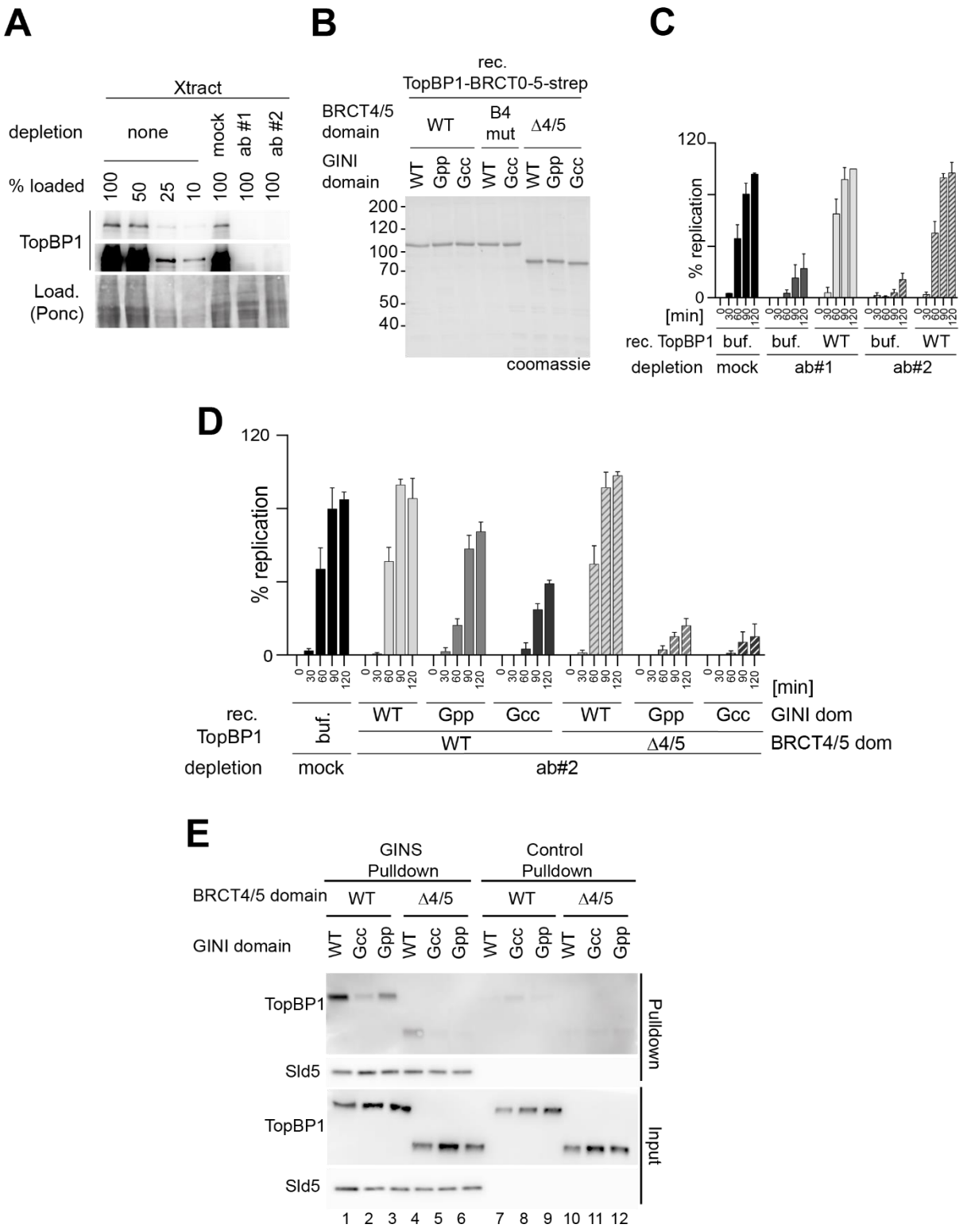

Figure 20. GINI domain and BRCT4 region cooperate to support DNA replication
A) Coomassie-stained SDS PAGE gel of the indicated purified TopBP1 proteins. **B)**The provided quantities of immunodepleted and undepleted Xenopus egg extracts were examined by utilizing TopBP1 antibodies #1 and #2 as well as IgG (mock). **C-D)** DNA replication analysis in Xenopus egg extracts immunodepleted with #ab2 upon adding back buffer (buf) or recombinant TopBP1-WT or mutants shown in A. (Experiment by Milena Parlak) **E)** Immobilized recombinant GINS was used to pulldown of indicated recombinant TopBP1-strep versions using 100mM NaAc in the binding buffer. The pulldown was analysed by immunoblotting.

3.3.7. The GINI domain and the BRCT4 domain cooperate to support CMG formation

We moved on to ask whether the origin firing step of DNA replication requires TopBP1-GINS interaction. For this purpose, we utilized the *Xenopus* egg extract system. We first depleted the endogenous TopBP1 from the extract, then we added-back either TopBP1-BRCT0-5-WT or the mutant TopBP1 to the depleted extract. In order to increase the signal for the replisome factors, we added aphidicolin which inhibits DNA polymeraseα and allows the accumulation of the replisomes on the chromosome. The chromatin was re-isolated from the extract after 75-minute incubation period, and the re-isolated chromatin was analysed by immunoblotting in cooperation with Milena Parlak. The immunoblotting against the Mcm subunits, Mcm4 and Mcm6, showed that the Mcm2-7 helicase was loaded onto the chromatin similarly for the addition of TopBP1-BRCT0-5-WT, the mutants and buffer control, while there was no Mcm signal in the geminin control (Figure 21). This indicates that the licensing occurs independently of TopBP1-GINS interaction. In the immunoblotting of some of the replisome markers, GINS, Cdc45 and Pol ε, we could detect the incorporation of Sld5 (GINS), Cdc45 and Pol E2 (Pol ε) when we added-back TopBP1-BRCT0-5-WT to the depleted extract. If TopBP1-Gcc was added-back to the extract, the binding of the replisome markers was dramatically reduced. In the case of the addition of TopBP1-ΔBRCT4/5, the binding of Sld5 and PolE2 were significantly reduced, while the binding of Cdc45 was not affected. When we added-back TopBP1-Gcc-ΔBRCT4/5, both of the GINS interaction sites mutated, the binding of the replisome markers for GINS, Cdc45 and Pol ε were abolished. These results indicate that TopBP1-GINS interaction is required for the replisome formation upstream of the CMG formation, and the GINI domain and the BRCT4 domain cooperates to form the CMG helicase.

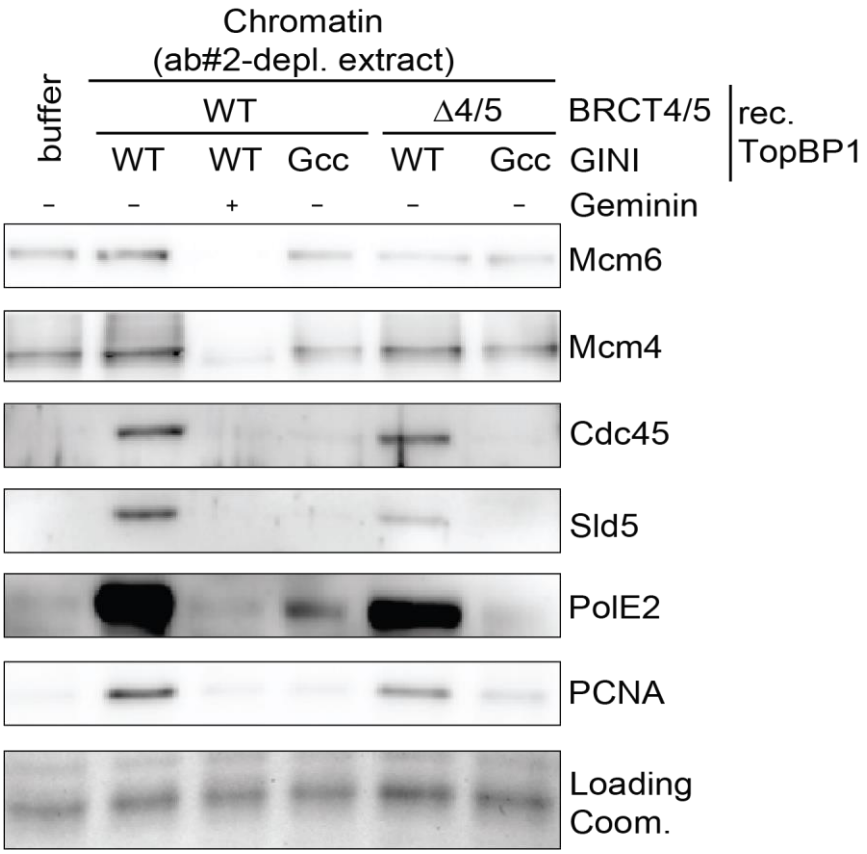

Figure 21. The GINI and the BRCT4 regions cooperates to assemble the CMG
Immunoblotting of chromatin-bound proteins after re-isolation of the chromatin from the Xenopus egg extract. Before the chromatin was re-isolated from the extract, either purified WT TopBP1 or the mutant TopBP1 was added to the XTopBP1 depleted extract and incubated for 75 minutes in the presence of aphidicolin. (Experiment By Milena Parlak)

4. Discussion

The aim of this thesis is to unravel the molecular details of the interaction between TopBP1 and GINS, and to provide insight into how their interaction supports vertebrate replication origin firing. Recent studies on the origin firing in yeast focused on elucidating the contribution of the Mcm2-7 helicase as a molecular machine to build replication forks (Costa and Diffley 2022; Deegan, Yeeles, and Diffley 2016; Douglas et al. 2018; Douglas and Diffley 2016; Greiwe et al. 2022; Heller et al. 2011; Lewis et al. 2022; Blackford et al. 2015; Yeeles et al. 2015; Saleh et al. 2022). However, there has been limited investigation into the process of helicase activation through the loading of GINS and Cdc45 to form the CMG complex. In this project, we are providing novel molecular insights into how TopBP1 may load GINS onto pre-RCs.

The CMG complex formation plays a crucial role as a key regulatory step in origin firing. In metazoan and yeast, the signal integrators TopBP1/Dpb11, Treslin/Sld3, MTBP/Sld7, RecQ4/Sld2 and the Mcm2-7 helicase itself are involved in the CMG formation as a regulatory platform by coupling replication origin firing to the S-phase. In addition to the coupling origin firing to the S-phase, these signal integrators are targeted by diverse regulatory pathways, including the DNA damage checkpoint to regulate origin firing (Zegerman and Diffley 2010; Lopez-Mosqueda et al. 2010; Natsume et al. 2013; Reusswig et al. 2016; Toledo et al. 2013). This regulation is essential to maintain the genomic stability (Burrell et al. 2013; Toledo et al. 2013).

The pre-IC formation step in replication origin firing is the major regulatory step in replication initiation. Although the molecular details of the pre-IC formation have been well characterized in yeast, it is poorly understood in vertebrates (Boos and Ferreira 2019). In order to understand the molecular mechanisms of the pre-IC formation in vertebrates, the long-term aim of the Boos laboratory is to biochemically reconstitute pre-IC *in vitro* using recombinant proteins and the isolated pre-RCs from *Xenopus* egg extract. For this purpose, isolation of the pre-RCs from Xenopus egg extract has been optimized (by Milena Parlak). During this PhD thesis, the purification of the core origin firing factors, Treslin-MTBP, TopBP1, DNA polymerase epsilon (Polε), helicase components Cdc45 and GINS and kinases DDK and CDK have been completed. These recombinant proteins and kinases with isolated pre-RCs will help to understand better the molecular processes of the origin firing regulations.

4.1. Molecular processes of the CMG formation

The CMG complex formation during origin firing is a crucial step in replication initiation and plays a fundamental role in ensuring accurate and efficient genome duplication.

The Mcm2-7 helicase is inactive in the pre-RCs, which are formed during the licensing in G1-phase. Activation of the Mcm2-7 helicase in S-phase begins with the stepwise assembly of a transient pre-IC, the main regulatory step of DNA replication initiation, onto its pre-RC precursor. In yeast and metazoan, formation of the pre-IC is dependent on high levels of CDK and DDK activity (Zegerman and Diffley 2007, 2010). DDK phosphorylates the inactive Mcm2-7 in the pre-RCs, and this phosphorylation recruits Treslin-MTBP/Sld3-Sld7 to the phosphorylated Mcm2-7 (Francis et al. 2009; Greiwe et al. 2022; Deegan, Yeeles, and Diffley 2016; Randell et al. 2010). Pre-RC recruitment experiments *in vitro* and in cell lysates suggested that this initial DDK dependent recruitment of Treslin-MTBP/Sld3-Sld7 delivers the CMG component Cdc45 to the Mcm2-7 (Deegan, Yeeles, and Diffley 2016; Heller et al. 2011; Zaffar et al. 2022). In addition to DDK, the CMG formation is also dependent on CDK, which is required to recruit all other CMG formation factors downstream of Mcm2–7-Treslin-MTBP/Sld3-Sld7-Cdc45. N-terminal BRCT0-2 repeats of TopBP1 bind to Treslin in a strictly CDK phosphorylation-dependent manner. CDK phosphorylates two conserved phosphorylation sites in Treslin and Sld3, and this phosphorylation facilitates the binding of Treslin/Sld3 to the N-terminal tandem BRCT0-2 repeats of TopBP1 which are the homologue BRCT1/2 repeats of Dpb11. In this way, TopBP1/Dpb11 couples the origin firing to the S-phase (Kumagai, Shevchenko, and Dunphy 2011; Boos et al. 2011). In yeast cells, Sld2-Dpb11 forms the pre-loading complex (pre-LC) with GINS and Polε in a CDK dependent manner, and the pre-LC is recruited to the pre-RCs, which are already associated with Sld3-Sld7-Cdc45. CDK-dependent binding of Sld3 to Dpb11 facilitates this recruitment (Muramatsu et al. 2010). After stable association of Cdc45 and GINS with the Mcm2-7 in the pre-RCs, the regulatory firing factors Treslin/Sld3, MTBP/Sld7 and TopBP1/Dpb11 dissociate, resulting in the formation of the active CMG helicase (Gambus et al. 2006; Kanemaki and Labib 2006).

Recent electron microscopy studies of the CMG complex in yeast and Drosophila have revealed the major re-configurations during the formation of the CMG from the pre-RC. These studies have demonstrated that the Mcm2-7 ring in the CMG is a single hexamer bound to Cdc45 and GINS, rather than forming a double hexamer (Costa et al. 2011; Costa et al. 2014; Yuan et al. 2016). Cdc45 and GINS interact with the N-terminal tier of the Mcm2-7 ring and bridge the weak Mcm2-5 interface. The Psf2 subunit of GINS binds to the side of the A domain of Mcm5 in the Mcm2-7 ring and stabilizes Mcm5:3 interface, while Cdc45 binds to the N-terminal tier

of the Mcm2-7 and stabilizes the Mcm2:5 interface (Frigola et al. 2017; Costa et al. 2011; Zaffar et al. 2022; Abid Ali et al. 2017). Association of Cdc45 and GINS with Mcm2-7 appears to activate the Mcm2-7 helicase. This indicates that interactions of Cdc45 and GINS with the Mcm2-7 ring play a crucial role in the assembly and the activation of the CMG complex. The CMG complex associates with Polε and forms CMGE (CMG-Polε) during the origin firing reaction. In CMGE, Polε has a role in the poorly investigated re-configurations of the helicase and its engagement with the DNA (Zaffar et al. 2022; Langston et al. 2014; Yuan et al. 2020; Goswami et al. 2018). Recent cryo-EM studies of human CMGs, which either purified from human cell line or biochemically reconstituted *in vitro*, revealed that the association of Cdc45 and GINS with the Mcm2-7 is conserved and the overall architecture of human CMG is remarkably similar to the yeast CMG. These findings point out the crucial role of the CMG complex in the origin firing (Jones et al. 2021; Rzechorzek et al. 2020).

4.1.1. TopBP1-GINS interaction is required to activate the CMG helicase

TopBP1 is a key regulator in replication initiation, as it mediates the coupling of the activation of the CMG helicase to the S-phase. As explained previously, CDK phosphorylated Treslin/Sld3 binds to the N-terminal BRCT repeats of TopBP1/Dpb11. This binding mode of TopBP1 couples the activation of the CMG helicase to the S-phase (Kumagai, Shevchenko, and Dunphy 2011; Boos et al. 2011). In addition, BRCT3/4 of Dpb11 and BRCT4/5 of TopBP1 share homology, whereas BRCT3 of TopBP1 is metazoan specific (Makiniemi et al. 2001; Garcia, Furuya, and Carr 2005). The rescue experiments in TopBP1-depleted *Xenopus* egg extract showed that TopBP1-BRCT4/5, the equivalent of Dpb11-BRCT3/4 which mediates the essential phospho-binding of Sld2, is dispensable for supporting DNA replication (Kumagai, Shevchenko, and Dunphy 2010). This TopBP1 fragment contains the inter BRCT3 and BRCT4 region where the GINS interaction domain (GINI domain) is located (Tanaka and Araki 2013). The interaction between Dpb11 and GINS occurs via the GINI domain and Psf3 subunit of GINS, and it is required for the GINS loading onto the pre-RC to activate the CMG helicase (Takayama et al. 2003). It was previously shown by the yeast two-hybrid experiments and *in vivo* biochemical binding assays that the GINI domain in yeast is located between BRCT2 and BRCT3 of Dpb11, and it is sufficient to interact with GINS *in vivo* (Tanaka and Araki 2013). Tanaka et al., also showed that the GINI domain is essential for the cell viability in yeast. It was also suggested that the GINI domain exists in vertebrates as well, and it is located between inter BRCT3 and BRCT4 region on TopBP1 (Tanaka et al. 2013).

4.1.2. The TopBP1 GINI core helix interacts with GINS Psf1 and Psf3

As explained above, the GINI domain in TopBP1 is broadly defined as the region between BRCT3 and BRCT4 (Tanaka et al. 2013). In this project, our multiple amino acid sequence alignment of the inter BRCT3 and BRCT4 region among vertebrate species revealed that the GINI domain is located between amino acids 487 and 495 in TopBP1. Moreover, our cryo-EM structure of TopBP1-GINS showed that there is a short α-helix motif at the core of the conserved GINI region (GINI-core helix), and when we mutated the GINI domain to break this α-helix structure (TopBP1-Gcc), the interaction was severely weakened. This indicates that this α-helix forms an essential part of the binding surface necessary for robust interaction with GINS. However, TopBP1-Gpp was able to rescue DNA replication in the endogenous TopBP1 depleted *Xenopus* egg extract with a moderate reduction when compared with WT, indicating that the weak interaction between TopBP1-Gcc and GINS is sufficient to restore DNA replication. Our cryo-EM model also revealed that this α-helix motif mainly interacts with the distal end of the Psf1 A domain and the adjacent region of Psf3. These findings are consistent with the previous yeast two-hybrid experiments (Tanaka et al. 2013).

4.1.3. BRCT4 region on TopBP1 is a novel binding site for GINS

Our cryo-EM structure of TopBP1-BRCT4/5 and GINS suggested that TopBP1-VTV590/606/610 in BRCT4 forms an interaction surface with T91 and I97 on Psf1 side. We confirmed these predictions by *in vitro* pulldown experiments using WT and the mutant versions of recombinant TopBP1 (TopBP1-B4mut or TopBP1-ΔBRCT4/5) and GINS (Psf1-I97R). This represents a novel mode for a BRCT4 domain-mediated interaction and ascribes for the first time a specific molecular function to TopBP1-BRCT4. TopBP1-B4mut or TopBP1-ΔBRCT4/5 rescued DNA replication in *Xenopus* egg extracts to the similar level with WT, indicating that the weak interaction is sufficient to restore DNA replication in DNA replication deficient egg extract.

4.1.4. GINI domain and the novel binding site BRCT4 cooperate

Our project revealed two binding sites in TopBP1 for GINS: GINI domain which we identified the location between BRCT3 and BRCT4, and BRCT4 domain which was previously unknown. Our *in vitro* pulldown experiments showed that each binding site alone has a weak binding affinity for GINS (Figure 20E). In the presence of the two intact binding sites, the binding affinity is markedly higher. This indicates that the GINI domain and BRCT4 cooperate to form a composite high-affinity interface which is required for stable TopBP1-GINS interaction. However, each binding site alone is able to rescue DNA replication to the substantial levels in the depleted *Xenopus* egg extract, indicating that the weak TopBP1-GINS interaction is sufficient for origin firing. Despite the GINI domain and BRCT4 are not individually required

for origin firing, their combined action is essential, suggesting that neither site has a unique molecular role beyond GINS binding. The explanation of this could be that their common essential molecular role is to chaperone GINS onto pre-RCs, and that the partial redundancy between the two binding sites provides an explanation for the unrecognised role of TopBP1-BRCT4/5 in replication. Notably, both binding sites in TopBP1 are fully accessible for GINS in the context of either the unbound GINS tetramer or in the CMG complex. This is consistent with a model that TopBP1 recruits GINS to the pre-RCs using both binding sites. In this model, it is plausible that TopBP1 may simultaneously bind phosphorylated Treslin-MTBP via its N-terminal BRCT0-3 module, and then Treslin may recruit Cdc45 to the pre-RCs from (Matthew Day, Bilal Tetik and Milena Parlak et al., 2023).

Studies in yeast and *Xenopus* egg extract have revealed that Treslin, MTBP and TopBP1 are limiting DNA replication initiation factors. This indicates that after delivery of Cdc45 and GINS onto the pre-RCs, the subsequent release of Treslin, MTBP and TopBP1 is necessary, and presumably they must be 'recycled' to allow the use of late firing origins (Collart et al. 2013; Mantiero et al. 2011). However, such a release mechanism has not been elucidated yet. Our data suggests that the two individual GINS binding sites in TopBP1 have only low binding affinities for GINS. This finding allows a model that release of one site, in a 'zipper'-like fashion, would significantly destabilise the TopBP1-GINS complex to trigger dissociation of TopBP1. To release of TopBP1 after CMG is formed, there is no obvious steric clash in the context of the CMG that would force TopBP1 dissociation. However, a steric clash may be possible in the CMGE (CMG-Pol ε) context, where binding of DNA Pol ε would be incompatible with binding of GINS to BRCT4 in TopBP1, suggesting that the two proteins exchange (In collaboration with Matthew Day, Extended Figure 10). It is still unclear that whether the association of DNA Polε requires the disassociation of TopBP1 from the complex or Polε competes with TopBP1 to bind to the CMG. Therefore, the important but mechanistically unclear role of Polε in CMG formation still remains to be elucidated. In our cryo-EM model and previous crystallisation studies, the B domain of Psf1 subunit of GINS is flexible. This B-domain is not required for the GINS tetramer formation, whereas it is essential for the CMG formation (Chang et al. 2007; Kamada et al. 2007; Carroni et al. 2017). We here propose a model that during CMG formation, reconfiguration of the Psf1-B domain facilitates the disassociation of TopBP1 from the CMG. In our cryo-EM model, the B domain seems flexible in the TopBP1-GINS complex, and when GINS interacts with Cdc45, the B domain reconfigures from flexible state into the well-ordered state to form the CMG. This new configuration of the B domain might be favour for Pol ε binding over TopBP1-BRCT4,

resulting in the release of TopBP1 (Figure 22) (Matthew Day, Bilal Tetik and Milena Parlak et al., 2023).

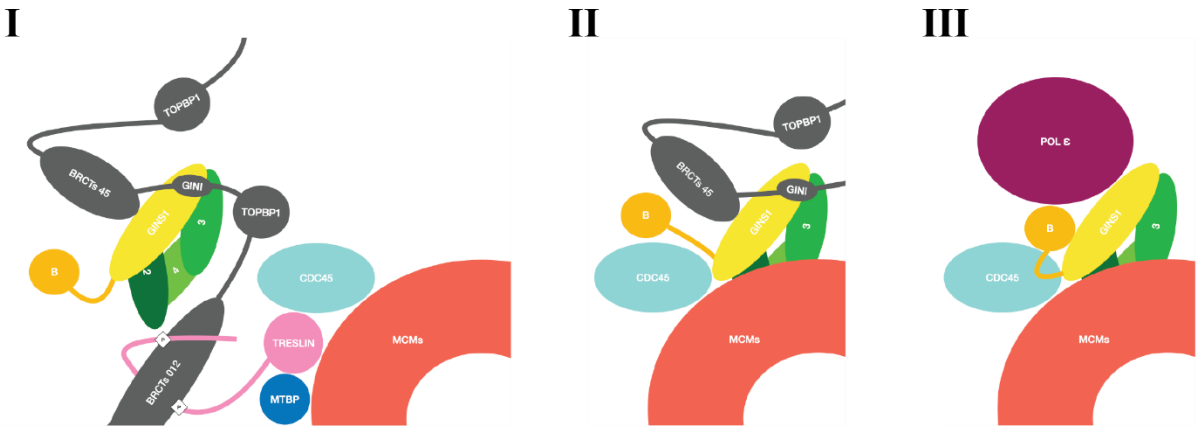

Figure 22. Hypothetical model of TopBP1-facilitated GINS incorporation into pre-RCs
According to our hypothetical model, TopBP1-mediated GINS incorporation into the pre-RCs takes place in three steps. I) CDK phosphorylation of Treslin-MTBP recruits TopBP1 to the pre-RC. This recruitment mediates the delivery of GINS to the Mcm2-7-Cdc45 complex. II) Psf1 B-domain reconfigures upon interaction with Cdc45, simultaneously locking the Mcm2-7 ring and weakening the interface between TopBP1-BRCT4 and the GINS complex. III) The new configuration of the B-domain is more favour for binding of Polε, resulting in TopBP1 dissociation, allowing Polε to bind to form the CMGE complex. Adapted from (Matthew Day, Bilal Tetik and Milena Parlak et al., 2023).

In yeast, GINS and Polε simultaneously bind to Dpb11 and they are delivered to the pre-RCs (Muramatsu et al. 2010). According to our hypothetical model, the delivery of GINS and Polε is mechanistically changed. However, the coupling of origin firing to the S-phase remains fundamental, yet flexible.

4.2. Control of genome duplication by replication origin firing

DNA replication is tightly controlled to ensure precise duplication of the genome. Since the eukaryotic genome is large, multiple replication origins are required to duplicate the large genome within a typical replication period. This makes the completeness of genome duplication in eukaryotes particularly complex issue. Multiple origins bring the risk of gaps between two replication initiation sites that are positioned too far away from each other to be replicated by two replication forks within the duration of one S-phase. In most of the eukaryotes including metazoan, since the positioning of origins is not strictly defined by specific DNA sequences, the origins might be placed randomly, resulting in smaller and larger inter-origin distances. To guarantee the completeness, the number of large inter-origin gaps needs to be kept minimal. For this reason, two requirements must be met: 1) the placement of the origins must be placed regularly, not too far from each other in the genome and 2) since the unfired origin increases the gap size, origins must fire reliably (Figure 23) (Boos and Ferreira 2019).

Some origin firing factors, including the regulation platform TopBP1 and Treslin-MTBP are present in limiting amounts in the cells. Therefore, not all origins can fire simultaneously in the beginning of the S-phase (Collart et al. 2013; Tanaka and Araki 2011; Wong et al. 2011; Mantiero et al. 2011). If the relatively rare firing events were scattered throughout the genome, this may cause large inter-origin distances and result in stalled forks. To avoid these scattered replication events, higher eukaryotic cells presumably replicate their genomes in the replication domains/factories (Berezney, Dubey, and Huberman 2000; Nakamura, Morita, and Sato 1986). In these replication domains, neighboring domains fire sequentially, suggesting a domino-like model where replication progress from the initial domain to the adjacent domain (Figure 23) (Sadoni et al. 2004; Maya-Mendoza et al. 2010; Sporbert et al. 2002). In this domino-like model, timing transition regions (TTRs), defined as the regions between two adjacent domains that replicate with a significant time delay, represent an exception. Replication of TTRs must be blocked and the replication timing of late replication domains has to be determined newly (Figure 23) (Boos and Ferreira 2019).

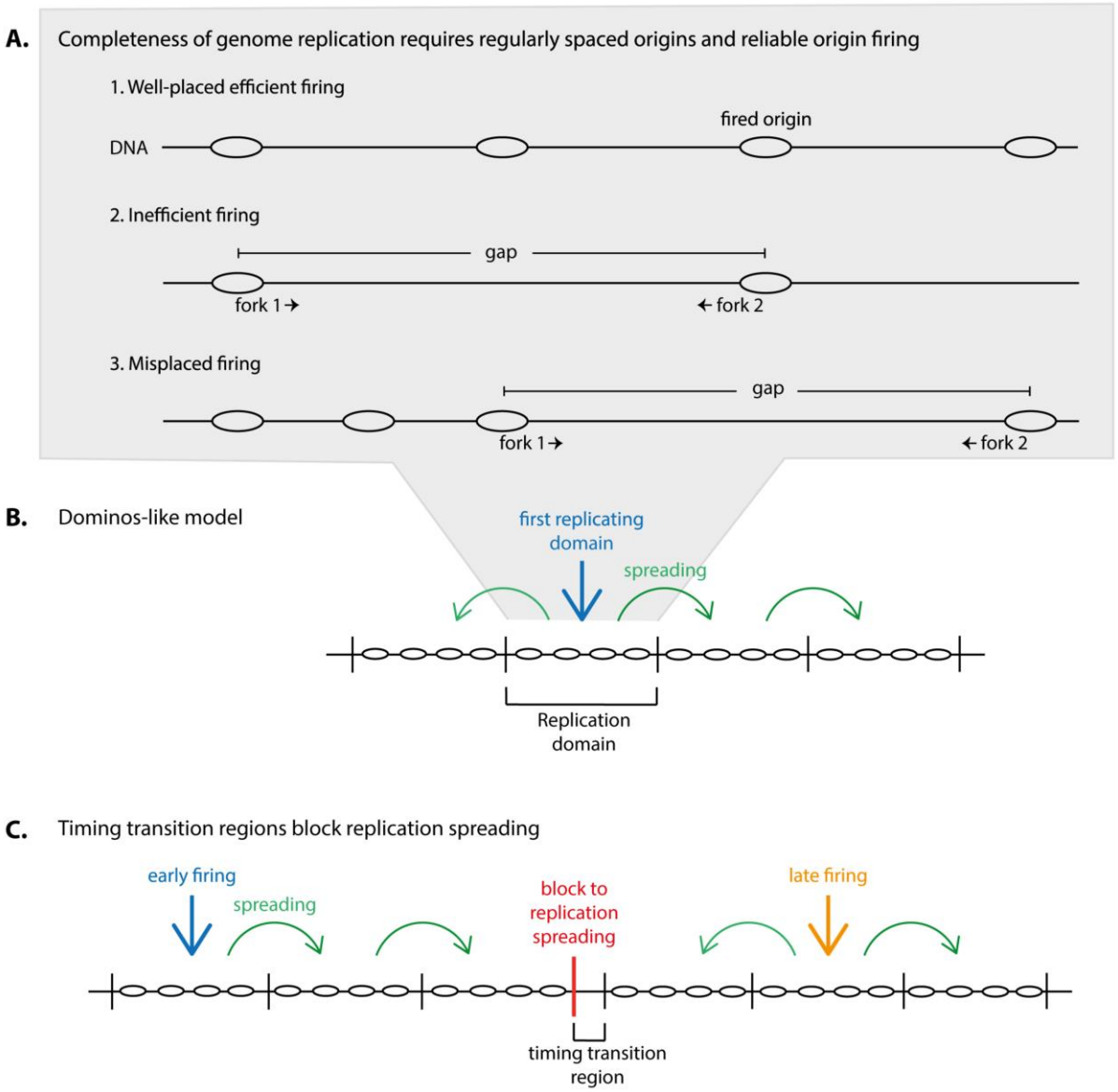

Figure 23. Proper control of origin firing is required for complete genome duplication
A) Complete genome replication requires well-placed origins and efficient firing. Misregulations of origins and inefficient origin firing can cause gaps in the replicating genome that are too big to be replicated by two forks during an S-phase. **B,C)** Domino-like model of origin firing where replication progress from the initial domain to the adjacent domain. Replication at TTRs is blocked. **C)** The replication timing of late replication domains must be newly determined. Adapted from (Boos and Ferreira 2019)

The domino-like model of eukaryotic genome presented here is highly simplified. In this model, there are many open questions, such as how is the first domain (the first domino) in a row determined? How is the replication progress is achieved and how is it blocked at TTRs? What are the replication parameters and chromatin processes to influence the timing? It is known that, origin firing factors that involve the formation of regulatory platform, Treslin-MTBP and TopBP1, have metazoan specific regions in addition to the yeast homologue regions. We speculate that these regions may constitute regulatory units that mediate the proper control of origin firing (Boos and Ferreira 2019).

4.2.1. Treslin-MTBP-TopBP1 complex is the regulatory hub of origin firing

Treslin-MTBP-TopBP1 (TMT) complex mediates CDK-dependent S-phase specific origin firing like its yeast counterpart Sld3-Dpb11-Sld2 (SDS) complex. First, Treslin-MTBP complex facilitates the activation of the CMG helicase. Phosphorylation of the Mcm2-7 helicase by DDK promotes the recruitment of Treslin-MTBP complex with Cdc45 (Reusswig et al. 2016; Greiwe et al. 2022; Saleh et al. 2022; Francis et al. 2009; Volpi et al. 2021). The high CDK activity in S-phase facilitates the phosphorylation of Treslin and CDK phosphorylated Treslin allows the recruitment of TopBP1-GINS to the Mcm2-7 (Zegerman and Diffley 2007; Kumagai, Shevchenko, and Dunphy 2010; Boos et al. 2011; Tanaka and Araki 2013; Volpi et al. 2021). In case of DNA damage, Chk1 suppresses replication origin firing by disrupting the interaction between Treslin and TopBP1. Two models have been proposed for regulation of Treslin-TopBP1 interaction by Chk1. In the first model, Chk1-induced decrease in CDK activity leads to a decrease in Treslin phosphorylation which is required for TopBP1 binding. In the second model, Treslin is directly phosphorylated by Chk1, resulting in dissociation of TopBP1 (Boos et al. 2011; Guo et al. 2015; Kelly et al. 2022). The recent *in vitro* biochemical reconstitution studies of the human replisome using purified recombinant proteins revealed that these regulatory firing factors are not required for the assembly of the CMG helicase *in vitro*, although they are essential *in vivo* (Kumagai, Shevchenko, and Dunphy 2010; Boos et al. 2011; Ferreira et al. 2021; Jones et al. 2021).

In archaea, a simplified version of the eukaryotic replication machinery is present. Although, the homologue of the CMG helicase has been identified, the regulatory origin firing factors and regulatory cell cycle kinases CDK and DDK are not present in archaea. As explained above, in eukaryotic cells, origin firing is strictly coupled to the S-phase to ensure accurate and complete genome replication, in contrast to archaea. The S-phase coupling of origin firing is mediated by SDS complex in yeast, while it is mediated by TMT complex in metazoan. Moreover, the activation of the CMG complex also depends on the TMT/SDS complex. Thus, it is presumable that these firing factors and regulatory kinases might be evolved with the eukaryotic cell cycle (Barry et al. 2007). In eukaryotes, the checkpoint kinases Rad53 (yeast) and Chk1 (vertebrates) inhibit origin firing upon DNA damage and replication stress. These checkpoint activities in archaea have not been identified yet (Marshall and Santangelo 2020).

In addition to the conserved functions, Treslin, MTBP and TopBP1 have evolved additional functions in DNA replication and DNA damage-dependent origin firing inhibition. The study of Sansam et al., revealed that in vertebrates, Treslin mutant harboring phospho-mimetic mutations on the two CDK sites stimulates shortening of the S-phase length by increasing the

replication clusters and the number of replication forks within each cluster, indicating that Treslin has a function to control the length of the S-phase (Sansam et al. 2015). In addition to origin firing, Treslin plays a direct role in the checkpoint response in vertebrates. It has been shown that Treslin activates ATR-mediated and TopBP1-dependent Chk1 phosphorylation (Hassan et al. 2013). Vertebrate specific structure of Treslin harbors N-terminal and C-terminal domains which are required for normal replication in human cells. Individual deletion of each domain showed mild effects on DNA replication. However, in case of deletion of both domains, a core Treslin protein is not sufficient to support DNA replication and origin firing in human cells. This indicates that these two vertebrate specific domains of Treslin have a cooperation to facilitate replication origin firing in parallel pathways (Ferreira et al. 2022). Furthermore, Treslin contributes to epigenetic control of DNA replication. Transcriptional regulatory proteins BRD2 and BRD4 bind to acetylated histones and recruit the multiprotein complexes to enhance the transcriptional activity (Fujisawa and Filippakopoulos 2017; Rahman et al. 2011). It is known that transcriptionally active chromatin is replicated early in the S-phase (Boos and Ferreira 2019; Yekezare, Gomez-Gonzalez, and Diffley 2013). It has been shown that Treslin interacts with BRD2 and BRD4, and then it is recruited to acetylated chromatin. Abrogation of this interaction disrupts binding of Treslin to the acetylated chromatin and impairs normal S-phase progression (Sansam et al. 2018).

MTBP is the vertebrate orthologue of Sld7 in yeast, and in contrast to Sld7, it is essential for DNA replication (Kohler et al. 2019; Kumagai and Dunphy 2017). MTBP forms a complex with Treslin, and if this interaction is disrupted by mutating the Treslin-binding region on MTBP, the overall levels of the Treslin and MTBP are decreased in human cells, suggesting that Treslin and MTBP stabilize each other (Kumagai and Dunphy 2017; Boos, Yekezare, and Diffley 2013). In addition to the interaction with Treslin, MTBP is dimerized by its C-terminal domain (Kohler et al. 2019). This dimerization acts as a control to ensure simultaneous activation of both Mcm2-7 helicases and loading of Cdc45 and GINS onto these helicases. Therefore, the activation of the single replisomes is prevented to ensure bidirectional replication. Furthermore, recent studies suggested that MTBP is phosphorylated by the ATM/ATR and Chk1/Chk2 DNA damage checkpoint kinases, in contrast to Sld7. The evolution of additional regulation platform may reflect the need for stringent control (Ferreira et al. 2021).

TopBP1 is a dual protein that has essential functions in both DNA replication and in DNA damage response. In DNA damage, to stimulate the kinase activity, TopBP1 binds to the checkpoint kinase ATR and regulates the checkpoint response (Kumagai et al. 2006). TopBP1 has numerous BRCT domains for additional interactors to fulfill its dual role in DNA replication

and DNA damage response. Besides conserved functions, TopBP1 also has vertebrate-specific functions, as discussed in more detail in the following sections.

Taken together, the complexity of the metazoan genome requires these mechanistical changes in the TMT complex to maintain genomic homeostasis. The TMT complex with these mechanistical changes has evolved to be able to facilitate the complex regulations of DNA replication and DNA damage response.

4.1.1. Molecular roles of TopBP1

Our project provides a novel insight into the molecular functions of TopBP1. In comparison to its yeast orthologue Dpb11, it contains additional BRCT domains. Besides conserved N-terminal BRCT0/1/2 and the BRCT4/5 domains, TopBP1 includes vertebrate specific additional five BRCT repeats in its C-terminus and additional inter-BRCT3 domains (Garcia, Furuya, and Carr 2005; Yamane, Kawabata, and Tsuruo 1997). TopBP1 has dual functions in DNA replication and DNA damage response. ATM and ATR are two essential checkpoint kinases that regulate the upstream of the DNA damage signalling. ATM is primarily activated by double-strand breaks (DSB), whereas ATR is mainly activated by replication stress or single-strand breaks (Blackford et al. 2015).

ATR-activation domain (AAD) of TopBP1, located between BRCT6 and BRCT7, interacts either directly with ATR or the ATR-interacting protein (ATRIP) to stimulate the checkpoint kinase (Kumagai et al. 2006; Mordes et al. 2008). BRCT0/1/2 repeats of TopBP1 interacts with RAD9-HUS1-9-RAD (9-1-1) checkpoint complex to activate ATR in a phosphorylation dependent manner. To recruit TopBP1 to ATR, it is considered that BRCT5 in TopBP1 phospho-dependently interacts with the Bloom syndrome kinase (BLM) (Blackford et al. 2015). In addition to ATR, ATM also regulates TopBP1 by phosphorylating serine-1131 in TopBP1, and this phosphorylation enhances the ATR activity at DSBs (Yoo et al. 2007).

ATM/ATR like kinases preferentially phosphorylate their targets on SQ or TQ motifs (Traven and Heierhorst 2005). In our project, we identified one of these SQ motif within the GINI domain. This SQ motif may be a target for ATM to regulate TopBP1-GINS interaction in case of DNA damage. Our fluorescent polarization assay in collaboration with Matthew Day using the phosphorylated SQ motif of the GINI peptide and GINS tetramer showed that binding of TopBP1 to GINS is significantly reduced. This may indicate a switch-on/switch off mechanism for TopBP1 between DNA replication and DNA damage response. This probability will be investigated in detail in the Boos laboratory.

4.2. Isolated pre-RCs and recombinant proteins are tool to reconstitute the metazoan pre-IC *in vitro*

Replication origin firing is a highly regulated process that requires the stepwise assembly of the pre-IC from the inactive pre-RC to activate the CMG helicase. Although pre-IC formation is the main regulatory step of origin firing, it has been poorly understood in metazoan, in contrast to yeast pre-IC (Zaffar et al. 2022). Recent *in vitro* reconstitution studies of yeast pre-IC have revealed that Sld3-Sld7, Sld2, Dpb11 and Polε are the core firing factors and sufficient with Mcm2-7, GINS and Cdc45 to support origin firing (Yeeles et al. 2015; Yeeles et al. 2017).

In order to understand the molecular mechanisms of the pre-IC formation in vertebrates, the long-term aim of the Boos laboratory is to biochemically reconstitute pre-IC *in vitro* using recombinant proteins and the isolated pre-RCs. For this purpose, isolation of the pre-RCs from *Xenopus* egg extract has been optimized (by Milena Parlak). During this PhD thesis, the purification of the core origin firing factors, Treslin-MTBP, TopBP1, Polε, helicase components Cdc45 and GINS and kinases DDK and CDK have been completed. These recombinant proteins and kinases with isolated pre-RCs will help to understand better the molecular processes of the origin firing regulations.

5. Material & Methods

5.1. Purification of recombinant proteins

5.1.1. Purification of TopBP1 from Sf9 insect cells

Sf9 insect cells were grown as a suspension culture in insect cell media (Pan biotech, P04-850 500) at 27 °C. Baculoviruses were generated using pLIB-based constructs (Addgene, 80610). 500 ml Sf9 cells (1 x 106 cells/ml) were infected with a 1:100 dilution of recombinant baculovirus carrying an expression construct for TopBP1-1-766-Strep WT or mutants and were incubated at 27 °C for 72 hours. Cell pellets were lysed by douncing in 30 ml of lysis buffer (20 mM HEPES pH 8.0, 150 mM NaCl, 0.1 % (v/v) Tween-20, 0.5 mM TCEP, protease inhibitor cocktail (Roche complete protease inhibitor cocktail, 05056489001)). The lysate was centrifuged at 44800 g for 45 minutes, and the supernatant was loaded onto the StrepTrapHP-1ml column (Cytiva, 28907546) using an Äkta FPLC system. The bound protein was eluted with elution buffer (20 mM HEPES pH 8.0, 150 mM NaCl, 0.01 % Tween-20 (v/v), 0.5 mM TCEP, 2 % (v/v) glycerol, 2.5 mM desthiobiotin). (Day et al., 2023).

5.1.2. Purification of GINS from Sf9 insect cells

Sf9 insect cells cultured as described above were co-infected with 1:50 dilution of each four recombinant baculoviruses for expressing 6xHis-3xFlag-Sld5, Psf1, Psf2 and Psf3, respectively. 72 h post infection, pellets from one litre cells were lysed by douncing in 60 ml of lysis buffer (20 mM HEPES pH 8.0, 300 mM NaCl, 0.1% (v/v) Tween-20, 25 mM imidazole, 0.5 mM TCEP, protease inhibitor cocktail (Roche Complete protease inhibitor cocktail, 05056489001)). The lysate was centrifuged at 44800 g for 45 min and the supernatant was incubated with 2.5 ml Ni-NTA agarose beads (Qiagen,30210) for 1 h at 4°C. The bound protein was eluted with six bead volumes elution buffer (20 mM HEPES pH 8.0, 300 mM NaCl, 0.01% (v/v) Tween-20, 250 mM imidazole, 0.5 mM TCEP, 2% (v/v) glycerol). The eluate was dialysed into 20 mM HEPES pH 8.0, 150 mM NaCl, 0.01% (v/v) Tween-20, 0.5 mM TCEP, 2% (v/v) glycerol, and then applied onto an HiTrap HP Q anion exchange column (Cytiva, 17115301). To elute the bound protein, a linear gradient of NaCl (from 150 mM to 1 M) in elution buffer (20 mM HEPES pH8.0, 0.01% (v/v) Tween-20, 0.5mM TCEP, 2% (v/v) glycerol) was used. Peak fractions including GINS were pooled and loaded onto gel filtration column (running buffer: 20 mM HEPES pH8.0, 300mM NaCl, 0.01% (v/v) Tween-20, 0.5mM TCEP, 2% (v/v) glycerol). (Day et al., 2023).

5.1.3. Purification of geminin from *E.coli*

GST tagged Xenopus geminin (Xgeminin) in pGEX was purified from 6 l of Rosetta E. coli culture. Expression of GST-Xgeminin was induced with 1 mM IPTG at OD600 = 0.8 at 25 °C for overnight. Cells were harvested by centrifugation at 6000 rpm (JLA-8.1, Avanti JXN-26 Beckman Culture) for 15 min. Subsequently, cells were resuspended in lysis buffer (5 mg/ ml lysozyme, 20 mM Hepes pH 7.7, 200 mM NaCl, 5 mM β-mercaptoethanol, 5 % glycerin) and lysed by sonication. Cell suspension was centrifuged at 20000 rpm (SS-34, Sorvall RC 6 PLUS) for 20 min at 4 °C. Supernatant was incubated with glutathione-sepharose (GE Healthcare 17513201) for 3 h before elution with lysis buffer + 50 mM glutathion (Applichem A2084,0025)??? (buffer). Peak fractions were pooled and dialysed into XBE2 buffer (100 mM KCl, 2 mM MgCl2, 0.1 mM CaCl2, 1.71 % w:v sucrose, 5 mM K-EGTA, 10 mM HEPES-KOH, pH 7.7) and concentrated to 360 µM Xgeminin. Aliquots were frozen at - 80 °C. Recombinant geminin was purified by Milena Parlak (Day et al., 2023).

5.1.4. Purification of RecQ4 from Sf9 insect cells

Sf9 insect cells were grown as a suspension culture in insect cell media (Pan biotech, P04-850 500) at 27 °C. Baculoviruses were generated using pLIB-based constructs (Addgene, 80610). 500 ml Sf9 cells (1 x 106 cells/ml) were infected with a 1:100 dilution of recombinant baculovirus carrying an expression construct for RecQ4-Strep and were incubated at 27 °C for 72 hours. Cell pellets were lysed by douncing in 30 ml of lysis buffer (20 mM HEPES pH 8.0, 150 mM NaCl, 0.1 % (v/v) Tween-20, 0.5 mM TCEP, protease inhibitor cocktail (Roche complete protease inhibitor cocktail, 05056489001)). The lysate was centrifuged at 44800 g for 45 minutes, and the supernatant was loaded onto the StrepTrapHP-1ml column (Cytiva, 28907546) using an Äkta FPLC system. The bound protein was eluted with elution buffer (20 mM HEPES pH 8.0, 150 mM NaCl, 0.01 % Tween-20 (v/v), 0.5 mM TCEP, 2 % (v/v) glycerol, 2.5 mM desthiobiotin).

5.1.5. Purification of DNA polymerase epsilon from Sf9 insect cells

Sf9 insect cells cultured as described above were co-infected with 1:50 dilution of individual recombinant baculoviruses for expressing 6xHis-3xFlag-PolE11263-2287 and PolE2. 72 h post infection, pellets from one liter cells were lysed by douncing in 60 ml of lysis buffer (20 mM HEPES pH 8.0, 300 mM NaCl, 0.1% (v/v) Tween-20, 25 mM imidazole, 0.5 mM TCEP, protease inhibitor cocktail (Roche Complete protease inhibitor cocktail, 05056489001)). The lysate was centrifuged at 44800 g for 45 min and the supernatant was incubated with 2.5 ml Ni-NTA agarose beads (Qiagen,30210) for 1 h at 4°C. The bound protein was eluted with six bead volumes elution buffer (20 mM HEPES pH 8.0, 300 mM NaCl, 0.01% (v/v) Tween-20, 250

mM imidazole, 0.5 mM TCEP, 2% (v/v) glycerol). The eluate was dialysed into 20 mM HEPES pH 8.0, 150 mM NaCl, 0.01% (v/v) Tween-20, 0.5 mM TCEP, 2% (v/v) glycerol, and then applied onto an HiTrap HP Q anion exchange column (Cytiva, 17115301). To elute the bound protein, a linear gradient of NaCl (from 150 mM to 1 M) in elution buffer (20 mM HEPES pH8.0, 0.01% (v/v) Tween-20, 0.5mM TCEP, 2% (v/v) glycerol) was used. Peak fractions including Polε were pooled and loaded onto gel filtration column (running buffer: 20 mM HEPES pH8.0, 300mM NaCl, 0.01% (v/v) Tween-20, 0.5mM TCEP, 2% (v/v) glycerol).

5.1.6. Purification of Treslin1-1258-MTBP from Sf9 insect cells

Sf9 insect cells were grown as a suspension culture in insect cell media (Pan biotech, P04-850 500) at 27 °C. Baculoviruses were generated using pLIB-based constructs (Addgene, 80610). 2 liter Sf9 cells (1 x 106 cells/ml) were infected with a 1:50 dilution of recombinant baculovirus carrying an expression construct for MTBP-Strep and 6xHis-Treslin1-1258 and were incubated at 27 °C for 72 hours. Cell pellets were lysed by douncing in 120 ml of lysis buffer (20 mM HEPES pH 8.0, 500 mM NaCl, 0.1 % (v/v) Tween-20, 0.5 mM TCEP, 1 mM EDTA, protease inhibitor cocktail (Roche complete protease inhibitor cocktail, 05056489001)). The lysate was centrifuged at 44800 g for 45 minutes, and the supernatant was incubated with streptactin Sepharose beads (Cytiva, 28907546. The bound protein was eluted with elution buffer (20 mM HEPES pH 8.0, 150 mM NaCl, 0.01 % Tween-20 (v/v), 0.5 mM TCEP, 2 % (v/v) glycerol, 2.5 mM desthiobiotin). Peak fractions including Treslin1-1258-MTBP were pooled and loaded onto Superose 6 gel filtration column (running buffer: 20 mM HEPES pH8.0, 500mM NaCl, 0.01% (v/v) Tween-20, 0.5mM TCEP, 2% (v/v) glycerol).

5.1.7. Purification of Cdc45 from *E.coli*

N-terminally 6xHis-tagged human Cdc45 was cloned into pET28 plasmid and was purified from 1 l of Rosetta *E. coli* culture. Expression of 6xHis-Cdc45 was induced with 1 mM IPTG at OD600 = 0.8 at 20 °C over night. Cells were harvested by centrifugation at 6000 rpm (JLA-8.1, Avanti JXN-26 Beckman Culture) for 20 min. Subsequently, cells were resuspended in lysis buffer (20 mM Hepes pH 7.7, 300 mM NaCl, 1 mM DTT, 5 % glycerol) and lysed by sonication. Cell suspension was centrifuged at 20000 rpm (SS-34, Sorvall RC 6 PLUS) for 30 min at 4 °C. Supernatant was incubated with Ni-NTA agarose beads for 1 h before elution with 250 mM imidazole in lysis buffer. Peak fractions were pooled and dialysed into lysis buffer without imidazole (20 mM HEPES, 150 mM NaCl, 1 mM DTT, 0.01 % w:v Tween20, 5% w:v glycerol).

5.1.8. Purification of DDK from *E.coli*

N-terminally GST-tagged human CDC7/Dbf4 construct was provided by the Santocanale lab. This construct was transformed into Rosetta *E.coli* cells and was purified from 1 l of Rosetta *E. coli* culture. Expression of GST-Cdc7/Dbf4 was induced with 1 mM IPTG at OD600 = 0.8 at 20 °C over night. Cells were harvested by centrifugation at 6000 rpm (JLA-8.1, Avanti JXN-26 Beckman Culture) for 30 min. Subsequently, cells were resuspended in lysis buffer (20 mM Hepes pH 8.0, 150 mM NaCl, 1 mM DTT, 5 % glycerol) and lysed by sonication. Cell suspension was centrifuged at 20000 rpm (SS-34, Sorvall RC 6 PLUS) for 30 min at 4 °C. Supernatant was incubated with glutathione agarose beads for 1 h before elution with precision protease.

5.2.Biochemical methods

5.2.1. Pulldown of recombinant TopBP1 fragments by immobilized GINS

For in vitro pulldown experiments using recombinant GINS and TopBP1, magnetic anti-Flag beads (1 µl slurry for western blot/silver staining-scale experiments, 4 µl for Coomassie-scale experiments) were coupled with 600 ng (western/silver-scale) or 2400 ng (coomassie-scale) GINS via 3xFlag-Sld5. 100 nM final concentration of TopBP1-Strep-WT or mutants in 20□l (western/silver-scale) or 80 ul (coomassie-scale) of interaction buffer (20 mM HEPES pH8.0, 150mM NaCl, 0.01% (v/v) Tween-20, 0.5mM TCEP, 2% (v/v) glycerol) were added to GINS-coupled beads in 5 ul (western/silver-scale) or 20 µl (coomassie-scale) interaction buffer. The reaction was incubated for 45 min at 4°C rotating. Then, beads were washed three times for 5 min with interaction buffer and boiled in 50 µl Laemmli buffer (10% SDS, 200 mM Tris-HCL pH 6.0, 20% glycerol, 2.16 M β-mercaptoethanol,0.01% bromphenolblue) before SDS PAGE. (Day et al., 2023).

5.2.2. Pulldown from cell lysates with recombinant TopBP1-BRCT0-5-strep

For pulldown assays from soluble lysates non-transfected 293T cells, 5 µl streptactin Sepharose HP (Cytiva, 28935599) beads were coupled with 10 □g recombinant TopBP1-1-766-strep-WT or different mutants in coupling buffer (20 mM HEPES pH8.0, 150mM NaCl, 0.1% (v/v) Tween-20, 0.5mM TCEP, 2% (v/v) glycerol) for 45 min at 4 °C before washing two times with coupling buffer and then once in cell lysis buffer (20 mM HEPES pH8.0, 150mM NaCl, 0.1% (v/v) Tween-20, 0.5mM TCEP, 2% (v/v) glycerol, protease inhibitor cocktail (Roche Complete protease inhibitor cocktail, 05056489001). 293T cells were lysed in ten times pellet volume of cell lysis buffer, and centrifuged at 20000 g for 15 min at 4 °C. Soluble lysate from cells equivalent to 50 % of a 15 cm tissue culture plate was added to the TopBP1-coupled beads and incubated for 2 h at 4°C rotating. Beads were washed three times with 5 min incubation in lysis

buffer and boiled in 50 µl Laemmli buffer (10% SDS, 200 mM Tris-HCL pH 6.0, 20% glycerol, 2.16 M β-mercaptoethanol,0.01% bromphenolblue) before SDS PAGE. (Day et al., 2023).

5.2.3. Immunoprecipitations from transiently transfected 293T cells

Transient transfections of 293T cells (ATCC CRL-11268) were carried out as described using PEI (polyethyleneimine) according to a protocol kindly shared by David Cortez' lab. 4 µg plasmid DNA in 100 µl DMEM (Thermofisher, 41965039) without penicillin-streptomycin were combined with 2.4 µl Polyethylenimin (Sigma, 408727; 10 mg/ml) and incubated for 20 minutes before addition to 4 x 106 cells on a 10 cm dish. Transfected cells were used 72 h post transfection.

6xMyc-Tev2-TopBP1 was immunoprecipitated from native lysates of transiently transfected 293T cells. 72 h post transfection, 293T cells were lysed by douncing in ten times cell pellet volume of lysis buffer (20 mM HEPES pH8.0, 150mM NaCl, 0.1 % (v/v) Tween-20, 0.5mM TCEP, 2% (v/v) glycerol, protease inhibitor cocktail (Roche, Complete protease inhibitor cocktail, 05056489001)), and centrifuged at 20000 g for 15 min at 4 °C. The soluble fraction was added to magnetic anti-Myc beads (5 µl slurry per sample; Thermofischer, 88842) and incubated for 2 hours at 4 °C rotating. Cells equivalent to 50 % of a 15 cm dish were used per sample. Beads were washed three times in lysis buffer with 5 min incubation each, and finally boiled in 50 µl Laemmli buffer (10% SDS, 200 mM Tris-HCL pH 6.0, 20% glycerol, 2.16 M β-mercaptoethanol, 0.01% bromphenolblue). (Day et al., 2023).

5.2.4. Fluorescence polarisation experiments

Fluorescein-labelled peptides (WT: 'Flu'-GYGAPSEKHEQADEDLLSQYENG or LLPP: 'Flu'-GYGAPSEKHEQADEDPPSQYENG) (Peptide Protein Research Ltd, Bishops Waltham, UK) at a concentration of 100nM, were incubated at room temperature with increasing concentrations of GINS in 25 mM HEPES pH 7.5, 150 mM NaCl, 1 mM EDTA, 0.25 mM TCEP, 0.02 % (v/v) Tween 20 in a black 96-well polypropylene plate (VWR, Lutterworth, UK). Fluorescence polarisation was measured in a POLARstar Omega multimode microplate reader (BMG Labtech GmbH, Offenburg, Germany). Binding curves represent the mean of 3 independent experiments, with error bars of 1 standard deviation. (Experiment by Mtthew Day) (Day et al., 2023).

5.2.5. Generation of replicating *Xenopus* egg extracts

Xenopus laevis egg extracts were prepared from metaphase II arrested eggs as described in (1). After washing with MMR (100 mM NaCl, 2 mM KCl, 1 mM MgCl2, 2 mM CaCl2, 0.1 mM EDTA, 5 mM HEPES–NaOH, pH 7.8) eggs were dejellied (2% cysteine w:v in H2O,pH 7.8

with NaOH.). Subsequently, eggs were rinsed in XBE2 (100 mM KCl, 2 mM MgCl2, 0.1 mM CaCl2, 1.71 % w:v sucrose, 5 mM K-EGTA, 10 mM HEPES-KOH, pH 7.7). Eggs were transferred into centrifuge tubes containing 1 ml XBE2 + 10 µg/ ml protease inhibitor (aprotinin Sigma A6279, leupeptin Merck 108975, pepstatin Carl Roth 2936.1) + 100 µg/ ml cytochalasin D (Sigma C8273). For packing, eggs were centrifuged for 1 min at 1400 g at 16 °C in a swingout rotor. Excess buffer, activated and apoptotic eggs were removed before crushing the eggs at 16000 g for 10 min at 16 °C. Extract were collected with a 20 G needle and supplemented with 10 µg/ml cytochalasin D, 10 µg/ml protease inhibitors, 1:80 dilution of energy regenerator (1M phosphocreatine K salt, 600 µg/ ml creatine phosphokinase in 10 mM HEPES–KOH pH 7.6) and LFB1/50 (10% w:v sucrose, 50 mM KCl, 2 mM MgCl2, 1 mM EGTA, 2 mM DTT, 20 mM K2HPO4/KH2PO4 pH 8.0, 40 mM HEPES–KOH, pH 8.0.) to 15 % v:v. Extract was cleared at 84000 g at 4 °C for 20 min in a swingout rotor. The cytoplasmatic layer was collected and supplemented with 2 % glycerol v:v. Extract was frozen by dropping 20 µl aliqouts into liquid nitrogen and stored at - 80 °C. (Experiment by Milena Parlak) (Day et al., 2023).

5.2.6. Immunodepletion of TopBP1 from Xenopus egg extract

For XTopBP1 depletion from Xenopus egg extract, 0.5 µg antibody #1, #2 or IgG (rabbit) were coupled per µl magnetic Protein G dynabeads (Life Technologies 10004D) for 1 h at RT. Freshly thawed extracts were supplemented with 1/40 energy regenerator (1M phosphocreatine K salt, 600 µg/ ml creatine phosphokinase in 10 mM HEPES–KOH pH 7.6) and 250 µg/ml cycloheximide and released into interphase by adding 0.3 mM CaCl2 for 15 min at 23 °C. Subsequently, extracts were depleted for 45 min on ice with 0.675 µg antibody per µl extract. After depletion the extract was aliquoted, snap frozen and stored at - 80 °C for replication assays and chromatin isolations. (Experiment by Milena Parlak) (Day et al., 2023).

5.2.7. Replication analysis

Interphase Xenopus egg extracts were supplemented with 5 ng sperm DNA (kindly provided by the lab of O Stemmann) per µl extract and 50 nCi/µl α32P-dCTP (Perkin Elmer NEG513A250UC) at 23°C. 1 µl extract was spotted for each time point onto a glass fibre membrane. For addback experiments, 6 ng/ µl recombinant TopBP1 protein or buffer was added before sperm nuclei addition to TopBP1 depleted egg extract. Unbound α32P-dCTP was removed by rinsing the membrane three times 15 min with ice cold 5 % TCA in water and once with ice cold EtOH. Newly synthesized DNA was detected by phospho-imaging. (Experiment by Milena Parlak) (Day et al., 2023).

5.2.8. Chromatin isolation

For chromatin isolation, XTopBP1 depleted interphase egg extract was supplemented with 50 µg/ml aphidicolin and aliquoted into 15 µl samples before addition of buffer or recombinant TopBP1 to a final concentration 6 ng/µl. 2.25 µM geminin or buffer were added before incubation for 10 min on ice. To start the replication reaction 9 ng sperm DNA/µl (I think this is sperm DNA, not 9ng sperm) extract was added and incubated for 75 min at 23°C. Reactions were stopped with 300 µl ice cold ELB salt (10 mM HEPES-KOH pH 7.7, 50 mM KCl, 2.5 mM MgCl2) + 250 mM sucrose + 0.6 % triton X-100. Diluted extract was loaded onto 150 µl ELB salt + 25 % sucrose and centrifuged for 10 min at 2500 g at 4 °C in a swingout rotor. Liquid above the sucrose cushion was removed and the suface of the cushion was washed twice with 200 µl EBL salt containing 250 mM sucrose. Subsequently the cushion was removed leaving about 15 µl behind and centrifuged for 2 min at 10000 g at 4 °C in a fixed angle rotor to remove rest of the cushionFor western blotting, the chromatin pellet was resuspended in 24 µl 1x Laemmli SDS sample buffer (6.5 % glycerol, 715 mM β-mercaptoethanol, 3% SDS, 62.5 mM Tris-HCl pH 7.9, 0.005 % Bromphenol blue) and 5 µl were separated by denaturing SDS PAGE. (for anti-XCdc45 and anti-XSld5 samples were diluted again 1:5 before loading. (Experiment by Milena Parla) (Day et al., 2023).

5.2.9. BS3 crosslinking of TopBP1-BRCT0-5 and GINS

50 µg (7 µM) of each GINS and TopBP1-BRCT0-5-strep (amino acids 1-766) were incubated for 45 min on ice in cross-linking buffer (20mM HEPES pH8.0, 150mM NaCl, 0.01% Tween20, 2% Glycerol, 0.5mM TCEP). 600 µM or 2500 µM of BS3 crosslinker were added and incubated for 30 min at 35°C with shaking. The reaction was stopped by adding ammonium bicarbonate to a final concentration of 100 mM. 90 % of the cross-linked sample was used for mass spectrometry analysis of crosslinks. For mass spectrometry of gel-extracted samples, 10% of the reaction were separated by SDS-PAGE. The coomassie-stained gel was cut in slices above the molecular weight of monomeric TopBP1-BRCT0-5-strep for subsequent mass spectrometry. (Experiment with Heike Siegert) (Day et al., 2023).

5.2.10. Processing of BS3 crosslinked protein preparations for mass spectrometry

Sample preparation of crosslinked samples for LC/MS/MS is essentially based on the SP3 protocol published by (5). A volume corresponding to 30 µg of protein from each cross-linking sample was taken up in 100 µL 1× SP3 Lysis Buffer (final concentrations: 5% (wt/vol) SDS; 10 mM TCEP; 200 µL 40 mM Chloracetamide; 200 mM HEPES pH 8) and heated for 5 min at 90°C. After cooling the samples to room temperature (on ice) a mix of 150 µg hydrophobic (#65152105050250) and 150 µg hydrophilic (#45152105050250) SeraMag Speed Beads (Cytiva) was added to the denatured and alkylated protein containing solution (bead to protein

ratio 10 to 1) and gently mixed. Then 1 volume of 100% vol/vol Ethanol (EtOH) was added and the protein/bead/EtOH suspension was then incubated for 20 min at 24°C on a Thermomixer C (Eppendorf) while shaking at 1200 rpm. After this binding step, the beads collected on a magnet washed 4× with 80% EtOH (collection time on the magnet minimum of 4 min). After the final wash & collect step the beads were taken up in 25 mM Ammoniumbicarbonate (ABC) containing 1 µg Trypsin (Protein:Trypsin ratio 30:1). To help bead dissociation samples were incubated for 5 min in a sonification bath (preheated to 37°C). After this step samples were transferred to a Thermomixer C (preheated to 37°C) and incubated over night while shaking at 1300 rpm. Next morning the samples were acidified with formic acid (FA, final 1% vol/vol). The beads were collected on a magnet and the supernatant transferred to a fresh Eppendorf tube. The samples were then put again on a magnet for at least 5 min to remove remaining beads. The cleared tryptic digests were then desalted on home-made C18 StageTips as described (4). Briefly, peptides were immobilized and washed on a 2 disc C18 StageTip. After elution from the StageTips, samples were dried using a vacuum concentrator (Eppendorf) and the peptides were taken up in 0.1% formic acid solution (10 µL) and directly used for LC-MS/MS experiments (see below for details). (In collaboration with Prof. Dr. Farnusch Kahani) (Day et al., 2023).

5.2.11. Analytical size exclusion chromatography

TOPBP1 and GINS constructs were mixed in an equimolar ratio to give a final concentration of 20 uM of each component and incubated on ice for at least 30 minutes prior to application to a Superdex200increase 10 300 column (GE Healthcare, Little Chalfont, UK) equilibrated in 10 mM HEPES pH 7.5, 150 mM NaCl, 0.5 mM TCEP. (Experiment by Matthew Day) (Day et al., 2023).

5.2.12. SDS-PAGE

Discontinuous SDS-PAGE was employed to analyze protein samples based on their size. Protein separation was achieved using either self-made polyacrylamide gels with a concentration range of 5-14% and 10%, or precast gels with 4-12% (CriterionTM XT Bis-Tris Precast) and 3-8% (CriterionTM XT Tris-Acetate Precast). The stacking gels for the self-made gels were composed of 125 mM Tris (pH 6.9), 0.1% SDS, and 5.12% acrylamide. To denature the protein samples, they were boiled at 95 °C for 10 minutes in SDS loading buffer, which consisted of 6.5% glycerol, 715 mM β-mercaptoethanol, 3% SDS, 62.5 mM Tris-HCl (pH 7.9), and 0.005% Bromphenol blue. During separation, the protein samples were loaded onto the gels and subjected to a constant electrical voltage of 200 V for 45-75 minutes. The running buffer used for the self-made gels was Laemmli running buffer, containing 25 mM Tris base, 192 mM

glycine, and 0.5 g/l SDS. Alternatively, MOPS or MES buffer was used for Bis-Tris gels, and Tricine buffer for Tris-Acetate gels.

5.2.13. Western blot

In order to transfer proteins onto a nitrocellulose membrane, the following steps were taken. Firstly, proteins were separated using SDS-PAGE as described in section 5.2.1. The transfer of proteins was carried out at a constant voltage of 90 V for 90 minutes in an electrophoresis chamber filled with Towbin transfer buffer (containing 25 mM Tris base, 192 mM glycine, and 20% methanol). To maintain a cooled environment during the transfer, external ice and a sealed ice block were utilized. To confirm the successful protein transfer and to mark the protein leader for later size discrimination, the membrane was stained with Ponceau S. After this step, the membranes were rinsed with distilled water and then blocked for 10-30 minutes at room temperature (RT) using 1.5% BSA in TBST (comprising 135 mM NaCl, 2.5 mM KCl, 14 mM Tris HCl, 11 mM Tris base, and 0.01% Tween-20) to prevent non-specific binding of antibodies. To detect the proteins, the membrane was incubated overnight at 4 °C with specific antibodies listed in Table 5. Following the primary antibody incubation, the membranes were washed three times for 10 minutes each with TBST and subsequently incubated with an HRP-conjugated secondary antibody for 2 hours at RT. Finally, the detection of proteins was carried out using an appropriate method. Finally, the membranes underwent three washes with TBST, each lasting 10 minutes. To detect the secondary antibody through chemiluminescence, the membranes were coated with a 1:1 mixture of Clarity™ Western ECL Blotting Substrates, a peroxidase solution, and a luminol/enhancer solution. Signals were then detected at various time intervals using the Amersham Imager 600.

Table 2 Antibodies used for protein detection in Western Blot

name	**Antigen/source**
Anti-DB4	TopBP11-360, rabbit, self-made
Anti Sld5	Sld5/Rabbit, self-made
Anti-Flag	Flag peptide, mouse
Anti-53BP1	53BP1, rabbit
Anti-Myc	Myc tag, mouse
Anti-TopBP1 #1	XTopBP1 1-365, rabbit, self-made

Anti-TopBP1 #2	XTopBP1 999-1299, rabbit, self-made
Anti-XCdc45	XCdc45/ rabbit, self-made
Anti-XSld5	XSld5, rabbit, self-made
Anti-XPolE2	XPolE25, rabbit, self-made
Anti-Mcm6	Mcm6 775-821/ rabbit, BETHYL A300-194A
Anti-Mcm4	Mcm4 750-850/ rabbit, Abcam ab4459

5.2.14. Coomassie staining of proteins separated by SDS-PAGE

The proteins that were separated using SDS-PAGE were visualized by immersing the gels in Colloidal Coomassie staining solution, which consisted of 900 mM (NH4)2SO4, 12% Phosphoric Acid (v/v), and 1 mg/ml Coomassie Brilliant G-250, supplemented with 20% methanol. Following the staining process, the gels were destained using distilled water. Once destained, the gels were imaged using an Amersham Imager 600.

5.2.15. Silver staining of proteins separated by SDS-PAGE

The gels were incubated for 45 minutes in a fixation solution containing 50% methanol, 12% acidic acid, and 0.02% formaldehyde. After that, the gels were washed twice for 10 minutes each, first in 50% ethanol and then in 30% ethanol. Next, the gels were sensitized for 1 minute in a 0.014% sodium thiosulfate reagent and washed three times with H2O for 20 seconds each. The gels were then incubated for 20 minutes in a staining solution composed of 0.1% AgNO3 and 0.03% formaldehyde and washed twice with H2O for 20 seconds each. Subsequently, the gels were incubated with a developer solution containing 60 g/l Na2CO3, 0.02% formaldehyde, and 2 g/l Na2S2O3 x 5H2O. The protein staining was monitored, and when the bands became visible, the reaction was stopped by adding 5% acidic acid.

5.3. Computational modeling

We used the local implementation of AlphaFold-Multime (deepmind.com) to predict the binding interfaces of GINS and TopBP1 using the full-length sequence of each chain. 25 models were obtained by default and ranked with the combined score of ipTM+pTM implemented in AlphaFold-Multimer (13).

To gain more insights into the GINI binding region, we performed blind molecular docking calculations taking the GINI sequence DEDLLSQY of TopBP1 (residues 487-494) with Cluspro (14), HPEPDOCK (15), and MDockPeP (16) web servers, for 200 solutions per server. We further extended, refined, and re-scored the sampling, by generating 10 additional conformations per web server solution (for a total of 6000 solutions) with FlexPepDock (17). The top-10 best-scored solutions were selected for analysis and visualization.

The binding free energies of GINS with BRCT45 and GINI were estimated with the PRODIGY (18) and PPI-Affinity (19) web servers. For the estimations, the best scored AlphaFold model was used. The region of GINI employed for the estimation of the binding free energies comprised residues 481 to 496. (Experiment by Yasser Almeida-Hernandez) (Day et al., 2023).

5.4. Molecular biology methods

5.4.1. Polymerase chain reaction (PCR)

The process of DNA amplification using specific oligonucleotide primers was achieved through the Polymerase Chain Reaction (PCR). The PCRs were conducted using Phusion High-Fidelity DNA Polymerase (NEB) following the guidelines provided by the manufacturer. A thermal cycler was employed, and the amplification was carried out under the following cycling conditions:

Table 3 PCR cycling conditions

Time	Temperature	Cycles
5 min	98 °C	Initial denaturation
20 sec	98°C	30x
20 sec	65°C	
2 min	72°C	
5 min	72°C	1X

5.4.2. Agarose gel electrophoresis

DNA was subjected to agarose gel electrophoresis to separate it based on its size. The gels were prepared by boiling agarose with concentrations ranging from 0.75% to 2% in TAE buffer, which consisted of 8 mM Tris base, 0.02 mM EDTA, and 0.4 mM acetic acid. Once the solution cooled down, it was supplemented with DNA stain HDGreen (3 µl/50 ml TAE), and the gels were cast in an agarose gel electrophoresis chamber. After polymerization of the gels, the chamber was filled with TAE buffer. DNA samples were mixed with 1x DNA loading buffer and loaded onto the gel. To determine the size of DNA fragments, the DNA size standard

O'GeneRuler 1 kb DNA Ladder (Thermo Scientific) was loaded as a reference. Separation of DNA fragments based on their size was achieved by applying a constant voltage of 80-120 V for 30-60 minutes. A Gel Doc system (Bio-Rad) was utilized to visualize the DNA, which bound to HDGreen, by using UV light excitation. After visualizing the DNA, it was excised from the gel and purified for cloning purposes. The purification process was carried out using the NucleoSpin PCR and Gel-Clean Up Kits (Machery-Nagel) following the instructions provided by the manufacturer.

5.4.3. Cloning

To incorporate DNA fragments into plasmid vectors, the process involved several steps. Initially, the DNA fragments were amplified through PCR, utilizing primers that introduced restriction sites for the enzymes FseI (forward primer) or AscI (reverse primer). After amplification, both the DNA fragments and the plasmid vector underwent digestion with FseI and AscI enzymes, respectively. Following this, the DNA inserts were ligated into the vector with the aid of T4 DNA ligase (NEB). The ligation reaction was left to incubate overnight at 14 °C. Lastly, the plasmid vectors containing the integrated DNA fragments were purified using NucleoSpin PCR and Gel-Clean Up Kits (Machery-Nagel), following the manufacturer's instructions.

5.4.4. Transformation into the chemical competent *E. coli*

NEB5α and Rosetta E. coli cells were thawed while kept on ice, in preparation for DNA plasmid amplification. Chemically competent cells in the range of 10-20 µl were mixed with the appropriate amount of transforming DNA and incubated for 30 minutes on ice. Subsequently, the cells underwent heat shock at 42 °C for 45 seconds, followed by a 2-minute return to ice. E. coli cells were then supplemented with 90-180 µl of LB-medium and incubated at 37 °C for one hour. Finally, the cells were plated onto LB plates containing ampicillin for selection and incubated overnight at 37 °C.

5.4.5. Plasmid isolation from *E.coli*

To extract plasmid DNA from E. coli single colonies, individual colonies were selected from LB plates and placed in 5 ml of LB-medium with ampicillin. After an overnight incubation at 37 °C, the plasmid DNA was isolated using either NucleoSpin Plasmid Kits or NucleoSpin Midi Kit (Machery-Nagel), following the guidelines provided by the manufacturer.

5.4.6. Cell culture

Cell lines were maintained in incubators at a temperature of 37 °C with a CO2 concentration of 5%. To ensure sterility, media and solutions used for culturing the cell lines were passed through

a sterile filter. Biosafety cabinets were disinfected with 70% ethanol both before and after treating or splitting the cells. Before use, media and solutions were warmed to 37 °C in a water bath. For cell culturing, DMEM (Dulbecco's Modified Eagle Medium) containing 10% fetal calf serum and 1% penicillin/streptomycin was employed. Cell lines were split twice a week, involving the removal of spent cell culture media and washing of cells with DPBS (Dulbecco's Phosphate Buffered Saline). To detach the cells from the culture dish, TrypLE Express was used, and the incubation process lasted 2-5 minutes at 37 °C. Gentle dispersal of media over the cell layer surface facilitated cell dissociation. Subsequently, cells were resuspended, and the desired cell concentration was achieved by pipetting the appropriate volume into new cell culture dishes. Finally, the cells were returned to the incubator for further growth.

5.4.7. Transiently transfection of 239 T cells

Twenty-four hours prior to transfection, 0.8 x 10^6 239T cells were seeded onto a 6 cm dish. For calcium phosphate transfection, a mixture of 4.4 µg plasmid DNA listed in Table 7, 2 M CaCl2, 200 µl sterile filtered water, and 2x HEPES buffered saline was incubated for 5 minutes. During this time, 25 µl of chloroquine was added to the cells. Following the incubation, the cells were transfected with the prepared transfection mix. After 12-16 hours, the media was replaced with fresh DMEM containing 10% FCS and 1% penicillin/streptomycin. For proximity biotinylation, cells were processed according to the method described in section 5.5.4, starting 12 hours after the cells were supplemented with fresh medium.

Table 4 Buffers for purification

Buffer/Solution	Composition
Lysis buffer for TopBP1/ RecQ4 purification	20 mM HEPES pH 8.0 150 mM NaCl 0.1% w/v Tween20 0.5 mM TCEP 2% w/v glycerol Protease inhibitor coctail
Lysis buffer for GINS/Treslin-MTBP/ Polε/Cdc45 purification	20 mM HEPES pH 8.0 300 mM NaCl 0.1% w/v Tween20 0.5 mM TCEP 2% w/v glycerol 25 mM imidazole Protease inhibitor coctail

Elution buffer for TopBP1/RecQ4 purification	20 mM HEPES pH 8.0 150 mM NaCl 0.01% w/v Tween20 0.5 mM TCEP 2% w/v glycerol 2.5 mM desthiobiotin
Elution buffer for GINS/Treslin-MTBP/ Polε/Cdc45 purification	20 mM HEPES pH 8.0 300 mM NaCl 0.01% w/v Tween20 0.5 mM TCEP 2% w/v glycerol 250 mM imidazole
Lysis buffer for Treslin-MTBP purification	20 mM HEPES pH 8.0 500 mM NaCl 0.1% w/v Tween20 0.5 mM TCEP 2% w/v glycerol Protease inhibitor coctail
Elution buffer buffer for Treslin-MTBP purification	20 mM HEPES pH 8.0 500 mM NaCl 0.01% w/v Tween20 0.5 mM TCEP 2% w/v glycerol 2.5 mM desthiobiotin
Running buffer for Size exclusion chromatography for Treslin-MTBP	20 mM HEPES pH 8.0 500 mM NaCl 0.01% w/v Tween20 0.5 mM TCEP 2% w/v glycerol
	20 mM HEPES pH 8.0 300 mM NaCl 0.01% w/v Tween20

Running buffer for Size exclusion chromatography for GINS and Polε	0.5 mM TCEP 2% w/v glycerol

Table 5 GINS pulldown buffer

Coupling buffer	20mM HEPES pH 8.0 300 mM NaCl 2% glycerol 0.5mM TCEP 0.01% Tween20
Binding/wash buffer	20mM HEPES pH 8.0 150mM NaCl 2% glycerol 0.5mM TCEP 0.01% Tween20
Binding/wash buffer (less stringent conditions)	20mM HEPES pH 8.0 100mM NaAc 2% glycerol 0.5mM TCEP 0.01% Tween20

Table 6 buffers for western blot

3x SDS laemmli sample loading buffer	For 10ml: 2ml Glycerol 1.5ml β-mercaptoethanol 4.5ml 20% SDS 1.875ml 1M Tris HCl pH 6,9 0.125ml 1% Bromophenol Blue
Ponceau S (10 times)	2% ponceau S 30% trichloroacetic acid dd H_2O
TBST	TBS 0.1% Tween

Towbin (10 times)	250mM Tris base 1.92 M glycin 1:10 dilute before use, 20% methanol
Tris-buffered Saline (TBS) (10 times)	For 10 l: 800g NaCl 20g KCl 222g Tris HCl 132.5 g Tris Base pH 8,0

Table 7 Buffers for silver-staining and Coomassie-staining

Fixation solution	50 % methanol 12 % acidic acid 0.02 % formaldehyde
Quenching buffer	10 mM sodium azide 10 mM sodium ascorbate 5 mM Trolox in DPBS
Sensitizer solution	0.014 % sodium thiosulfate
Staining solution	0.1 % AgNO3 0.03 % formaldehyde
Colloidal Coomassie	900 mM (NH4)2SO4 12 % Phosphoric Acid (v/v) 1 mg/ml Coomassie Brilliant G-250

Table 8 Chemical and Components

Substance	**Company**
2 % Bis-Acrylamide	Bio-Rad Laboratories GmbH
40 % Acrylamide Solution	Bio-Rad Laboratories GmbH
Acetic Acid	VWR Chemicals
Agarose (for gel electrophoresis)	Carl Roth
AgNO3	Sigma-Aldrich
Ammonium Bicarbonate	Sigma-Aldrich
Aphidicolin	Sigma-Aldrich
APS	Merck
AscI (10,000 units/ml)	New England BioLabs
Bromphenol blue	AppliChem
BSA (Bovine Serum Albumin)	Carl Roth GmbH + Co. KG (Karlsruhe, Deutschland)

CaCl2	Carl Roth
Clarity™ Western ECL Substrate	Bio-Rad Laboratories GmbH (Hercules, USA)
cOmplete™, EDTA-free Protease Inhibitor Cocktail	Hoffmann-La Roche (Basel, Switzerland)
Coomassie blue	AppliChem (Darmstadt, Germany)
Desthiobiotin	Sigma-Aldrich (St. Louis, USA)
DMEM (Dulbecco's Modified Eagle Medium)	Thermos Fisher Scientific
DPBS (Dulbecco's Phosphate Buffered Saline)	Thermos Fisher Scientific
DTT Dithiothreitol	Sigma-Aldrich
EDTA Disodium Salt	AppliChem (Darmstadt, Germany)
Fetal Calf Serum	Thermos Fisher Scientific
Formaldehyde	Carl Roth
FseI (2,000 units/ml)	New England BioLabs
Gibco Penicillin-Streptomycin (10,000 U/ml)	Thermos Fisher Scientific
Glycerol	Carl Roth GmbH + Co. KG (Karlsruhe, Deutschland)
HDGreen Plus	Intas Science Imaging
HEPES	Carl Roth GmbH + Co. KG (Karlsruhe, Deutschland)
IPTG	Thermos Fisher Scientific
Isopropanol	Bernd Kraft
LB-Agar	Carl Roth
Methanol	Fisher Chemicals
NaAc	Sigma-Aldrich (St. Louis, USA)
NaCl	Thermo Fisher Scientific (Waltham, USA)
NaOH	Bernd Kraft
NEB 5-alpha	New England BioLabs
O'GeneRuler 1 kb	Thermos Fisher Scientific
Opti-MEM Thermo	Thermos Fisher Scientific
PageRulerTM Prestained Protein Ladder Thermo Fisher	Thermos Fisher Scientific
Phenylmethylsulfonyl fluoride (PMSF)	Carl Roth GmbH + Co. KG (Karlsruhe, Deutschland)
Phusion High-Fidelity DNA Polymerase	New England BioLabs
Ponceau S	Sigma-aldrich
Protein-ladder unstained	Thermo Fisher Scientific (Waltham, USA), 26614
SDS	Carl Roth

Sodium Thiosulfate	Sigma-Aldrich
Spodopan, Protein free medium with L-Glutamine and 0.35 g/L $NaHCO_3$	PAN Biotech (Aidenbach, Germany)
Streptactin Sepharose Beads	GE Healthcare
TCEP	Sigma-Aldrich (St. Louis, USA)
TEMED	Merck
Trichloroacetic Acid	AppliChem
Tris Hydrochloride	Carl Roth
Tris Base	Carl Roth
Tween® 20	AppliChem GmbH (Darmstadt, Germany)
XT MOPS buffer	Bio-Rad Laboratories GmbH (Hercules, USA)
XT Tricine Running Buffer	Bio-Rad Laboratories GmbH (Hercules, USA)
α32P-dCTP	Perkin Elmer
β-mercaptoethanol	Carl Roth

Table 9 List of kits

Kits	**Manufacturer**
NucleoBond Xtra Midi/Maxi	Machery-Nagel
NucleoSpin Gel- and PCR-Clean up	Machery-Nagel
NucleoSpin Plasmid	Machery-Nagel

Table 10 List of plasmids

Plasmid name	**Vector backbone**	**Recombinant protein**
BT702	pLib	TopBP1-766 LL489/490PP-Strep
BT707	pLib	TopBP11-766-Strep
BT708	pLib	TopBP11-766 RegionI-Strep
BT709	pLib	TopBP11-766 RegionII-Strep
BT710	pLib	TopBP11-766 RegionIII-Strep
BT711	pLib	TopBP11-766 Gcore-Strep
BT712	pLib	TopBP11-766 Gcc-Strep

BT735	pLib	TopBP11-766 SKK654/661/704VRE-Strep
BT759	pLib	TopBP11-549-Strep
BT760	pLib	TopBP11-549 Gcc-Strep
BT761	pLib	TopBP11-549-LL489/490PP-Strep
BT770	pLib	TopBP11-766 B4mut-Strep
BT772	pLib	TopBP11-766Gcc/B4mut-Strep
BT805	pLib	6xHis-3xFlag-Sld5
BT806	pLib	Psf1
BT807	pLib	Psf2
BT808	pLib	Psf3
BT781	pLib	Psf1 NK43/51AE
BT782	pLib	Psf1 KH63/66AE
DB54	pCS2	6xMyc-TEV2-TopBP11-766
DB58	pCS2	6xMyc-TEV2-TopBP11-549

Table 11 List of primers

Name	**Sequence**	**Purpose**
TopBP1 5'F	AATGGCCGGCCAatgtccagaaatgacaaagaacc	cloning
TopBP1 3'A_open	tatGGCGCGCCtGTGTACTCTAGGTCGTTTGAT	cloning

Table 12 List of consumables

Anti-FLAG® M2 Magnetic Beads	Sigma-Aldrich
Dishes (10cm)	Sarstedt AG & Co
Eppendorf tubes (1,5ml, 2ml)	Sarstedt AG & Co
Falcon tubes (15ml, 50ml)	Sarstedt AG & Co
Neubauer chamber	LO-Laboroptik Ltd

Nitrocellulose Membran Amersham Premium	GE Healthcare Europe
PhotonSlide™, Ultra-low Fluorescence Counting Slides	Logos Biosystems (Anyang-si, South Korea)
Pipette tips ClearLine Refill (10 µl, 200 µl, 1250 µl)	Kisker Biotech GmbH & Co.
Precast Gel, 5-14% Criterion™ XT Bis-Tris Protein Gel, 26 well, 15 µl	Bio-Rad Laboratories GmbH
Serological Pipette	Sarstedt AG & Co
Strep-Tactin Column	GE Healthcare Europe
Whatman Paper	GE Healthcare Europe GmbH

Table 13 List of equipments and devices

Equipment/Device	**Company**
Amersham Imager 600	GE Healthcare Europe GmbH
Avanti JXN-26 Centrifuge	Beckman Coulter
Axio vert. A1 microscope	Zeiss
Countess II	Thermo Fisher Scientific
Centrifuge 5427 R	Eppendorf AG
Centrifuge 5810 R	Eppendorf AG
Criterion™ Blotter	Bio-Rad Laboratories GmbH
Douncer	
Easypet	Eppendorf AG
Eppendorf Research® Plus	Eppendorf AG
ETTAN	GE Healthcare Europe GmbH
FPLC	GE Healthcare Europe GmbH
Gel electrophoresis camber	Bio-Rad Laboratories GmbH
Infors HT Multitron Incubator Shaker	Infors AG
Luna-FL Dual Fluorescence Cell Counter	Logos Biosystems
Microscope: PrimoVert	Carl Zeiss Microscopy GmbH
Mini-Protean Tetra Cell	Bio-Rad Laboratories GmbH
Pipetboy acu 2	INTEGRA Biosciences GmbH

Power Pac Basic Power Supply	Bio-Rad Laboratories GmbH
ProBlot™ Rocker 25	Labnet International
Test Tube Rotator	Labinco
Thermomixer Compact (1,5-2ml Aufsatz)	Eppendorf AG
Sorvall™ RC 6 Plus Centrifuge	Thermo Fisher Scientific
Vortex Genie 2	Scientific Industries, Inc.
Water bath WNB 14	Memmert GmbH + Co. KG

Table 14 List of software

Software	**Provider**
Fiji	Open source
Adobe Illustrator 2023	Adobe
Microsoft Office	Microsoft
SecMan Pro	DNA Star
SeqBuilder	DNA Star

6. References

Abid Ali, F., M. E. Douglas, J. Locke, V. E. Pye, A. Nans, J. F. X. Diffley, and A. Costa. 2017. 'Cryo-EM structure of a licensed DNA replication origin', *Nat Commun*, 8: 2241.

Adam, S., S. E. Rossi, N. Moatti, M. De Marco Zompit, Y. Xue, T. F. Ng, A. Alvarez-Quilon, J. Desjardins, V. Bhaskaran, G. Martino, D. Setiaputra, S. M. Noordermeer, T. K. Ohsumi, N. Hustedt, R. K. Szilard, N. Chaudhary, M. Munro, A. Veloso, H. Melo, S. Y. Yin, R. Papp, J. T. F. Young, M. Zinda, M. Stucki, and D. Durocher. 2021. 'The CIP2A-TOPBP1 axis safeguards chromosome stability and is a synthetic lethal target for BRCA-mutated cancer', *Nat Cancer*, 2: 1357-71.

Barry, E. R., A. T. McGeoch, Z. Kelman, and S. D. Bell. 2007. 'Archaeal MCM has separable processivity, substrate choice and helicase domains', *Nucleic Acids Res*, 35: 988-98.

Bell, S. P. 2002. 'The origin recognition complex: from simple origins to complex functions', *Genes Dev*, 16: 659-72.

Bell, S. P., and B. Stillman. 1992. 'ATP-dependent recognition of eukaryotic origins of DNA replication by a multiprotein complex', *Nature*, 357: 128-34.

Berezney, R., D. D. Dubey, and J. A. Huberman. 2000. 'Heterogeneity of eukaryotic replicons, replicon clusters, and replication foci', *Chromosoma*, 108: 471-84.

Bigot, N., M. Day, R. A. Baldock, F. Z. Watts, A. W. Oliver, and L. H. Pearl. 2019. 'Phosphorylation-mediated interactions with TOPBP1 couple 53BP1 and 9-1-1 to control the G1 DNA damage checkpoint', *Elife*, 8.

Blackford, A. N., J. Nieminuszczy, R. A. Schwab, Y. Galanty, S. P. Jackson, and W. Niedzwiedz. 2015. 'TopBP1 interacts with BLM to maintain genome stability but is dispensable for preventing BLM degradation', *Mol Cell*, 57: 1133-41.

Boos, D., and P. Ferreira. 2019. 'Origin Firing Regulations to Control Genome Replication Timing', *Genes (Basel)*, 10.

Boos, D., L. Sanchez-Pulido, M. Rappas, L. H. Pearl, A. W. Oliver, C. P. Ponting, and J. F. X. Diffley. 2011. 'Regulation of DNA Replication through Sld3-Dpb11 Interaction Is Conserved from Yeast to Humans', *Curr Biol*, 21: 1152-7.

Boos, D., M. Yekezare, and J. F. Diffley. 2013. 'Identification of a heteromeric complex that promotes DNA replication origin firing in human cells', *Science*, 340: 981-4.

Burrell, R. A., S. E. McClelland, D. Endesfelder, P. Groth, M. C. Weller, N. Shaikh, E. Domingo, N. Kanu, S. M. Dewhurst, E. Gronroos, S. K. Chew, A. J. Rowan, A. Schenk, M. Sheffer, M. Howell, M. Kschischo, A. Behrens, T. Helleday, J. Bartek, I. P. Tomlinson, and C. Swanton. 2013. 'Replication stress links structural and numerical cancer chromosomal instability', *Nature*, 494: 492-96.

Carroni, M., M. De March, B. Medagli, I. Krastanova, I. A. Taylor, H. Amenitsch, H. Araki, F. M. Pisani, A. Patwardhan, and S. Onesti. 2017. 'New insights into the GINS complex explain the controversy between existing structural models', *Sci Rep*, 7: 40188.

Chang, Y. P., G. Wang, V. Bermudez, J. Hurwitz, and X. S. Chen. 2007. 'Crystal structure of the GINS complex and functional insights into its role in DNA replication', *Proc Natl Acad Sci U S A*, 104: 12685-90.

Collart, C., G. E. Allen, C. R. Bradshaw, J. C. Smith, and P. Zegerman. 2013. 'Titration of four replication factors is essential for the Xenopus laevis midblastula transition', *Science*, 341: 893-6.

Costa, A., and J. F. X. Diffley. 2022. 'The Initiation of Eukaryotic DNA Replication', *Annu Rev Biochem*, 91: 107-31.

Costa, A., I. Ilves, N. Tamberg, T. Petojevic, E. Nogales, M. R. Botchan, and J. M. Berger. 2011. 'The structural basis for MCM2-7 helicase activation by GINS and Cdc45', *Nat Struct Mol Biol*, 18: 471-7.

Costa, A., L. Renault, P. Swuec, T. Petojevic, J. J. Pesavento, I. Ilves, K. MacLellan-Gibson, R. A. Fleck, M. R. Botchan, and J. M. Berger. 2014. 'DNA binding polarity, dimerization, and ATPase ring remodeling in the CMG helicase of the eukaryotic replisome', *Elife*, 3: e03273.

Coster, G., and J. F. X. Diffley. 2017. 'Bidirectional eukaryotic DNA replication is established by quasi-symmetrical helicase loading', *Science*, 357: 314-18.

De Jesus-Kim, L., L. J. Friedman, M. Looke, C. K. Ramsoomair, J. Gelles, and S. P. Bell. 2021. 'DDK regulates replication initiation by controlling the multiplicity of Cdc45-GINS binding to Mcm2-7', *Elife*, 10.

Deegan, T. D., J. T. Yeeles, and J. F. Diffley. 2016. 'Phosphopeptide binding by Sld3 links Dbf4-dependent kinase to MCM replicative helicase activation', *EMBO J*, 35: 961-73.

Diffley, J. F. X. 2001. 'DNA replication: building the perfect switch', *Curr Biol*, 11: R367-70.

Diffley, J.F.X. 1996. 'Once and only once upon a time: Specifying and regulating origins of DNA replication in eukaryotic cells', *Genes Dev.*, 10: 2819-30.

Dimitrova, D. S., and D. M. Gilbert. 1999. 'The spatial position and replication timing of chromosomal domains are both established in early G1 phase', *Mol Cell*, 4: 983-93.

Douglas, M. E., F. A. Ali, A. Costa, and J. F. X. Diffley. 2018. 'The mechanism of eukaryotic CMG helicase activation', *Nature*, 555: 265-68.

Douglas, M. E., and J. F. X. Diffley. 2016. 'Recruitment of Mcm10 to Sites of Replication Initiation Requires Direct Binding to the Minichromosome Maintenance (MCM) Complex', *J Biol Chem*, 291: 5879-88.

Drury, L. S., G. Perkins, and J. F. X. Diffley. 1997. 'The Cdc4/34/53 pathway targets Cdc6p for proteolysis in budding yeast', *EMBO J*, 16: 5966-76.

———. 2000. 'The cyclin-dependent kinase Cdc28p regulates distinct modes of Cdc6p proteolysis during the budding yeast cell cycle', *Curr Biol*, 10: 231-40.

Elsasser, S., Y. Chi, P. Yang, and J. L. Campbell. 1999. 'Phosphorylation controls timing of Cdc6p destruction: A biochemical analysis', *Mol Biol Cell*, 10: 3263-77.

Evrin, C., P. Clarke, J. Zech, R. Lurz, J. Sun, S. Uhle, H. Li, B. Stillman, and C. Speck. 2009. 'A double-hexameric MCM2-7 complex is loaded onto origin DNA during licensing of eukaryotic DNA replication', *Proc Natl Acad Sci U S A*, 106: 20240-5.

Ferreira, P., V. Hofer, N. Kronshage, A. Marko, K. U. Reusswig, B. Tetik, C. Diessel, K. Kohler, N. Tschernoster, J. Altmuller, N. Schulze, B. Pfander, and D. Boos. 2021. 'MTBP phosphorylation controls DNA replication origin firing', *Sci Rep*, 11: 4242.

Ferreira, P., L. Sanchez-Pulido, A. Marko, C. P. Ponting, and D. Boos. 2022. 'Refining the domain architecture model of the replication origin firing factor Treslin/TICRR', *Life Sci Alliance*, 5.

Francis, L. I., J. C. Randell, T. J. Takara, L. Uchima, and S. P. Bell. 2009. 'Incorporation into the prereplicative complex activates the Mcm2-7 helicase for Cdc7-Dbf4 phosphorylation', *Genes Dev*, 23: 643-54.

Frigola, J., J. He, K. Kinkelin, V. E. Pye, L. Renault, M. E. Douglas, D. Remus, P. Cherepanov, A. Costa, and J. F. X. Diffley. 2017. 'Cdt1 stabilizes an open MCM ring for helicase loading', *Nat Commun*, 8: 15720.

Frigola, J., D. Remus, A. Mehanna, and J. F. Diffley. 2013. 'ATPase-dependent quality control of DNA replication origin licensing', *Nature*, 495: 339-43.

Fu, Y. V., H. Yardimci, D. T. Long, A. Guainazzi, V. P. Bermudez, J. Hurwitz, A. van Oijen, O. D. Scharer, and J. C. Walter. 2011. 'Selective Bypass of a Lagging Strand Roadblock by the Eukaryotic Replicative DNA Helicase', *Cell*, 146: 931-41.

Fujisawa, T., and P. Filippakopoulos. 2017. 'Functions of bromodomain-containing proteins and their roles in homeostasis and cancer', *Nat Rev Mol Cell Biol*, 18: 246-62.

Gambus, A., R. C. Jones, A. Sanchez-Diaz, M. Kanemaki, F. van Deursen, R. D. Edmondson, and K. Labib. 2006. 'GINS maintains association of Cdc45 with MCM in replisome progression complexes at eukaryotic DNA replication forks', *Nat Cell Biol*, 8: 358-66.

Garcia, V., K. Furuya, and A. M. Carr. 2005. 'Identification and functional analysis of TopBP1 and its homologs', *DNA Repair (Amst)*, 4: 1227-39.

Georgoulis, A., C. E. Vorgias, G. P. Chrousos, and E. P. Rogakou. 2017. 'Genome Instability and gammaH2AX', *Int J Mol Sci*, 18.

Goswami, P., F. Abid Ali, M. E. Douglas, J. Locke, A. Purkiss, A. Janska, P. Eickhoff, A. Early, A. Nans, A. M. C. Cheung, J. F. X. Diffley, and A. Costa. 2018. 'Structure of DNA-CMG-Pol epsilon elucidates the roles of the non-catalytic polymerase modules in the eukaryotic replisome', *Nat Commun*, 9: 5061.

Greenberg, R. A., B. Sobhian, S. Pathania, S. B. Cantor, Y. Nakatani, and D. M. Livingston. 2006. 'Multifactorial contributions to an acute DNA damage response by BRCA1/BARD1-containing complexes', *Genes Dev*, 20: 34-46.

Greiwe, J. F., T. C. R. Miller, J. Locke, F. Martino, S. Howell, A. Schreiber, A. Nans, J. F. X. Diffley, and A. Costa. 2022. 'Structural mechanism for the selective phosphorylation of DNA-loaded MCM double hexamers by the Dbf4-dependent kinase', *Nat Struct Mol Biol*, 29: 10-20.

Guo, C., A. Kumagai, K. Schlacher, A. Shevchenko, A. Shevchenko, and W. G. Dunphy. 2015. 'Interaction of Chk1 with Treslin negatively regulates the initiation of chromosomal DNA replication', *Mol Cell*, 57: 492-505.

Hassan, B. H., L. A. Lindsey-Boltz, M. G. Kemp, and A. Sancar. 2013. 'Direct role for the replication protein treslin (Ticrr) in the ATR kinase-mediated checkpoint response', *J Biol Chem*, 288: 18903-10.

Havens, C. G., and J. C. Walter. 2011. 'Mechanism of CRL4(Cdt2), a PCNA-dependent E3 ubiquitin ligase', *Genes Dev*, 25: 1568-82.

Heller, R. C., S. Kang, W. M. Lam, S. Chen, C. S. Chan, and S. P. Bell. 2011. 'Eukaryotic Origin-Dependent DNA Replication In Vitro Reveals Sequential Action of DDK and S-CDK Kinases', *Cell*, 146: 80-91.

Huberman, J. A., and A. D. Riggs. 1968. 'On the mechanism of DNA replication in mammalian chromosomes', *J Mol Biol*, 32: 327-41.

Hyrien, O., K. Marheineke, and A. Goldar. 2003. 'Paradoxes of eukaryotic DNA replication: MCM proteins and the random completion problem', *Bioessays*, 25: 116-25.

Itou, H., S. Muramatsu, Y. Shirakihara, and H. Araki. 2014. 'Crystal structure of the homology domain of the eukaryotic DNA replication proteins Sld3/Treslin', *Structure*, 22: 1341-47.

Jones, M. L., Y. Baris, M. R. G. Taylor, and J. T. P. Yeeles. 2021. 'Structure of a human replisome shows the organisation and interactions of a DNA replication machine', *EMBO J*, 40: e108819.

Kamada, K., Y. Kubota, T. Arata, Y. Shindo, and F. Hanaoka. 2007. 'Structure of the human GINS complex and its assembly and functional interface in replication initiation', *Nat Struct Mol Biol*, 14: 388-96.

Kanemaki, M., and K. Labib. 2006. 'Distinct roles for Sld3 and GINS during establishment and progression of eukaryotic DNA replication forks', *EMBO J*, 25: 1753-63.

Kanemaki, M., A. Sanchez-Diaz, A. Gambus, and K. Labib. 2003. 'Functional proteomic identification of DNA replication proteins by induced proteolysis in vivo', *Nature*, 423: 720-4.

Kang, S., M. D. Warner, and S. P. Bell. 2014. 'Multiple functions for Mcm2-7 ATPase motifs during replication initiation', *Mol Cell*, 55: 655-65.

Kelly, R. L., A. M. Huehls, A. Venkatachalam, C. J. Huntoon, Y. J. Machida, and L. M. Karnitz. 2022. 'Intra-S phase checkpoint kinase Chk1 dissociates replication proteins Treslin and TopBP1 through multiple mechanisms during replication stress', *J Biol Chem*, 298: 101777.

Knott, S. R., J. M. Peace, A. Z. Ostrow, Y. Gan, A. E. Rex, C. J. Viggiani, S. Tavare, and O. M. Aparicio. 2012. 'Forkhead transcription factors establish origin timing and long-range clustering in S. cerevisiae', *Cell*, 148: 99-111.

Kohler, K., L. Sanchez-Pulido, V. Hofer, A. Marko, C. P. Ponting, A. P. Snijders, R. Feederle, A. Schepers, and D. Boos. 2019. 'The Cdk8/19-cyclin C transcription regulator functions in genome replication through metazoan Sld7', *PLoS Biol*, 17: e2006767.

Kubota, Y., Y. Takase, Y. Komori, Y. Hashimoto, T. Arata, Y. Kamimura, H. Araki, and H. Takisawa. 2003. 'A novel ring-like complex of Xenopus proteins essential for the initiation of DNA replication', *Genes Dev*, 17: 1141-52.

Kumagai, A., and W. G. Dunphy. 2017. 'MTBP, the Partner of Treslin, Contains a Novel DNA-Binding Domain That Is Essential for Proper Initiation of DNA Replication', *Mol Biol Cell*.

Kumagai, A., J. Lee, H. Y. Yoo, and W. G. Dunphy. 2006. 'TopBP1 activates the ATR-ATRIP complex', *Cell*, 124: 943-55.

Kumagai, A., A. Shevchenko, and W. G. Dunphy. 2010. 'Treslin collaborates with TopBP1 in triggering the initiation of DNA replication', *Cell*, 140: 349-59.

———. 2011. 'Direct regulation of Treslin by cyclin-dependent kinase is essential for the onset of DNA replication', *J Cell Biol*, 193: 995-1007.

Labib, K., J. F. X. Diffley, and S. E. Kearsey. 1999. 'G1-phase and B-type cyclins exclude the DNA-replication factor Mcm4 from the nucleus', *Nat Cell Biol*, 1: 415-22.

Laine, A., S. G. Nagelli, C. Farrington, U. Butt, A. N. Cvrljevic, J. P. Vainonen, F. M. Feringa, T. J. Gronroos, P. Gautam, S. Khan, H. Sihto, X. Qiao, K. Pavic, D. C. Connolly, P. Kronqvist, L. L. Elo, J. Maurer, K. Wennerberg, R. H. Medema, H. Joensuu, E. Peuhu, K. de Visser, G. Narla, and J. Westermarck. 2021. 'CIP2A Interacts with TopBP1 and Drives Basal-Like Breast Cancer Tumorigenesis', *Cancer Res*, 81: 4319-31.

Langston, L. D., D. Zhang, O. Yurieva, R. E. Georgescu, J. Finkelstein, N. Y. Yao, C. Indiani, and M. E. O'Donnell. 2014. 'CMG helicase and DNA polymerase epsilon form a functional 15-subunit holoenzyme for eukaryotic leading-strand DNA replication', *Proc Natl Acad Sci U S A*, 111: 15390-5.

Leonard, A. C., and M. Mechali. 2013. 'DNA replication origins', *Cold Spring Harb Perspect Biol*, 5: a010116.

Leonhardt, H., H. P. Rahn, P. Weinzierl, A. Sporbert, T. Cremer, D. Zink, and M. C. Cardoso. 2000. 'Dynamics of DNA replication factories in living cells', *J Cell Biol*, 149: 271-80.

Lewis, J. S., M. H. Gross, J. Sousa, S. S. Henrikus, J. F. Greiwe, A. Nans, J. F. X. Diffley, and A. Costa. 2022. 'Mechanism of replication origin melting nucleated by CMG helicase assembly', *Nature*, 606: 1007-14.

Lopez-Mosqueda, J., N. L. Maas, Z. O. Jonsson, L. G. Defazio-Eli, J. Wohlschlegel, and D. P. Toczyski. 2010. 'Damage-induced phosphorylation of Sld3 is important to block late origin firing', *Nature*, 467: 479-83.

MacNeill, S. A. 2010. 'Structure and function of the GINS complex, a key component of the eukaryotic replisome', *Biochem J*, 425: 489-500.

Makiniemi, M., T. Hillukkala, J. Tuusa, K. Reini, M. Vaara, D. Huang, H. Pospiech, I. Majuri, T. Westerling, T. P. Makela, and J. E. Syvaoja. 2001. 'BRCT domain-containing protein TopBP1 functions in DNA replication and damage response', *J Biol Chem*, 276: 30399-406.

Mantiero, D., A. Mackenzie, A. Donaldson, and P. Zegerman. 2011. 'Limiting replication initiation factors execute the temporal programme of origin firing in budding yeast', *EMBO J*, 30: 4805-14.

Marinsek, N., E. R. Barry, K. S. Makarova, I. Dionne, E. V. Koonin, and S. D. Bell. 2006. 'GINS, a central nexus in the archaeal DNA replication fork', *EMBO Rep*, 7: 539-45.

Marshall, C. J., and T. J. Santangelo. 2020. 'Archaeal DNA Repair Mechanisms', *Biomolecules*, 10.

Masumoto, H., S. Muramatsu, Y. Kamimura, and H. Araki. 2002. 'S-Cdk-dependent phosphorylation of Sld2 essential for chromosomal DNA replication in budding yeast', *Nature*, 415: 651-5.

Matsuno, K., M. Kumano, Y. Kubota, Y. Hashimoto, and H. Takisawa. 2006. 'The N-terminal noncatalytic region of Xenopus RecQ4 is required for chromatin binding of DNA polymerase alpha in the initiation of DNA replication', *Mol Cell Biol*, 26: 4843-52.

Maya-Mendoza, A., P. Olivares-Chauvet, A. Shaw, and D. A. Jackson. 2010. 'S phase progression in human cells is dictated by the genetic continuity of DNA foci', *PLoS Genet*, 6: e1000900.

Mordes, D. A., G. G. Glick, R. Zhao, and D. Cortez. 2008. 'TopBP1 activates ATR through ATRIP and a PIKK regulatory domain', *Genes Dev*, 22: 1478-89.

Muramatsu, S., K. Hirai, Y. S. Tak, Y. Kamimura, and H. Araki. 2010. 'CDK-dependent complex formation between replication proteins Dpb11, Sld2, Pol (epsilon}, and GINS in budding yeast', *Genes Dev*, 24: 602-12.

Nakamura, H., T. Morita, and C. Sato. 1986. 'Structural organizations of replicon domains during DNA synthetic phase in the mammalian nucleus', *Exp Cell Res*, 165: 291-7.

Natsume, T., C. A. Muller, Y. Katou, R. Retkute, M. Gierlinski, H. Araki, J. J. Blow, K. Shirahige, C. A. Nieduszynski, and T. U. Tanaka. 2013. 'Kinetochores coordinate pericentromeric cohesion and early DNA replication by Cdc7-Dbf4 kinase recruitment', *Mol Cell*, 50: 661-74.

Nguyen, V. Q., C. Co, and J. J. Li. 2001. 'Cyclin-dependent kinases prevent DNA re-replication through multiple mechanisms', *Nature*, 411: 1068-73.

Peters, J. M. 2002. 'The anaphase-promoting complex: proteolysis in mitosis and beyond', *Mol Cell*, 9: 931-43.

Pfander, B., and J. F.X. Diffley. 2011. 'Dpb11 coordinates Mec1 kinase activation with cell cycle-regulated Rad9 recruitment', *EMBO J*, 30: 4897-907.

Rahman, S., M. E. Sowa, M. Ottinger, J. A. Smith, Y. Shi, J. W. Harper, and P. M. Howley. 2011. 'The Brd4 extraterminal domain confers transcription activation independent of pTEFb by recruiting multiple proteins, including NSD3', *Mol Cell Biol*, 31: 2641-52.

Randell, J. C., A. Fan, C. Chan, L. I. Francis, R. C. Heller, K. Galani, and S. P. Bell. 2010. 'Mec1 Is One of Multiple Kinases that Prime the Mcm2-7 Helicase for Phosphorylation by Cdc7', *Mol Cell*, 40: 353-63.

Remus, D., F. Beuron, G. Tolun, J. D. Griffith, E. P. Morris, and J. F. X. Diffley. 2009. 'Concerted loading of Mcm2-7 double hexamers around DNA during DNA replication origin licensing', *Cell*, 139: 719-30.

Reusswig, K. U., F. Zimmermann, L. Galanti, and B. Pfander. 2016. 'Robust Replication Control Is Generated by Temporal Gaps between Licensing and Firing Phases and Depends on Degradation of Firing Factor Sld2', *Cell Rep*, 17: 556-69.

Rhind, N. 2006. 'DNA replication timing: random thoughts about origin firing', *Nat Cell Biol*, 8: 1313-6.

Rzechorzek, N. J., S. W. Hardwick, V. A. Jatikusumo, D. Y. Chirgadze, and L. Pellegrini. 2020. 'CryoEM structures of human CMG-ATPgammaS-DNA and CMG-AND-1 complexes', *Nucleic Acids Res*, 48: 6980-95.

Sadoni, N., M. C. Cardoso, E. H. Stelzer, H. Leonhardt, and D. Zink. 2004. 'Stable chromosomal units determine the spatial and temporal organization of DNA replication', *J Cell Sci*, 117: 5353-65.

Sakasai, R., A. Sakai, M. Iimori, S. Kiyonari, K. Matsuoka, Y. Kakeji, H. Kitao, and Y. Maehara. 2012. 'CtIP- and ATR-dependent FANCJ phosphorylation in response to DNA strand breaks mediated by DNA replication', *Genes Cells*, 17: 962-70.

Saleh, A., Y. Noguchi, R. Aramayo, M. E. Ivanova, K. M. Stevens, A. Montoya, S. Sunidhi, N. L. Carranza, M. J. Skwark, and C. Speck. 2022. 'The structural basis of Cdc7-Dbf4 kinase dependent targeting and phosphorylation of the MCM2-7 double hexamer', *Nat Commun*, 13: 2915.

Sangrithi, M. N., J. A. Bernal, M. Madine, A. Philpott, J. Lee, W. G. Dunphy, and A. R. Venkitaraman. 2005. 'Initiation of DNA replication requires the RECQL4 protein mutated in Rothmund-Thomson syndrome', *Cell*, 121: 887-98.

Sansam, C. G., D. Goins, J. C. Siefert, E. A. Clowdus, and C. L. Sansam. 2015. 'Cyclin-dependent kinase regulates the length of S phase through TICRR/TRESLIN phosphorylation', *Genes Dev*, 29: 555-66.

Sansam, C. G., K. Pietrzak, B. Majchrzycka, M. A. Kerlin, J. Chen, S. Rankin, and C. L. Sansam. 2018. 'A mechanism for epigenetic control of DNA replication', *Genes Dev*, 32: 224-29.

Sclafani, R. A., and T. M. Holzen. 2007. 'Cell cycle regulation of DNA replication', *Annu Rev Genet*, 41: 237-80.

Shima, N., A. Alcaraz, I. Liachko, T. R. Buske, C. A. Andrews, R. J. Munroe, S. A. Hartford, B. K. Tye, and J. C. Schimenti. 2007. 'A viable allele of Mcm4 causes chromosome instability and mammary adenocarcinomas in mice', *Nat Genet*, 39: 93-8.

Siddiqui, K., K. F. On, and J. F. Diffley. 2013. 'Regulating DNA replication in eukarya', *Cold Spring Harb Perspect Biol*, 5.

Sporbert, A., A. Gahl, R. Ankerhold, H. Leonhardt, and M. C. Cardoso. 2002. 'DNA polymerase clamp shows little turnover at established replication sites but sequential de novo assembly at adjacent origin clusters', *Mol Cell*, 10: 1355-65.

Sun, L., Y. Huang, R. A. Edwards, S. Yang, A. N. Blackford, W. Niedzwiedz, and J. N. M. Glover. 2017. 'Structural Insight into BLM Recognition by TopBP1', *Structure*, 25: 1582-88 e3.

Tada, S., A. Li, D. Maiorano, M. Mechali, and J. J. Blow. 2001. 'Repression of origin assembly in metaphase depends on inhibition of RLF- B/Cdt1 by geminin', *Nat Cell Biol*, 3: 107-13.

Tak, Y. S., Y. Tanaka, S. Endo, Y. Kamimura, and H. Araki. 2006. 'A CDK-catalysed regulatory phosphorylation for formation of the DNA replication complex Sld2-Dpb11', *EMBO J*, 25: 1987-96.

Takayama, Y., Y. Kamimura, M. Okawa, S. Muramatsu, A. Sugino, and H. Araki. 2003. 'GINS, a novel multiprotein complex required for chromosomal DNA replication in budding yeast', *Genes Dev*, 17: 1153-65.

Tanaka, S. 2021. 'Interaction of replication factor Sld3 and histone acetyl transferase Esa1 alleviates gene silencing and promotes the activation of late and dormant replication origins', *Genetics*, 217: 1-11.

Tanaka, S., and H. Araki. 2010. 'Regulation of the initiation step of DNA replication by cyclin-dependent kinases', *Chromosoma*, 119: 565-74.

———. 2011. 'Multiple regulatory mechanisms to inhibit untimely initiation of DNA replication are important for stable genome maintenance', *PLoS Genet*, 7: e1002136.

———. 2013. 'Helicase activation and establishment of replication forks at chromosomal origins of replication', *Cold Spring Harb Perspect Biol*, 5: a010371.

Tanaka, S., and J. F. X. Diffley. 2002. 'Deregulated G1-cyclin expression induces genomic instability by preventing efficient pre-RC formation', *Genes Dev*, 16: 2639-49.

Tanaka, S., Y. Komeda, T. Umemori, Y. Kubota, H. Takisawa, and H. Araki. 2013. 'Efficient initiation of DNA replication in eukaryotes requires Dpb11/TopBP1-GINS interaction', *Mol Cell Biol*, 33: 2614-22.

Tanaka, S., T. Umemori, K. Hirai, S. Muramatsu, Y. Kamimura, and H. Araki. 2007. 'CDK-dependent phosphorylation of Sld2 and Sld3 initiates DNA replication in budding yeast', *Nature*, 445: 328-32.

Ticau, S., L. J. Friedman, N. A. Ivica, J. Gelles, and S. P. Bell. 2015. 'Single-molecule studies of origin licensing reveal mechanisms ensuring bidirectional helicase loading', *Cell*, 161: 513-25.

Toledo, L. I., M. Altmeyer, M. B. Rask, C. Lukas, D. H. Larsen, L. K. Povlsen, S. Bekker-Jensen, N. Mailand, J. Bartek, and J. Lukas. 2013. 'ATR prohibits replication catastrophe by preventing global exhaustion of RPA', *Cell*, 155: 1088-103.

Traven, A., and J. Heierhorst. 2005. 'SQ/TQ cluster domains: concentrated ATM/ATR kinase phosphorylation site regions in DNA-damage-response proteins', *Bioessays*, 27: 397-407.

Volpi, I., P. J. Gillespie, G. S. Chadha, and J. J. Blow. 2021. 'The role of DDK and Treslin-MTBP in coordinating replication licensing and pre-initiation complex formation', *Open Biol*, 11: 210121.

Wang, J., Z. Gong, and J. Chen. 2011. 'MDC1 collaborates with TopBP1 in DNA replication checkpoint control', *J Cell Biol*, 193: 267-73.

Wohlschlegel, J. A., B. T. Dwyer, S. K. Dhar, C. Cvetic, J. C. Walter, and A. Dutta. 2000. 'Inhibition of eukaryotic DNA replication by geminin binding to Cdt1', *Science*, 290: 2309-12.

Wong, P. G., S. L. Winter, E. Zaika, T. V. Cao, U. Oguz, J. M. Koomen, J. L. Hamlin, and M. G. Alexandrow. 2011. 'Cdc45 limits replicon usage from a low density of preRCs in mammalian cells', *PLoS One*, 6: e17533.

Yamane, K., M. Kawabata, and T. Tsuruo. 1997. 'A DNA-topoisomerase-II-binding protein with eight repeating regions similar to DNA-repair enzymes and to a cell-cycle regulator', *Eur J Biochem*, 250: 794-9.

Yeeles, J. T., T. D. Deegan, A. Janska, A. Early, and J. F. Diffley. 2015. 'Regulated eukaryotic DNA replication origin firing with purified proteins', *Nature*, 519: 431-5.

Yeeles, J. T., A. Janska, A. Early, and J. F. Diffley. 2017. 'How the Eukaryotic Replisome Achieves Rapid and Efficient DNA Replication', *Mol Cell*, 65: 105-16.

Yekezare, M., B. Gomez-Gonzalez, and J. F. Diffley. 2013. 'Controlling DNA replication origins in response to DNA damage - inhibit globally, activate locally', *J Cell Sci*, 126: 1297-306.

Yoo, H. Y., A. Kumagai, A. Shevchenko, A. Shevchenko, and W. G. Dunphy. 2007. 'Ataxia-telangiectasia mutated (ATM)-dependent activation of ATR occurs through phosphorylation of TopBP1 by ATM', *J Biol Chem*, 282: 17501-6.

Yuan, Z., L. Bai, J. Sun, R. Georgescu, J. Liu, M. E. O'Donnell, and H. Li. 2016. 'Structure of the eukaryotic replicative CMG helicase suggests a pumpjack motion for translocation', *Nat Struct Mol Biol*, 23: 217-24.

Yuan, Z., R. Georgescu, G. D. Schauer, M. E. O'Donnell, and H. Li. 2020. 'Structure of the polymerase epsilon holoenzyme and atomic model of the leading strand replisome', *Nat Commun*, 11: 3156.

Zaffar, E., P. Ferreira, L. Sanchez-Pulido, and D. Boos. 2022. 'The Role of MTBP as a Replication Origin Firing Factor', *Biology (Basel)*, 11.

Zegerman, P., and J. F. X. Diffley. 2007. 'Phosphorylation of Sld2 and Sld3 by cyclin-dependent kinases promotes DNA replication in budding yeast', *Nature*, 445: 281-5.

———. 2010. 'Checkpoint-dependent inhibition of DNA replication initiation by Sld3 and Dbf4 phosphorylation', *Nature*, 467: 474-8.

Zou, L., and B. Stillman. 1998. 'Formation of a preinitiation complex by S-phase cyclin CDK-dependent loading of Cdc45p onto chromatin', *Science*, 280: 593-6.

7. Extended Data

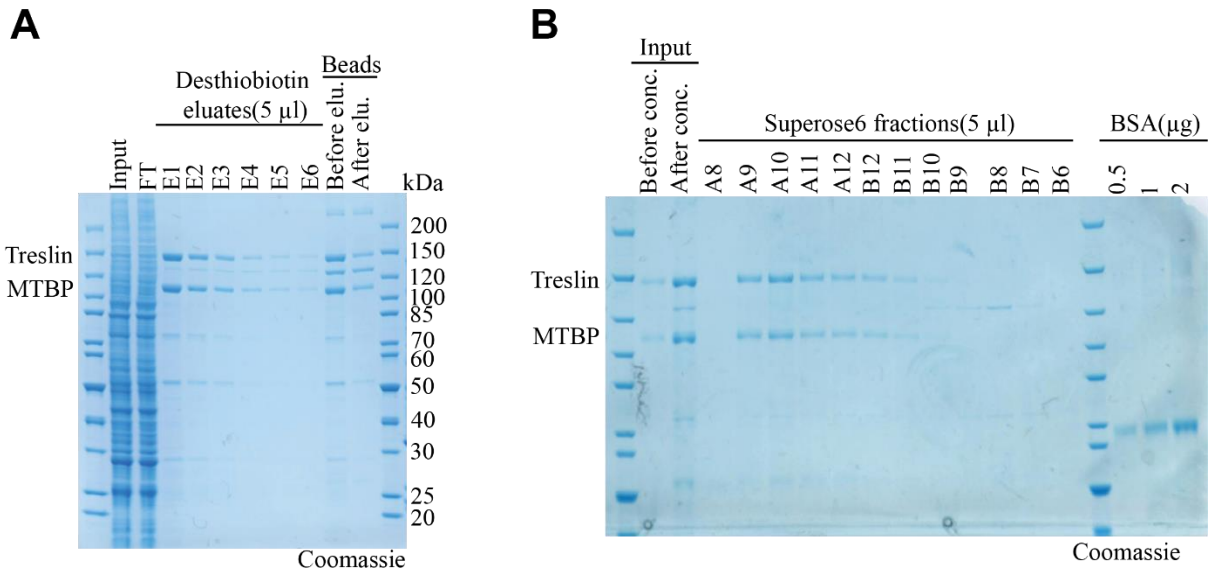

Extended figure 1. Purification of Treslin-MTBP
Treslin-MTBP was purified from Sf9 insect cells. Sf9 insect cells were co-infected with the individual viruses of 6xHis-Treslin1-1258 and MTBP-strep. **A)** The soluble lysate of the infected Sf9 cells was first applied onto the strep-tag affinity beads. The purification was analysed by Coomassie stained SD PAGE gel. **B)** The eluates from the strep-tag affinity purification were pooled and concentrated, and subsequently loaded to the size exclusion chromatography. The purification analysed using Coomassie stained SDS gel.

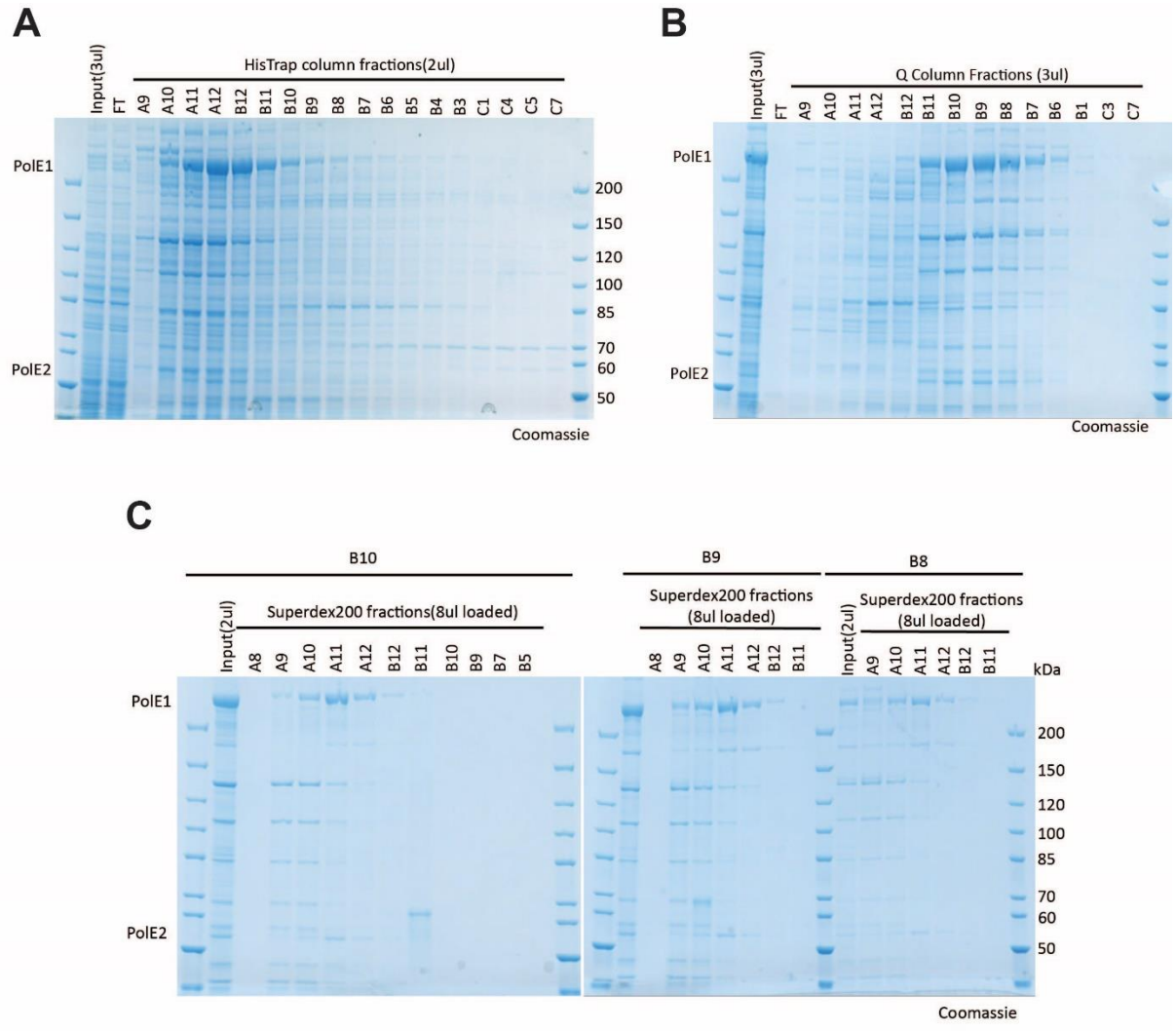

Extended figure 2. Purification of Pol ε

Pol ε was purified from Sf9 insect cells as a complex. For this, Sf9 cells were co-infected with the individual viruses of 6xHis-3xFlag-PolE1 and PolE2. **A)** the soluble lysate was first loaded to the His-tag affinity column using FPLC. The purification was analysed by Coomassie stained SDS gel. **B)** The peak fractions of the his-tag affinity column, from A10 to B11, were pooled and loaded to the anion exchange column on FPLC. Coomassie stained SD gel was used for the analysis of the purification. **C)** the peak fractions of the anion exchange chromatography, B10, B9 and B8, were separately run on size exclusion chromatography. Analysis was done with Coomassie-stained SDS gel.

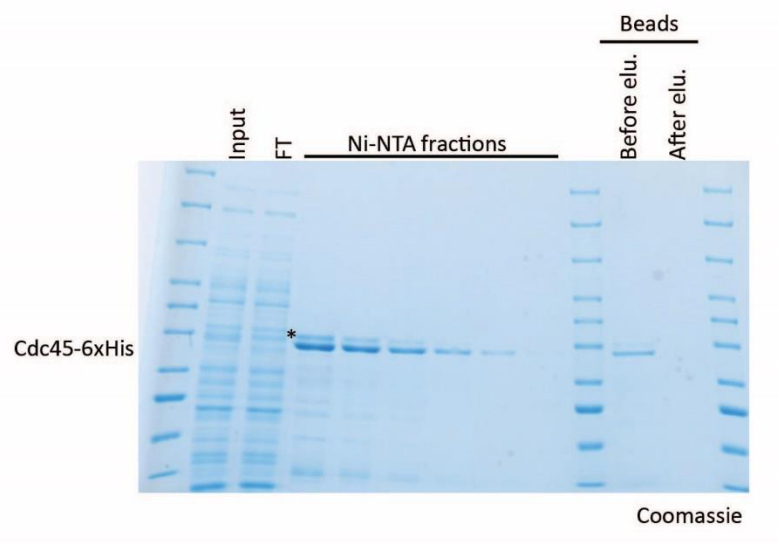

Extended figure 3. Purification of Cdc45
Cdc45-6xHis was purified from E.coli using Ni-NTA agarose beads by Yannik Glahn. The purification was analysed by Coomassie stained SDS gel.

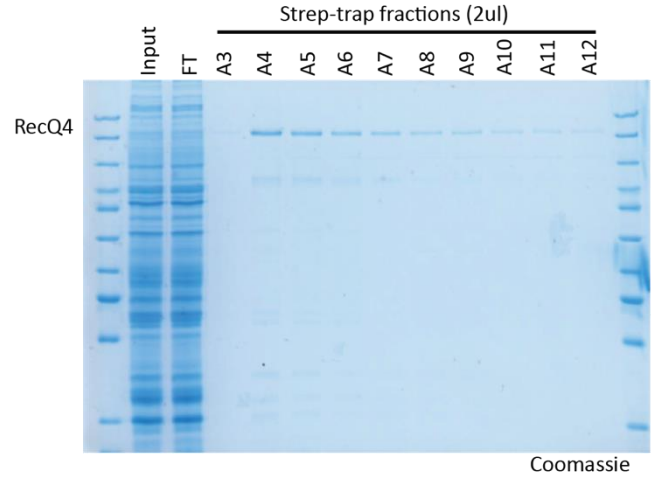

Extended figure 4. Purification of RecQ4
RecQ4-strep was purified from Sf9 insect cells using strep-tag affinity chromatography. Analysis was done with Coomassie-stained SDS gel.

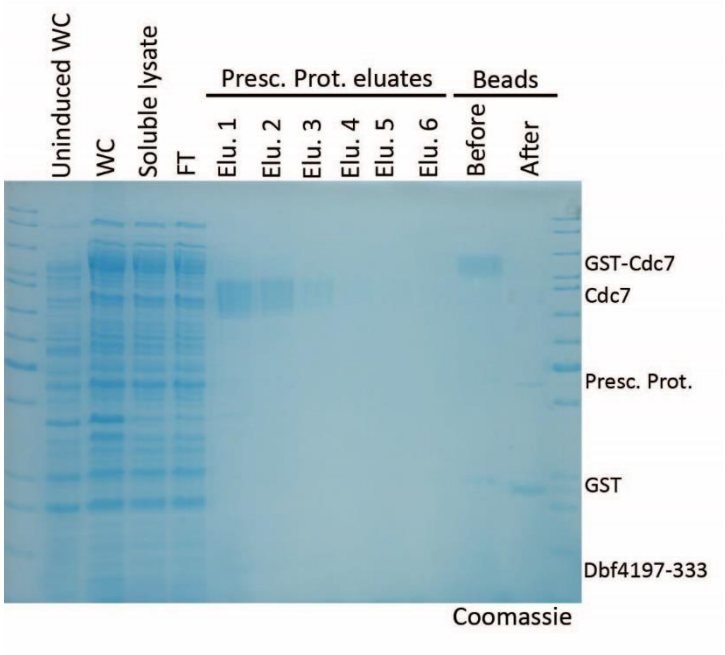

Extended figure 5. Purification of DDK
DDK was expressed in *E.coli* as a complex of GST-Cdc7 and Dbf4197-333. The soluble lysate of the *E.coli* was loaded onto the glutathione agarose beads by exploiting the GST-tag on the N-terminus of Cdc7, and subsequently, the bound DDK was eluted from the beads using precision protease. The purification was analysed by Coomassie-stained SDS gel.

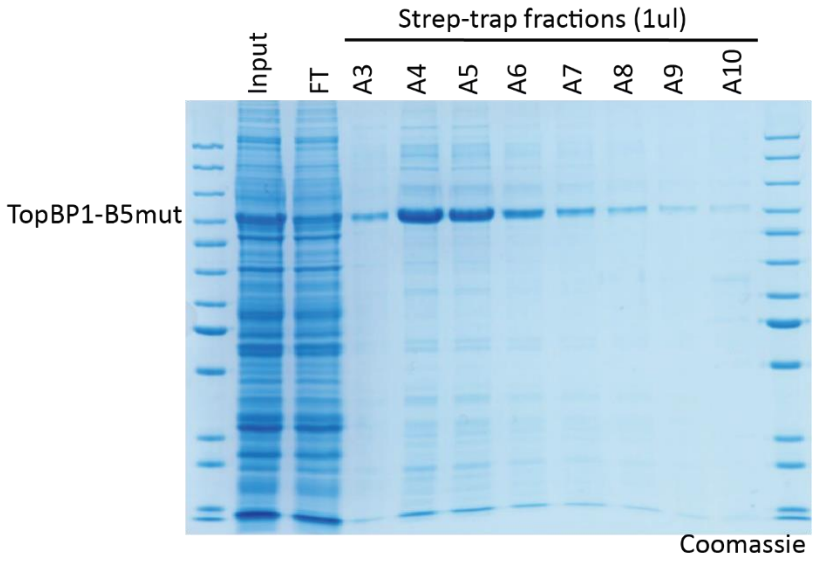

Extended figure 6. Purification of TopBP1-B5mut
TopBP1-B5mut with C-terminal strep-tag was purified from insect cells using using the strep-tag affinity chromatography. Purification was analysed by Coomassie-stained SDS gel.

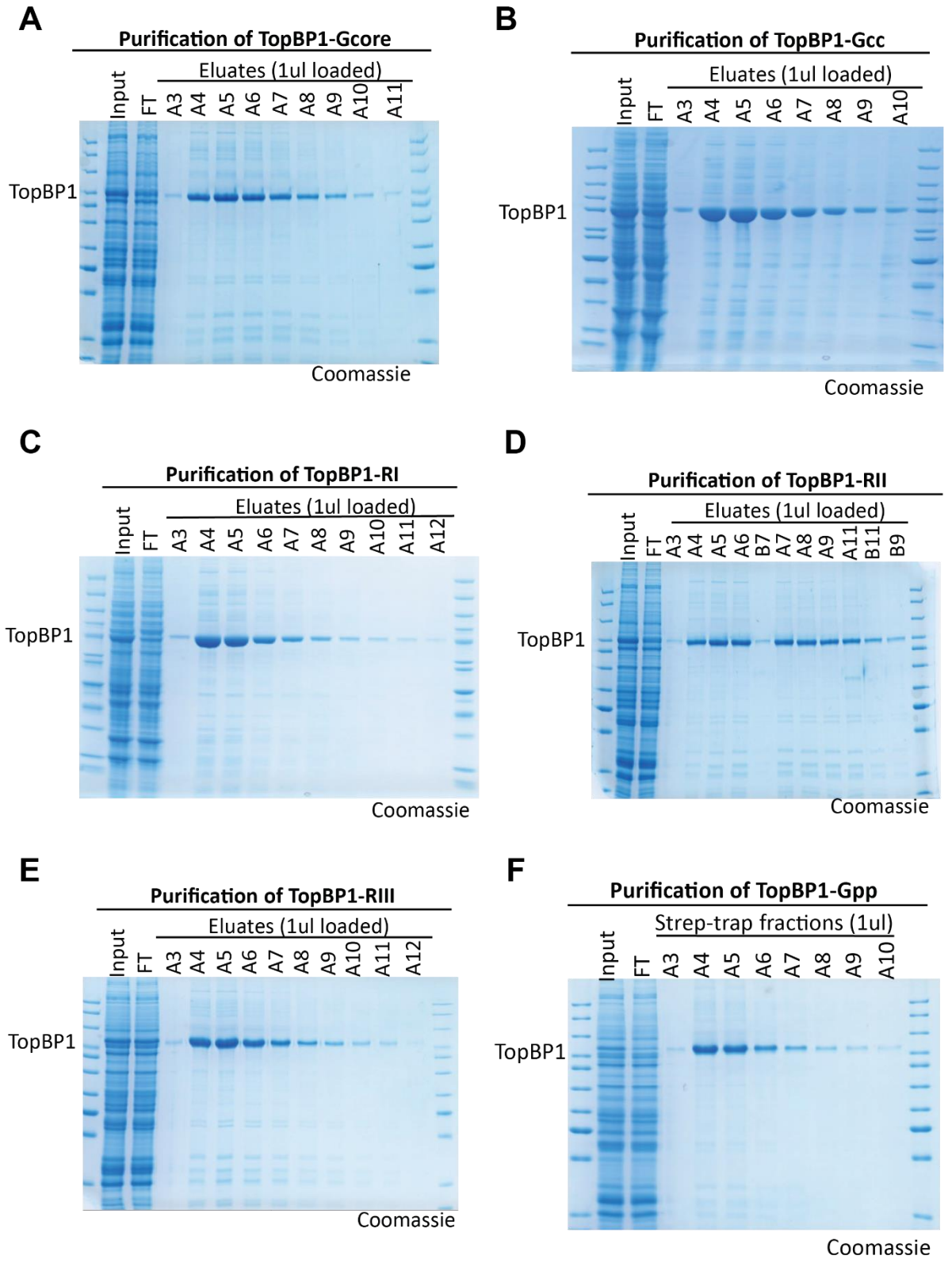

Extended figure 7. Purification of TopBP1-GINI domain mutants
Coomassie-stained SDS PAGE analysis of elution fractions of TopBP1-GINI domain mutants after strep-tag affinity chromatography.

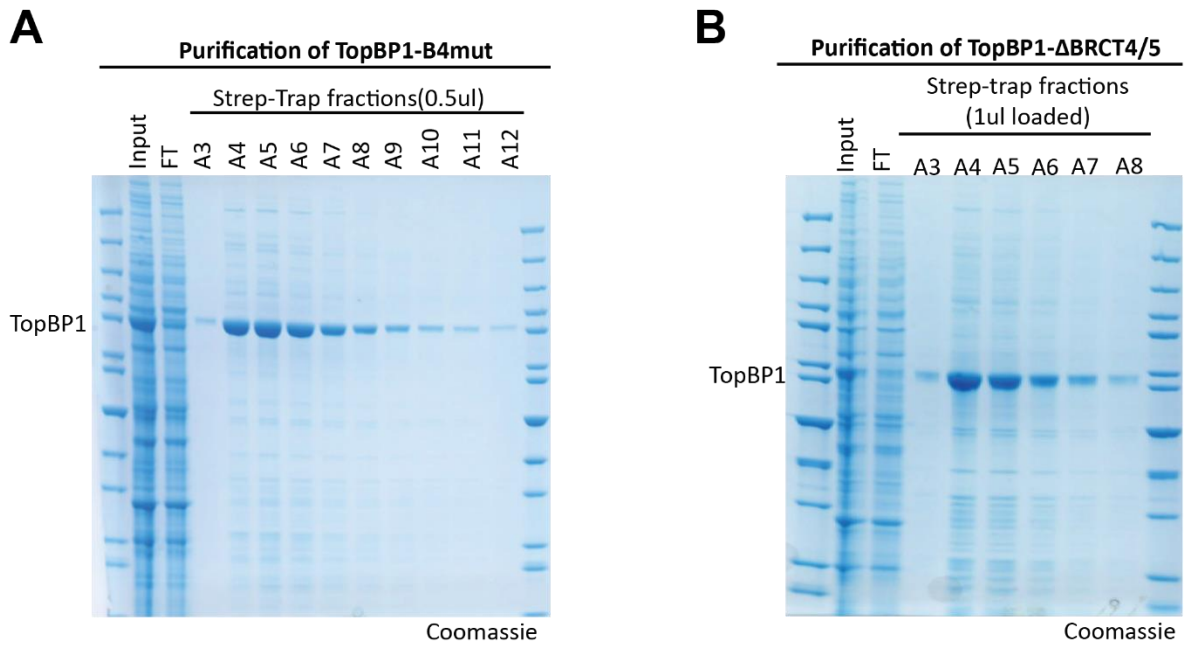

Extended figure 8. Purification of TopBP1-BRCT4 domain mutants
(A) TopBP1-B4mut (TopBP11-766 VTV590/606/610ERE-strep) and **(B)** TopBP1-ΔBRCT4/5 (TopBP11-549-strep) were purified from insect cells using strep-tag affinity chromatography by exploiting C-terminal strep-tag. Purifications were analysed by Coomassie-stained SDS gel.

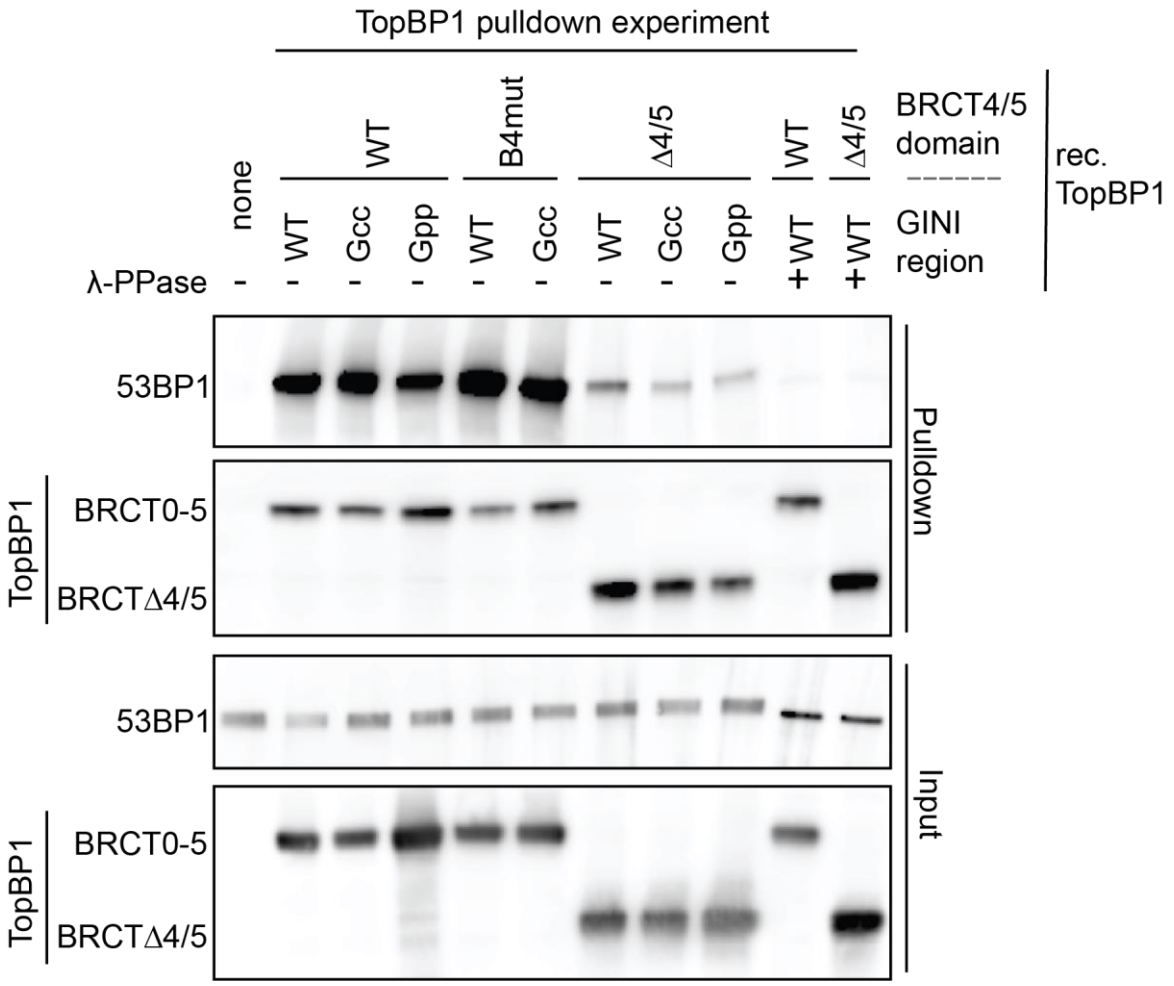

Extended figure 9. Recombinant TopBP1 mutants are not grossly misfolded
TopBP1-BRCT0-5-WT and indicated mutants were used to pull down endogenous 53BP1 from Hek293T cell lysates. Lysates and pulldowns were analysed using immunoblotting.

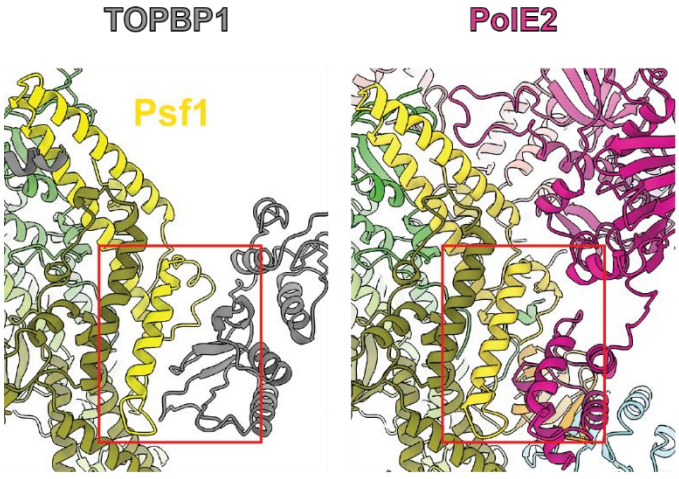

Extended figure 10. TopBP1 and DNA polymerase ε exclusively bind to GINS in the CMG context
Detailed *investigation* of the interaction regions on GINS with TopBP1-BRCT4 and PolE2

Curriculum Vitae

Der Lebenslauf ist in der Online-Version aus Gründen des Datenschutzes nicht enthalten.

Acknowledgements

First of all, I would like to express my sincere thanks to my supervisor and mentor Prof. Dr. Dominik Boos for giving me the opportunity to work on this fascinating project. His continuous support helped me through a challenging PhD.

Next, I would like to thank Prof. Dr. Stefan Westermann for reviewing my thesis and his scientific support.

I would like to particularly thank Milena Parlak for her support during writing my thesis and also her scientific contribution to this project.

I am very thankful to Matthew Day who provided the structural data for this project.

I am also very thankful for fruitful discussions in our lab meetings together with Prof. Dr. Stefan Westermann's group.

I thank all the current and former lab members for endless support, always helping out with lab work.

Special thanks to Anika Marko for her help during writing my thesis. Whenever I needed help, she was there for technical support.

A warm thank to Eman Zaffar and Katharina Pravi. I really enjoyed sharing my office with them.

Special thanks to Pedro Ferreira for always being there in the bad times and good times.

I would like to express my deepest gratitude to my parents, they have always been patient and supportive whenever I needed. They never left me alone during this long journey. A special thanks to my mother in law Ayla Kücük for her great support.

My last words go to my son Ege; and my wonderful wife Pelin, for always being by my side, believing and supporting me endlessly. Thank you for being there, your presence is irreplaceable. And Ege, you are the colour of my life, life would be meaningless without you.

Declarations

In accordance with § 7 (para. 2, clause d and f) of the Regulations Governing the Doctoral Proceedings of the Faculty of Biology for awarding the doctoral degree Dr. rer. nat., I hereby declare that I have written the herewith submitted dissertation independently using only the materials listed, and have cited all sources taken over verbatim or in content as such.

Essen, date _____ _____

Signature of the doctoral candidate

In accordance with § 7 (para. 2, clause e and g) of the Regulations Governing the Doctoral Proceedings of the Faculty of Biology for awarding the doctoral degree Dr. rer. nat., I hereby declare that I have undertaken no previous attempts to attain a doctoral degree, that the current work has not been rejected by any other faculty, and that I am submitting the dissertation only in this procedure.

Essen, date _____ _____

Signature of the doctoral candidate

In accordance with § 6 (para. 2, clause g) of the Regulations Governing the Doctoral Proceedings of the Faculty of Biology for awarding the doctoral degree Dr. rer. nat., I hereby declare that I represent the field to which the topic “Bipartite GINS binding mode of TopBP1 to activate the metazoan Mcm2-7 replicative helicase” is assigned in research and teaching and that I support the application of Bilal Tetik.

Essen, date _____ Prof. Dr. Dominik Boos _____

Name of the scientific supervisor/member of the University of Duisburg-Essen

Signature of the supervisor/ Member of the University of Duisburg-Essen